[redacted]

(NASA-CR-112055) HYPERSONIC RESEARCH ENGINE PROJECT. PHASE 2: STRUCTURES AND COOLING DEVELOPMENT Interim L.F. Jilly (AiResearch Mfg. Co., Los Angeles, Calif.) 1 Sep. 1970 98 p
CSCL 21E G3/28

N72-25711

Unclas
30758

GARRETT

AIRESEARCH MANUFACTURING COMPANY
A DIVISION OF THE GARRETT CORPORATION
9851-9951 SEPULVEDA BLVD. • LOS ANGELES, CALIFORNIA 90009
TELEPHONE: SPRING 6-1010, ORCHARD 0-0131 • CABLE: GARRETTAIR LOS ANGELES

AIRESEARCH MANUFACTURING COMPANY
Los Angeles, California

HYPERSONIC RESEARCH ENGINE PROJECT - PHASE II
STRUCTURES AND COOLING DEVELOPMENT
FOURTEENTH INTERIM TECHNICAL DATA REPORT
DATA ITEM NO. 55-7.14
3 MAY THROUGH 2 AUGUST 1970
NASA CONTRACT NO. NAS1-6666

Document No. AP-70-6640

Details of illustrations in this document may be better studied on microfiche

Number of pages 98

Original date 1 September 1970

Prepared by Engineering Staff

Edited by L. F. Jilly

Approved by Henry J. Lopez
HRE Program Manager

Revision	Date	Pages Affected (Revised, Added, Eliminated)

FORM 23 77, R-70

FOREWORD

This interim technical data report is submitted to the NASA-Langley Research Center by the AiResearch Manufacturing Company, Los Angeles, California. The document was prepared in accordance with the guidelines established by paragraph 5.7.3.2.2 of NASA Statement of Work L-4947-B (Revised).

Interim technical data reports are generated on a quarterly basis for major program tasks under the Hypersonic Research Engine Project. Upon completion of a given task effort, a final technical data report will be submitted.

The document in hand presents a detailed technical discussion of the structures and cooling development for the period of 3 May through 2 August 1970.

ACKNOWLEDGMENTS

Acknowledgments for completion of this document are herewith extended to the following contributors:

Design and Development:	O. A. Buchmann J. C. Gibson L. H. King C. M. Lee A. I. Stern
Heat Transfer Analyses:	A. A. Vuigner C. F. Young
Stress Analyses:	W. G. Flieder E. Katinszky
Materials Engineering:	O. Jones

CONTENTS

CONTENTS (Continued)

ILLUSTRATIONS

ILLUSTRATIONS (Continued)

ILLUSTRATIONS (Continued)

TABLES

1. SUMMARY OF STATUS

All design, manufacturing, and test activities during the reporting period have related to the Structures Assembly Model (SAM).

1.1 STRUCTURES ASSEMBLY MODEL MANUFACTURING

This activity involves adaptation and assembly of the HRE flightweight components to form the basic engine assembly, and fabrication of the water-cooled test adapters for use in the wind tunnel test. All fabrication and assembly activities were completed during the reporting period.

1.1.1 Flightweight Component Assemblies

Assembly of all of the flightweight component assemblies into the basic engine assembly was completed. The completed assembly was proof-pressure tested at 1050 psig and leak tested using a helium mass spectrometer. Results were satisfactory.

1.1.2 Water-Cooled Test Adapters

Manufacturing operations on the cowl/pylon assembly were completed and the unit was satisfactorily proof-pressure tested. All other water-cooled adapters had been previously completed.

1.1.3 Final Assembly

The assembly of the basic engine assembly and of the water-cooled test adapters was completed and satisfactorily leak tested. Final plumbing assemblies were prepared with the assembly mounted to the external manifolding to insure proper fitups.

1.2 SAM FUEL/COOLANT SYSTEMS

The coolant control system for SAM wind tunnel testing is being treated as facility-type equipment. In particular, the flightweight valves that were under development for the HRE will not be used. Instead, commercially available valves have been selected and procured. This is feasible because of the simplification of the temperature control concept and of the absence of weight and volume constraints.

1.2.1 Control Valves

Design, fabrication and testing of the pressure control valve has been completed and the valve is satisfactory for use with SAM. Work with all other valves required for the SAM fuel/coolant system had previously been completed. Dynamic testing, however, has shown problems involving venting of the pneumatic valves to a constant back pressure. Capacity of the vent lines apparently was inadequate and the resulting back pressure caused small oscillations. The vent line configuration has been modified to obviate this problem.

1.2.2 External Manifolding

Fabrication of the external manifolding for hydrogen and water has been completed. The assembly has been proof-pressure tested at 1050 psig and was found to be satisfactory.

1.3 SAM CALIBRATION TESTS

Hydraulic testing of the inlet spike actuation system was completed on the SAM final assembly. Calibration of spike position vs LVDT output and command dial settings were obtained. In addition, frequency response tests using input from a servo analyzer were run to 45 cps. No unacceptable conditions were encountered.

Upon completion of the hydraulic test, the SAM assembly was again mated to the external manifolding for flow calibration and system checkout. The pressure drop vs flow characteristics of the five water flows were obtained, and the differential pressure switches in the water flow routes calibrated to values corresponding to the test results. Pressure drops in two of the routes were higher than predicted but can be accommodated by the adjustment of the flow and slight increases in inlet pressure.

Pressure drop versus flow characteristics for the hydrogen system using isothermal air flow were obtained. Both the CRV and FDV settings were calibrated. Transition from dump flow to injection flow was checked out and calibrated. Operation of various abort signals and interlocks was verified. The response of the system during transients was measured and showed no unacceptable conditions such as flow reversals or large changes in relative flow of different routes. The pressure control valve and its controller were operated as part of the test and showed acceptable response for the air system. Operation of this valve as part of the hydrogen system was evaluated on the analog computer.

1.4 TEMPERATURE CONTROL SYSTEM

As noted above, integrated tests of the temperature control system have been completed. Nose and grounding problems have been resolved and circuit constants adjusted for satisfactory operation. Computer runs using the analog computer simulation of the temperature control system and the pressure control system have been completed and show that no compensation will be required. The need for damping in the pressure control loop, however, was established on the basis of these runs and the pressure control circuits appropriately modified.

1.5 TEST PLANNING

Detail test procedures for the testing of SAM at the NASA-Langley Research Center have been completed. In addition, fabrication of a shipping cart for SAM has been completed, as has fabrication of a special tool to be used to calibrate the spike position relative to the leading edge lip.

2. PROBLEM STATEMENT

The objective of the structures and cooling development program is to analyze, design, and fabricate the regeneratively cooled surfaces and their associated structures and to verify the performance of these surfaces and structures at conditions that simulate the operating conditions expected in the flight test engine.

The Hypersonic Research Engine requires regenerative cooling on all surfaces that contact the engine airstream. The use of ablative coating on the engine aerodynamic surfaces is barred by the Statement of Work to minimize extraneous effects on engine performance. No such restriction is imposed on the engine cowl; therefore, ablative protection is used for this component.

The characteristic design problem in regeneratively cooled structures for this type of application is associated with the large heat fluxes encountered over major portions of the engine surfaces. These heat fluxes range from values of approximately 10 Btu/sec-ft^2 to 1800 Btu/sec-ft^2 on the stagnation line of the support strut leading edge. The conservation of fuel requires that these heat fluxes be accommodated at temperature differences across the regeneratively cooled surfaces which range up to approximately 800°F in flat surfaces and 1200°F in leading-edge areas. These temperature differences, in turn, result in strains that cause plastic deformation of the hot surfaces. Design therefore is governed by low-cycle fatigue conditions. Uncertainties associated with the prediction of low-cycle fatigue performance have led to heavy emphasis, in the experimental portion of the program, on the evaluation of the low-cycle fatigue performance of the engine components.

The general performance objectives set for the cooled structures are as follows:

> Design life - 10 hr of hot operation, of which 3 hr are to be taken at Mach 7 to 8 flight conditions
>
> Cycle life - 100 cycles, at conditions which produce the highest plastic strain

3. TOPICAL BACKGROUND

The cooled structures, which are being designed, fabricated, and tested as part of this task, and the associated connecting structures constitute the basic structural elements of the engine. The cooled surfaces of these structures form the aerodynamic surfaces of the engine, as shown in Figure 3.0-1.

3.1 GENERAL DESIGN GUIDELINES

The regeneratively cooled surfaces must be designed and fabricated to minimize engine performance losses. In addition to providing the basic contours, the cooled surfaces must be fabricated and assembled in a way that avoids discontinuities; leading edges must use the minimum radius compatible with reliable structural design.

Because of the research nature of the HRE program, temperatures and pressures will be measured throughout the engine. Consequently, the engine structures must accommodate static pressure taps and metal temperature thermocouples.

The total amount of fuel available to the engine and for cooling of the structure is severely limited by X-15A-2 storage capabilities. Consequently, in cooling the structure, fuel usage in excess of combustion requirements must be minimized. To accomplish this goal, the cooled surfaces must function at maximum metal temperatures and temperature differences compatible with sound structural design.

Engine internal structures and plumbing must be designed to allow space for installing fuel system components, engine controls, instrumentation transducers, and signal conditioning equipment. Because of operating limitations, electronic equipment must be installed in locations having the least severe environment.

To permit the engine to operate over the flight Mach number range from 3 to 8, the inlet spike must be translated to various positions. To conserve coolant prior to and after engine operation, the inlet spike must be translated to a position nearly in contact with the outerbody leading edge. Consequently, it is necessary to have a spike actuation system capable of the desired positioning accuracy, with control provided by the control system computer.

Engine fuel pressurization is provided by a hydrogen turbopump. Therefore, the total pressure drop in the regeneratively cooled surfaces, manifolds, and associated plumbing must be compatible with the pressure output of the turbopump.

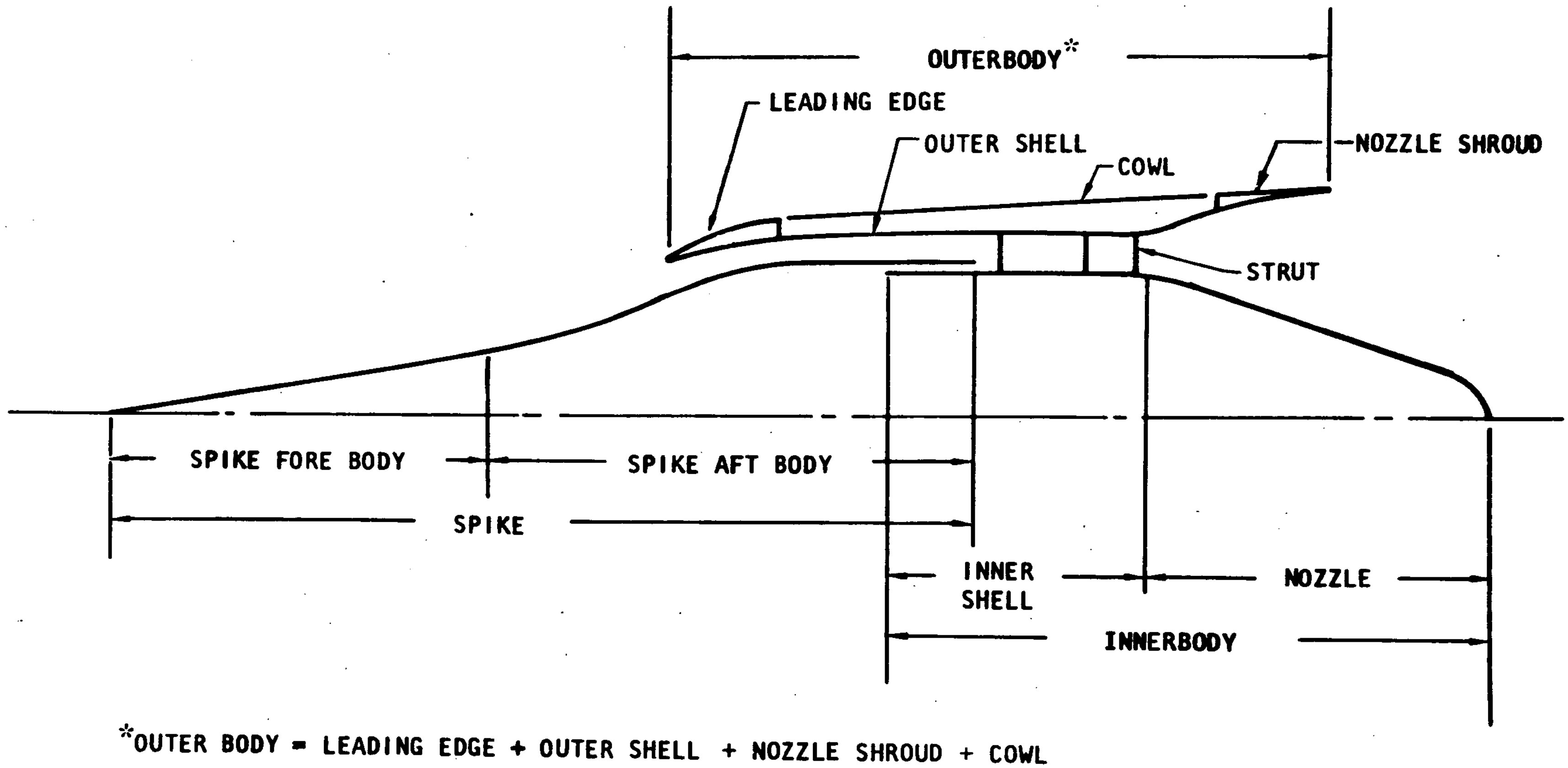

Figure 3.0-1. Cooled Structures Nomenclature

In addition to control of temperatures and temperature differences, the integrity of the coolant structures requires that the flow routes within the engine be matched in such a way as to minimize temperature differences at axial stations for innerbody and outerbody surfaces. This will minimize distortion of the engine internal passages. Axial temperature discontinuities as produced, for example, by the termination of two flow routes that differ greatly in temperature at the same station, are objectionable because of the severe thermal strains that result.

Measurement of engine internal thrust during flight is required. Consequently, external loads (drag and lift) that are transmitted directly to the thrust measuring device must be minimized. Specifically, the engine cowl has drag loads that are of the same order of magnitude as the engine thrust. Mounting of the cowl in such a way as to minimize this external drag load, and thus the uncertainties in calculation of thrust, is therefore required.

A basic engine design requirement is that malfunction of the engine will not endanger the safety of the aircraft or the life of the pilot. Therefore, provision must be made to jettison the engine. Because of probable hydrogen leakage to the engine cavities, the innerbody engine cavity must either be inerted or must be capable of containing an explosive mixture of hot hydrogen and air. To accomplish this, the engine cavity will be vented to near nozzle base pressure and provisions will be made for explosion containment. During ground checkout, the engine cavity will be inerted with nitrogen.

The weight of cooled structures, inlet spike actuation system, internal supporting structures, and plumbing is most of the total engine weight. Although optimization of the structures and structural components for minimum weight is not an objective, the specified weight limitation requires careful consideration of structural weight.

The instrumentation, controls, and fuel subsystems contained in the engine cavity will require servicing prior to and after each test. Consequently, the mechanical assembly of the engine cooled structure components must provide easy access to subsystem components for replacement in the field.

3.2 OPERATIONAL BOUNDARIES

3.2.1 General Design Ground Rules

The maximum dynamic pressure specified for the current phase of the program is 2000 psfa. This compares with the specified dynamic pressure of 2500 psfa, specified for the HRE Phase I program. Consequently, the minimum altitude at Mach 8, during which cooling must be provided, is 85,000 ft, as compared to the Phase I minimum altitude of 81,000 ft. The minimum design altitude for the current program is 88,000 ft. The increased altitude results in a reduction of heat flux throughout the engine, but this reduction is offset in part by an increase in engine contraction ratio from 10 in Phase I to 14.6 in Phase IIA. In summary, the operating envelope for the engine is as follows:

Engine Structural Design - With engine either lit or not lit, dynamic pressure (q) = 2000 psfa

Engine Cooling Design

Normal design, engine lit: q = 1750 psfa, h = 88,000 ft minimum

Emergency design, engine lit: q = 2000 psfa, h = 85,000 ft minimum

For the emergency design, engine lit conditions, all of the pump output pressure is available for coolant pressure drop. The dump valve opens and fuel injection valves close as the aircraft approaches these conditions from the normal operating line.

3.2.2 Engine Operating Cycles

A qualitative definition of the engine operating cycles has been formed for the purpose of providing a basis for analyzing heat transfer transients, evaluating the structural effect of transient temperature differences, establishing general control requirements and typical environmental conditions, and for defining acceptable operating cycles. The types of missions or conditions the engine must survive are as follows:

Case I - Constant M, with aircraft power on, at a constant high q

Case II - Constant M, with aircraft power off, aircraft diving

Case III - Variable M, expected to involve a change in M of 0.5 during 20-sec engine operating cycle

Case IV - Subsonic-supersonic combustion transition at M = 6

Case V - Inlet unstart, with shock expelled

Figure 3.2-1 is a qualitative representation of the critical cases. The common features, typical for all missions, are numbered on the figure and are as follows:

1. Launch to M = 3+, during which the engine structure is assumed to go from a soak at -65°F to a soak at 1140°F. No cooling is required. At the end of this period, the helium purge is performed and coolant flow started through all portions of the cooled structure.

2. Approach to test Mach number, inlet closed (leakage flow only), during which coolant flow is increased to maintain maximum structure temperature (cold surface) at 1140°F.

3. Time for retraction of inlet spike to desired position. The solid lines assume programmed cooling flow; the dashed line assumes controlled cooling flow based on temperature sensing. The approach selected will be a function of control system response and actuating system response. Controlled cooling is preferred.

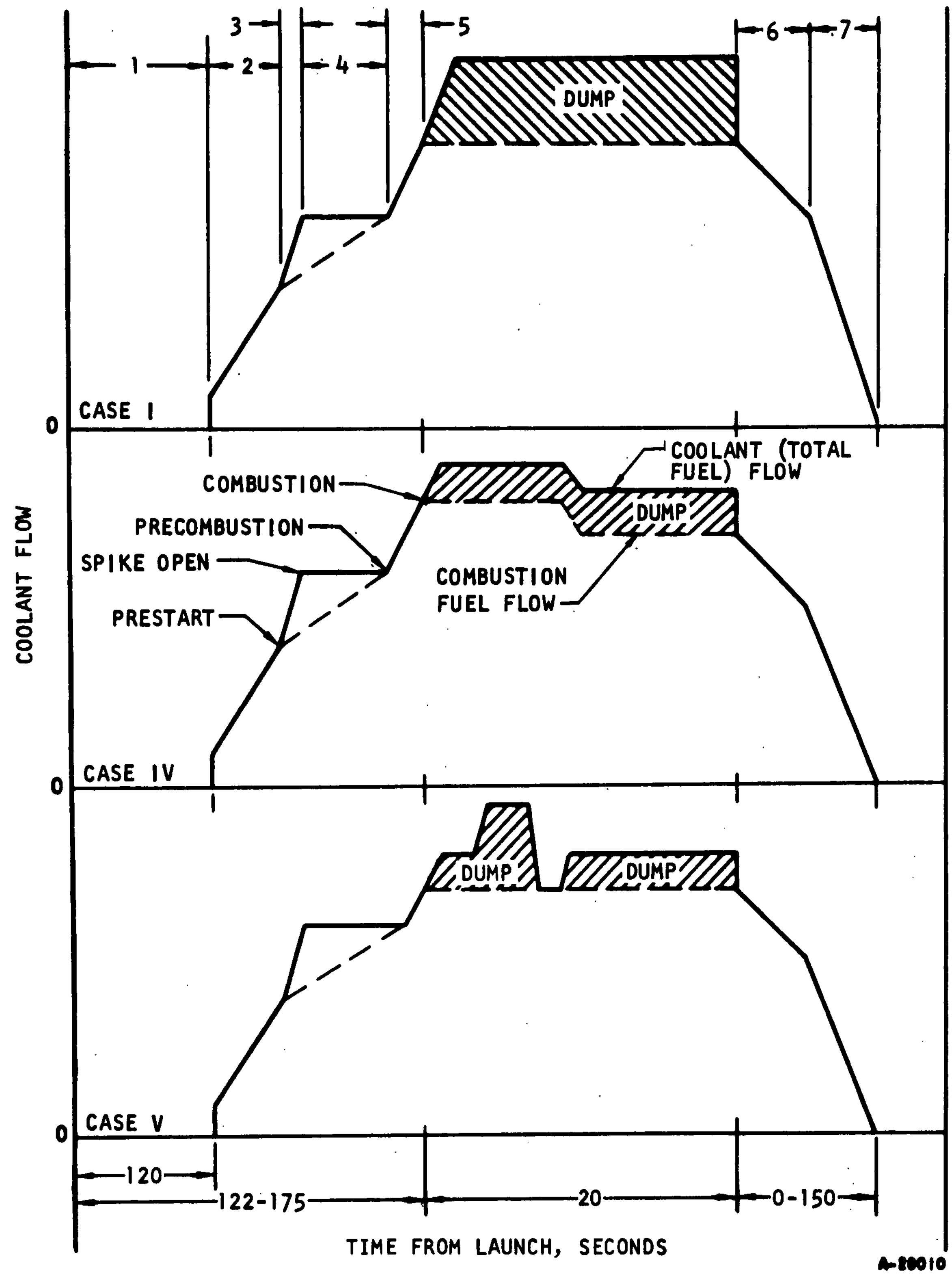

Figure 3.2-1. Typical Engine Operating Cycles

4. Inlet spike in starting position, full airflow through the engine, no combustion.

5. Programmed increase in cooling flow to starting combustion equivalence ratio (ϕ). This ϕ will be less than the test ϕ. Combustion ϕ will ramp to test ϕ (not shown).

6. Combustion terminated and inlet spike being extended to closed position.

7. Inlet closed (leakage flow only), deceleration to M = 4 +, with coolant flow decreased to maintain maximum structure temperature at 1140°F. Helium purge.

As combustion starts, the cooling ϕ must be controlled to accommodate increasing heat fluxes. The variations among missions occurring during the combustion phase are as follows:

Case I - Shown in Figure 3.2-1. Cooling ϕ is in excess of combustion ϕ. Combustion ϕ will ramp at beginning and end of test. Ramps of 5-sec duration to and from $\phi = 1$ may be assumed at beginning and end of test.

Case II - Not shown. Represents a gradual change in conditions shown for Case I and will involve less severe transients. Not considered a design point.

Case III - Same comments as Case II, but may become a design point at lower Mach numbers because of potential for increased test time and wider Mach number range.

Case IV - Shown in Figure 3.2-1. Involves a near-step change in gas-side engine conditions during test run.

Case V - Shown in Figure 3.2-1. The general rise in pressure would be expected to cause a step-change type increase in heat flux. Spike will extend and close, then retract to operating position for second attempt at starting. At this point, either normal operation or a second unstart is possible.

4. OVERALL APPROACH

The diverse requirements imposed on the cooled structures require iteration of the cooled structural design with (1) the engine aerodynamic design; (2) the instrumentation, control, and fuel subsystems designs; and (3) the airplane interface design. Internal contraints on cooled structural design are imposed by the close coordination required in thermal design, structural design, mechanical design, and manufacturing. It is generally not possible to treat any one of these areas independently of the others. During Phase I of the program, the basic design concepts for the engine were defined and are basically feasible in terms of the constraints imposed on the design. These concepts and the design data generated during Phase I are being used as the starting point for design of the Phase IIA cooled structures. Component layout drawings of acceptable mechanical design and with acceptable manufacturing features form the initial step in the iteration. These layout drawings have been evaluated to establish the required thermal and structural design features. Based on these inputs, layout drawings are revised to incorporate the required features, followed by substantiation of thermal and structural performance of the revised design.

Although the Phase I design is being used as the starting point of Phase IIA cooled structure design, each of the components is being reviewed with the objective of simplification in terms of mechanical design and manufacturing features. The interfaces between two or more components, in particular, will be reevaluated . The interfaces include engine-to-airplane mounting, outer-shell-to-innerbody mounting by means of the support struts, nozzle-to-inner-shell assembly, inlet spike-to-innerbody assembly, inlet spike actuator-to-inlet spike and innerbody mounting, leading edge-to-outer shell mounting, and cowl-to-outer shell support.

The general approach to cooled structures development places heavy emphasis on fabrication and testing of the full-scale components. A limited number of types of cooled structural elements and models is being fabricated and tested to evaluate the problems which are basic to the overall engine design, or which are sufficiently localized in nature to permit use of subscale evaluation. All significant manufacturing development and evaluation is being accomplished using the full-scale components. The nature of the required manufacturing operations for the components is such that use of subscale components would be expected to lead to only limited information on the adequacy of manufacturing techniques and processes.

4.1 THERMAL DESIGN

The overall thermal design approach is by analyses based on experimental data obtained from tests on similar geometric configurations and heat transfer situations. These experiment-based analyses, in turn, will be verified by experiments where the geometry or fluid conditions, or both, will be like those existing for the flight engine.

Where the discrepancy between calculated and experimental heat flux values is large, steps are being taken to improve the analytical techniques so that the correlation between calculated and experimental results can be improved.

The basic goals of all thermal analyses and designs are (1) limiting temperature and temperature differences to structurally acceptable values, while keeping hydrogen cooling flow equal to or less than hydrogen flow required for combustion, and (2) at the same time maintaining hydrogen pressure drop compatible with cooling jacket pressure containment and pump outlet pressure capabilities. The limiting values being used at present are (1) a maximum gas side metal temperature of 1700°F (2160°R), (2) a maximum primary structure temperature of 1140°F (1600°R), and (3) a hydrogen pump outlet pressure of 1100 psia.

The thermal design procedure involves separate calculation of aerodynamic heating and cooling jacket performance. The aerodynamic heating conditions are calculated (as during Phase I) primarily by use of the computer program H1940. Special aerodynamic heating conditions, such as shock wave/boundary layer interaction, are computed separately. Cooling jacket fin performance is calculated (as in Phase I) by use of computer program H1930. Special conditions, such as pressure and flow distributions for inlet, outlets, and bolted flange/manifolds, require separate calculations. Verification of aerodynamic and cooling jacket heat transfer and pressure drop calculations will be accomplished by actual tests. Specifically, aerodynamic heat transfer calculations will be verified by tests of engine component models, such as the combustor, and with the boilerplate engines. Calculated performance of cooled structures will be verified by full-scale component and some subscale component testing at heat flux levels and distributions comparable to those calculated for the flight engine components. The primary areas requiring verification in the cooled structures performance are flow distribution and associated temperature distribution and its effects on structural performance in terms of life and contour.

4.2 STRUCTURAL DESIGN

The structural design approach utilizes a combination of analytical and experimental methods. Experimental verification of detailed parts, such as short-term burst, creep-rupture, and thermal fatigue tests on sandwich plate-fin elements, will be employed wherever necessary. Generally, the structural tests will be performed on composite structural elements, such as the inlet spike and the innerbody assembly.

The bulk of the HRE structures consists of ring-stiffened orthotropic shell structures of variable thicknesses and contours. The ring stiffeners are also used for coolant flow manifolding and fuel injection rings for the engine combustor section. The structural loadings will produce axisymmetric and asymmetric forces and moments due to static normal pressures, acceleration, vibrational inputs, and aerodynamic flutter and buffeting effects.

Fully operational computer solutions are available to analyze axisymmetric isotropic thin shells of variable thicknesses and contours for stresses due to axisymmetric loads and temperature profiles. In addition, the isotropic shell analysis had been extended to treat orthotropic cylindrical shells with axisymmetric loads. Two MIT finite difference nodal circle solutions (SABOR III and DASHER I), which have been adapted for use on the AiResearch computer system (IBM-360/50), are available for use.

The SABOR III program is applicable for axisymmetric isotropic shells (local departures from ideal isotropy can be treated) that may be subjected to nonsymmetrical static forces. The SABOR III program may also be used to obtain the stiffness and mass matrixes for direct input into the DASHER I program to obtain dynamic response.

It would have required an extensive programming effort to modify the SABOR III and DASHER I programs to treat accurately many of the problems that will be encountered in the HRE. Rather than attempt this approach, a further survey of existing shell programs was carried out, and it was determined that an extremely applicable program had been developed under the auspices of the Analysis Group of the Theoretical Mechanics Branch, Structures Division of the Wright Patterson Air Force Base, Dayton, Ohio. This program is based upon the very recent improvement in matrix shell solutions generated by A. Kalnins (Department of Mechanics, Lehigh University). It solves the general axisymmetric orthotropic thin shell problem for symmetric and nonsymmetric loads due to static as well as dynamic inputs. The program has been successfully adapted for use on the AiResearch computer system. Although the program has been debugged, the final report describing the usability limitations, and methods of data input has not been completed, and will not be released by the Wright Patterson Air Force Base for at least twelve months. Until a program of this magnitude has been completely checked out by trying numerous test cases, a note of caution must be exercised regarding its capabilities. Another important point is the fact that the problem inputs and the data reduction of the outputs require considerable effort on the part of the user. The existence of the program also does not eliminate or substantially reduce the work needed to generate a sound design; however, it is the objective of careful analysis to discover design inadequacies that would otherwise not be recognized.

The eventual objective of the test program is to verify the actual performance capabilities of the structures as fabricated. Although it will not be possible to predict analytically the influence of realistic fabrication restrictions and limitations on the end product, the initial analysis will identify the serious design problem areas. Results of the test program will be used to assess the extent of the changes required to achieve the structural integrity goals.

4.3 MECHANICAL DESIGN

The guidelines used in mechanical design of the cooled structures components and assembly of the components into the engine require the use of known materials and joining techniques. Standard fasteners and seals are used to the greatest extent possible. Design for brazing is aimed at minimizing the total number of braze cycles to which a given part must be subjected. In some cases, this is done by redesigning the parts to allow use of prebrazed subassemblies, substitution of machined or welded subassemblies, or substitution of bolted interfaces for brazed or welded interfaces. Also, as a general rule, all welding into or close to braze joints is being avoided, although in certain cases, such a procedure may be acceptable.

The mechanical design effort will be supported by experimental verification in selected areas. In particular, selected configurations that present analytical problems and raise questions as to manufacturing feasibility will be fabricated and tested on a subscale basis. The purpose of such tests will be to provide design data and guidance for possible design revision. Currently planned tests, which are in support of mechanical design rather than thermal or structural design, include the following:

- Test specimen to evaluate feasibility of bolting the nozzle flange manifold to the inner shell through the removable nozzle cap
- Fabrication of a section of the inlet spike near the spike tip to help resolve questions regarding the best manufacturing approach, and hence, the best design for this portion of the inlet spike
- Fabrication of the spike-to-innerbody seal to evaluate the adequacy of the design solution
- Fabrication of a straight section of the bolted nozzle manifold to verify both the manufacturing aspects and structural integrity of the design solution

Fabrication and evaluation of the various mechanical seals used in the components to verify the adequacy of the design solution

Fabrication of flat panels using the various instrumentation and fuel injector fittings that penetrate the regeneratively cooled surfaces to verify manufacturing feasibility and structural integrity of the design. Tests results will be used to select the final configuration used in the engine.

4.4 MANUFACTURING

The manufacturing approach being used on this program has two aspects: (1) that dealing with the approach to development of manufacturing techniques and processes, and (2) that dealing with the specific manufacturing processes planned for use.

4.4.1 Development Approach

The development of the manufacturing techniques and processes will rely primarily on full-scale components. Except where isolated problems or basic data must be obtained, the use of subscale components represents a duplication of development effort. The compound forming of the shell-face sheets in half-scale, for example, results in working with radii of curvature which are half those encountered in the full-scale part. Use of lighter-gauge material to facilitate forming, on the other hand, is impractical. In addition, the size of the full-scale tooling, the machines required to use this tooling, and the unique problems associated with the forming of large thin wall shells cannot be duplicated in half-scale. As a result, a half-scale compound-curved model of the isentropic surface of the inlet spike is the only subscale component on which fabrication development work is being done. This part is being used to establish forming characteristics, evaluate electrohydraulic forming parameters, and investigate brazing problems.

4.4.2 Fabrication Approach

The most critical area of cooled structures fabircation is in the cooled surface shell face sheets. The starting point for these shells can either be rolled-and-welded-cone sections or flat sheets. The rolled-and-welded cones are bulge-formed, then final-sized, using electrohydraulic forming. Using flat sheets as a starting point, the shells must be deep drawn in about three stages. Final sizing of the shells occurs as for the welded cones. Of the two approaches, the one using the seam-welded cone has been selected. The weld seam is not considered structurally objectionable and the approach involves fewer steps than are required for deep drawing.

To ensure adequate braze fitup, forming accuracy for the shells must be high. Specifically, it is expected that the clearance between shells must be maintained within a tolerance of approximately ±0.001 in. Given this accuracy, the brazing of the fins between the face shape still requires special attention. To ensure sound braze joints, pressure must be exerted on the shells in such a way as to provide a crushing load on the fins. The methods available for providing this braze fixturing load include the following, as a function of the component being brazed:

Graphite fixtures, with an external piece containing the assembly and an internal piece using expanding segments to exert pressure.

Steel bags placed inside the shell and pressurized to a level sufficient to deform the shell with which the bag is in contact. Containment on the external face sheet may or may not be required with this approach.

Evacuation and backfilling of the space between the two shell face sheets, using atmospheric pressure to provide the load.

Integrity of the shell joining will be experimentally evaluated and adjustments in shell forming tools and brazing procedures and fixtures made to correct problems that appear.

4.4.3 Nondestructive Testing

The critical area in fabrication of the full-scale components involves the shells themselves, as discussed in the two previous paragraphs. For structural integrity of the shells, only very limited areas of unbrazed joint areas are tolerable. These joints are detectable by proof pressure testing at sufficiently high pressure levels. Only in exceptional cases, however, will a defect that is revealed by proof pressure test be repairable. In general, a nondestructive test capable of revealing braze voids is preferable and offers better opportunity for subsequent repair. The two techniques available are radiographic inspection of the entire shell surface and the use of temperature-sensitive paint on one of the face sheets with a heating transient imposed on the other face sheet. These methods will show a braze void; that is, an unbonded joint. Weak joints are not discernable as such. In general, however, the existence of a brazed joint is reasonable assurance that adequate joint strength can be achieved. Verification of the result of radiographic or thermal inspection of the shells will be done by proof-pressure testing.

The repair techniques available for unbonded joints in the shells would generally be the following:

Recycling of the complete shell to a slightly higher temperature than used during the first braze cycle. In this way, remelt and flow of the braze alloy is obtained with the objective of filling the void. Orientation of the shell in the brazing furnace can be used to assist the process.

Removal of a portion of the face sheet in the unbrazed area, addition of filler alloy and closeout using a patch, with the entire shell recycled in the brazing furnace. The applicability of this repair procedure will be a function of the location of the affected shell area in the engine gas stream.

5. ANALYTICAL DESIGN

5.1 SAM HYDROGEN COOLANT ROUTES

The inlet lines for the strut-sides coolant have been re-routed so that this coolant flow is now supplied from the same inlet manifold as the other four engine routes (spike, innerbody, leading edge, and outer shell). Formerly, the coolant flow for the strut sides was tapped off the outer shell flow route at the aft support manifold. The modified strut-side flow routing and the overall engine flow routing are described below.

5.1.1 Strut Sides Flow Re-Routing

The modified coolant-flow routing for the strut sides is shown in Figure 5.1-1. The coolant flow rate will be measured with sharp-edge orifices in a measuring section using corner taps. Two orifice plates (0.1615 and 0.2420 in. dia) will be used alternately to cover the expected range of hydrogen flow rates during test, and of nitrogen flow rates during calibration. Flow will be controlled with a needle valve downstream of the orifice section. Flow is distributed to each of the six struts from a 1-in. dia manifold through six 1/4-in.-dia tubes (0.028 in. wall thickness). The tubes formerly connecting the aft support manifold to the struts sides have been removed and the connections on the aft support manifold have been capped off. To eliminate flow maldistribution between struts, 0.110-in.-dia orifices have been placed in each of the six 1/4-in.-dia tubes at the distribution manifold. Without orifices, the maximum flow deviation between struts was estimated at 6.3 percent. This deviation was caused by differences in flow restrictions between struts and different lengths of the six 1/4-in.-dia tubes (from 12 to 40 in.). With orifices, the maximum flow deviation was estimated at 3.3 percent. A 5-percent deviation was reported for the former configuration (Reference 5-1).

5.1.2 Overall Flow Route Configuration

The schematic of the SAM coolant circuits with the modified strut-sides route is shown in Figure 5.1-2. Because the strut-sides route is supplied from the common inlet manifold, approximately 185 psi pressure drop (735 psi in the main inlet manifold to 553 psi in the fuel plenum) is now available compared with 4 psi for the former inlet configuration. In addition, the modified configuration allows independent strut-sides coolant control. The strut sides hydrogen inlet temperature will now be 200°R (the main hydrogen inlet temperature) compared with the former temperature of 540°R at SAM design point conditions (3300 psia, 3600°R tunnel total conditions). This decrease in inlet temperature allows for a decrease in design point flow rate from 0.026 lb/sec (six struts) to 0.021 lb/sec. The increased structural temperature mismatch between the aft strut and the inner and outer shells is acceptable, because structural temperature differences are moderately low in this area and

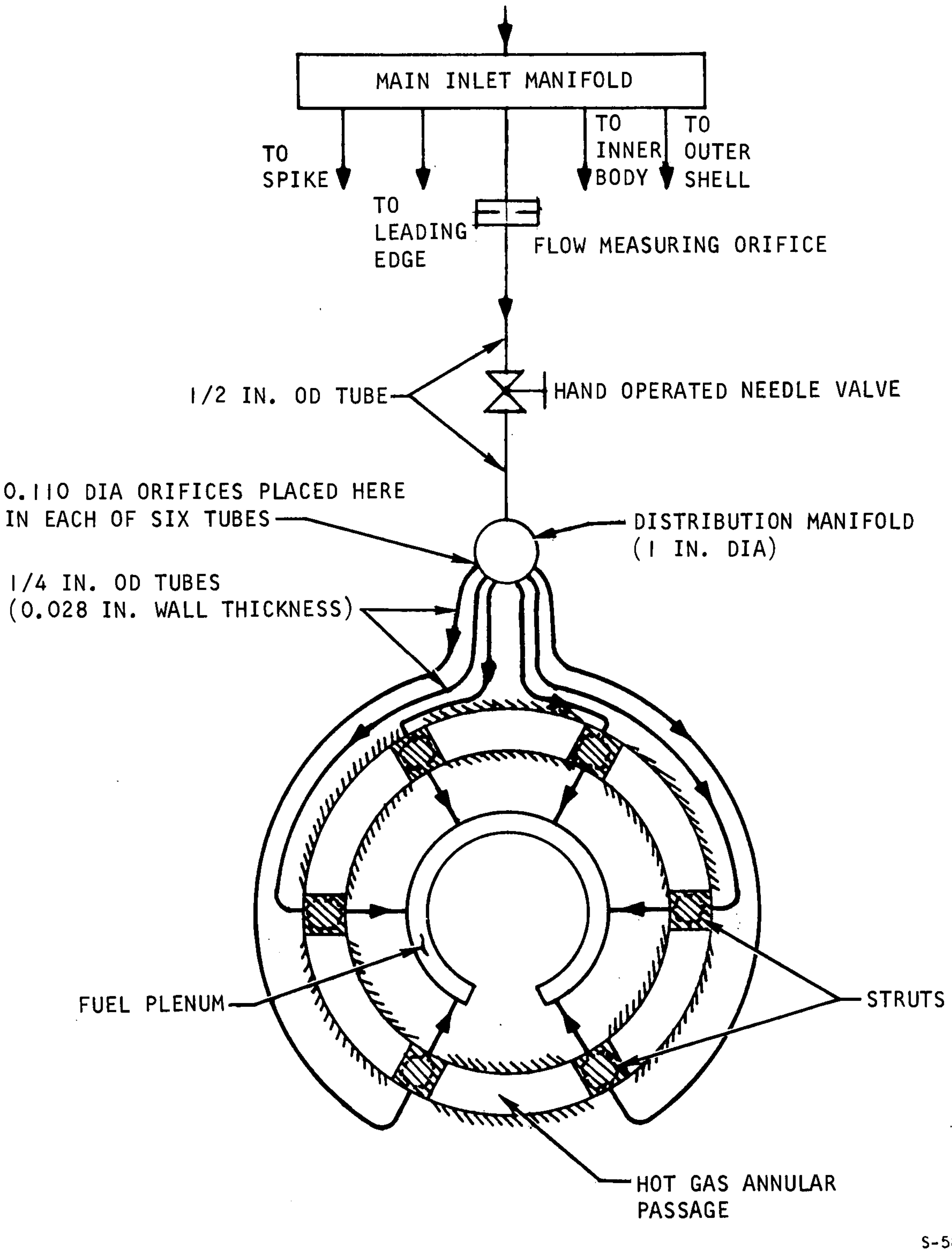

Figure 5.1-1. Modified Strut-Sides Coolant Routing

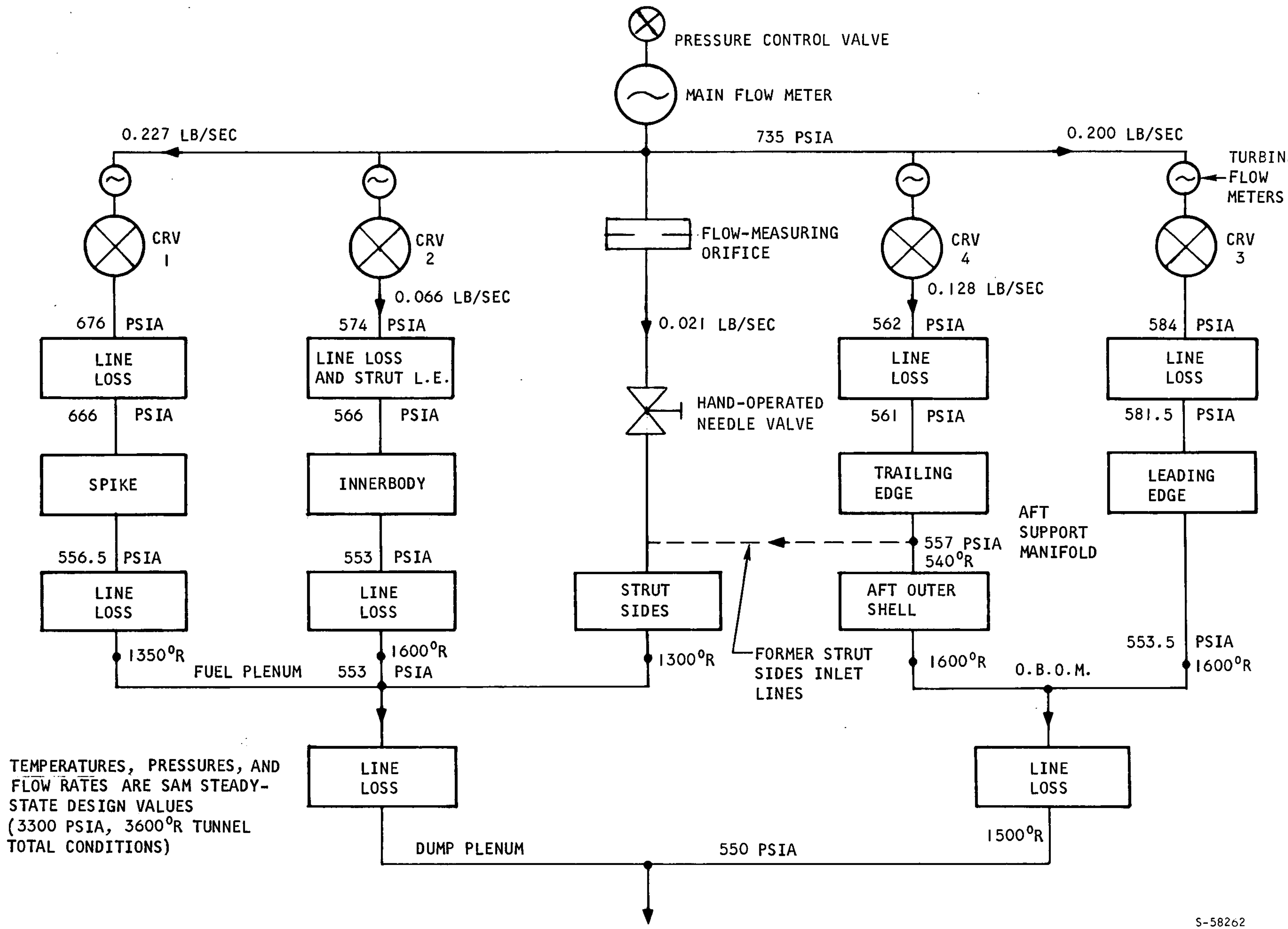

TEMPERATURES, PRESSURES, AND FLOW RATES ARE SAM STEADY-STATE DESIGN VALUES (3300 PSIA, 3600°R TUNNEL TOTAL CONDITIONS)

Figure 5.1-2. HRE/SAM Hydrogen Coolant Flow Schematic were not considered critical to engine thermal fatigue performance.

5.2 WIND TUNNEL TEST ERROR ANALYSIS

An error analysis was conducted as part of the SAM data evaluation program. Both measured parameters, such as temperature, pressures, and flowmeter frequency, and computed parameters, such as temperature differentials and heat loads, were considered. The calculation procedures being programmed for the SAM data reduction computer program were used for the error analysis of computed parameters. Additive errors were based on the square root of the sum of the squares of the individual errors. Figures 5.2-1 and 5.2-2 show the location of the SAM heat loads and flow routes which correspond to the error-results tables.

5.2.1 Instrumentation Accuracy

The probe-type thermocouples used in the SAM water circuits are accurate to $\pm 1^{o}$F. Hydrogen inlet temperature is sensed using platinum resistance probes which have an overall accuracy of $\pm 1^{o}$F in the temperature range of the tests. The SAM engine temperature control thermocouples were calibrated and have the following T/C calibration errors:

2.0^{o}F error at 1220^{o}F

1.0^{o}F error at 787^{o}F

0.5^{o}F error at 494^{o}F

The pressure transducers used for sensing engine static pressures are accurate to 0.5 percent of full scale. The four main hydrogen flow routes use turbine flowmeters for measuring hydrogen flow rates and are accurate to ± 1.5 percent of reading, including allowance for signal conditioning errors. The flow-measuring orifice in the strut-sides coolant circuit has an accuracy of better than ± 2.0 percent.

5.2.2 Heat Loads

Estimated errors in the hydrogen (coolant-side) heat loads for the various areas of the SAM engine are presented in Table 5.2-1. The first column lists the errors for tunnel total conditions of 3300 psia and 3600^{o}R (SAM design), and the second column presents the errors for tunnel conditions of 1350 psia and 2640^{o}R (SAM cycling). The notations in Table 5.2-1 correspond to Figure 5.2-1 and the errors shown represent the magnitude of uncertainty that will exist in the SAM coolant-side heat load reduced data.

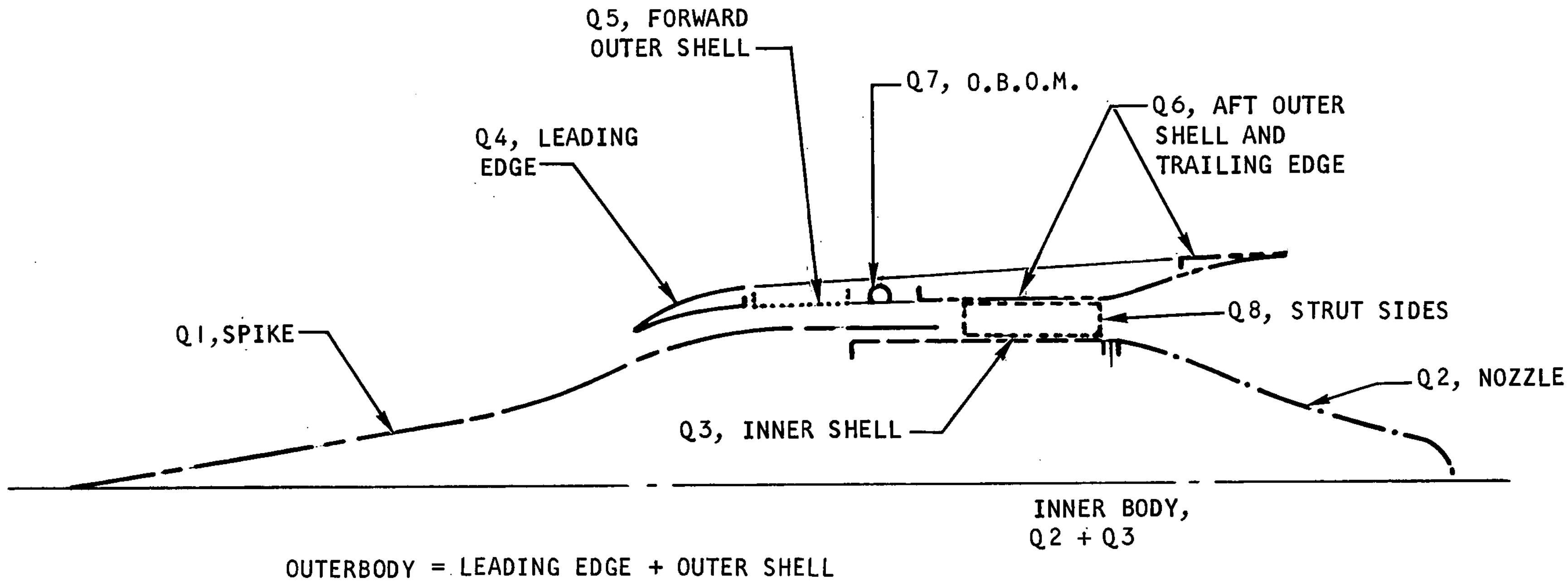

Figure 5.2-1. SAM Heat Load Designations

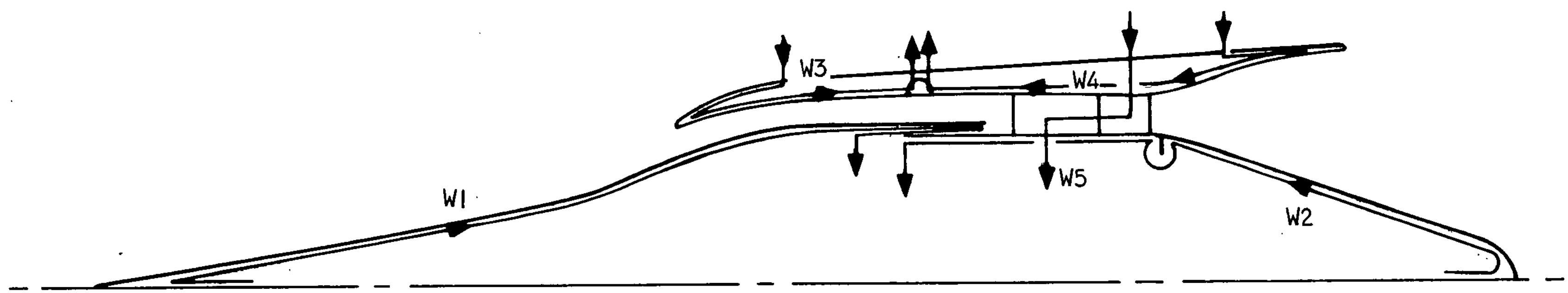

S-58585

Figure 5.2-2. Sam Hydrogen Flow Route Designations

TABLE 5.2-1

COOLANT-SIDE HEAT LOAD ERRORS

Coolant Route	Design Condition, ± percent	Cycling Condition, ± percent
Spike, Q1	4.2	7.2
Nozzle, Q2	8.0	11.9
Inner shell, Q3	7.8	11.8
Inner body, Q2+Q3	7.8	11.8
Leading edge, Q4	4.4	7.1
Forward outer shell, Q5	6.9	8.1
Aft outer shell and trailing edge, Q6	8.3	11.2
O.B.O.M., Q7	12.9	15.0
Strut sides, Q8	11.6	15.5
Entire SAM, Q9	7.9	11.0

Errors were also estimated for the heat loads on the water-cooled test adapters. Five water flow routes are used. Errors in the five water flow routes are all approximately the same; namely, ±6.4 percent. This ±6.4-percent error in heat load results from a ±5-percent error in water-flow rate (derived from a pressure drop calibration) and a ±4-percent error in water temperature difference. The results in the above analysis were based on the following assumptions:

(a) Magnitudes of the various parameters (Cp, T, W, Q, etc.) were taken from SAM design-point conditions (3300 psia and 3600°R)

(b) The cycling condition case was ratioed from the design case

(c) Flows in the various routes were assumed uniformly distributed

(d) Instrumentation accuracy of Section 5.2.1 was used

Error estimates for the hydrogen (coolant) flow rates for the SAM engine are presented in Table 5.2-2. The first column gives error values for indirect flow measurement using the experimental data from the SAM component air-pressure-drop tests which are reported in Section 8 of Reference 5-2. The second and third columns list the flow errors for the tunnel operating conditions based on direct-flow measurement using the flowmeters installed on SAM. The notations in Table 5.2-2 correspond to Figure 5.2-2.

TABLE 5.2-2

COOLANT-SIDE FLOW-RATE ERRORS

Coolant Route	Experimental, percent	Design, percent	Cycling, percent
Spike, W1	3.5	4.2	6.1
Nozzle, W2	4.9	6.6	10.2
Inner shell, W2	4.0	6.7	11.0
Leading edge, W3	6.7	4.0	6.0
Forward outer shell, W3	5.0	4.3	6.2
Trailing edge, W4	5.2	4.6	8.3
Struts, W5	7.0	2.0	2.0

The error values of column 1 in Table 5.2-2 assume $\rho\Delta p$ is exactly known and used to look up the flow rate in the test results ($\rho\Delta p$ versus flow rate). For purposes of data reduction, the uncertainty in the $\rho\Delta p$ results at most SAM operating conditions is too great to allow use of this method to determine component flow rates. Therefore, the flow rate errors in the second and third columns of Table 5.2-2 were used in evaluating the errors in coolant heat loads previously discussed. All the thermocouple errors were included in computing the errors in the coolant heat loads. Errors in temperature differences (hydrogen outlet minus hydrogen inlet) for the SAM coolant heat loads were usually less than 2.5 percent and are presented in Table 5.2-3. No correction for hydrogen thermocouple errors is planned for inclusion in the SAM data reduction program.

TABLE 5.2-3

HYDROGEN ΔT ERRORS

Coolant Route	Approximate ΔT, ^{o}R	Error, ± percent
Spike	1040	1.4
Nozzle	240	2.5
Inner shell	1140	1.4
Inner body	1140	1.4
Leading edge	640	1.6
Forward outer shell	400	5.5
O.B.O.M.	850	3.6
Aft outer shell	800	2.1
Trailing edge	240	2.5
Strut sides	1100	2.1

5.2.3 Heat Transfer Coefficients

Gas side aerodynamic heating will be evaluated by balancing the heat loads between the coolant and gas sides. Errors were computed for the gas side heat transfer coefficients using the coolant heat loads and the recovery-to-wall temperature differences. This analysis resulted in an estimated error in gas side coefficient of ±9 percent for the SAM design condition and of ±13.2 percent for the SAM cycling condition in the wind tunnel.

5.2.4 Metal Temperatures

Errors in measurement of metal temperatures on SAM result from radiation, conduction, and convection. Thermocouple errors were checked for the specific thermocouple installations used in the SAM engine. They are expected to be about one percent of the thermocouple reading for all SAM installations except for the insert type of installation used for measuring the hot wall temperature. Hot wall temperatures are expected to be in error by about two percent of the thermocouple reading. This results because the thermocouple mount surface temperature may vary by as much as ten percent from the actual surface temperature because of installation tolerances. This ten-percent error can be corrected analytically to about one percent and results in a total thermocouple error of two percent for the hot wall temperature measurements. The procedure for correcting hot wall temperature measurements will be included in the SAM data reduction program.

5.3 TEMPERATURE/PRESSURE CONTROL SYSTEMS

Previous analysis of the HRE temperature and pressure controls indicated interaction instability can exist under various operating conditions, when individual control response frequencies are of similar magnitudes. Networks may be added to provide stability compensation; however, the fixed parameters of the networks are very dependent upon individual test conditions and control response characteristics which vary greatly under various test conditions. For this reason, it was determined necessary to increase the frequency response of the pressure control valve sufficiently to eliminate this interaction.

5.3.1 System Configuration

The control system was changed to a high response electromechanical servovalve with an electronic control and sensor. The servomotor is a very low-inertia motor (printed circuit armature) which can develop high accelerating torques. The valve element is a low-friction ball that was retained from the previous pneumatically actuated controller.

The open-loop response of the control, including the control electronics and feedback potentiometer, was determined by testing, to be nearly that of a second-order system with a natural frequency of 25 Hz and a damping factor of 0.1 (see also Section 8.1). The low damping factor results from the low inertia and small viscous damping inherent in the servomotor and ball valve.

5.3.2 System Simulation

The analog simulation was changed to reflect the new pressure control.

Hysteresis and dead-band effects were determined as negligible in the valve tests, so were not considered in the simulation.

5.3.3 Computer Run Conditions

Conditions were run on the computer corresponding to heat loads of 100 percent, 50 percent, and 25 percent of the tunnel design conditions. The 100 percent point is for a steady-state hydrogen flow of approximately 0.62 lb-sec. These conditions were run for inlet temperatures of 200^0R and 530^0R.

5.3.4 Computer Results

To achieve optimum control for test measurement (i.e., minimize pressure or flow fluctuations) it was found some additional damping was required in the servo control. The damping factor was increased to 0.5 by adding a capacitor in parallel with the feedback potentiometer summing resistor.

Computer traces of the system for the various run conditions with the increased damping are shown in Figures 5.3-1, 5.3-2, and 5.3-3. Performance indicated by these traces is considered satisfactory.

INPUT DISTURBANCE: APPROX ±15% FDV AREA 530°R

INLET TEMP: 200°R

HEAT LOAD: 100%

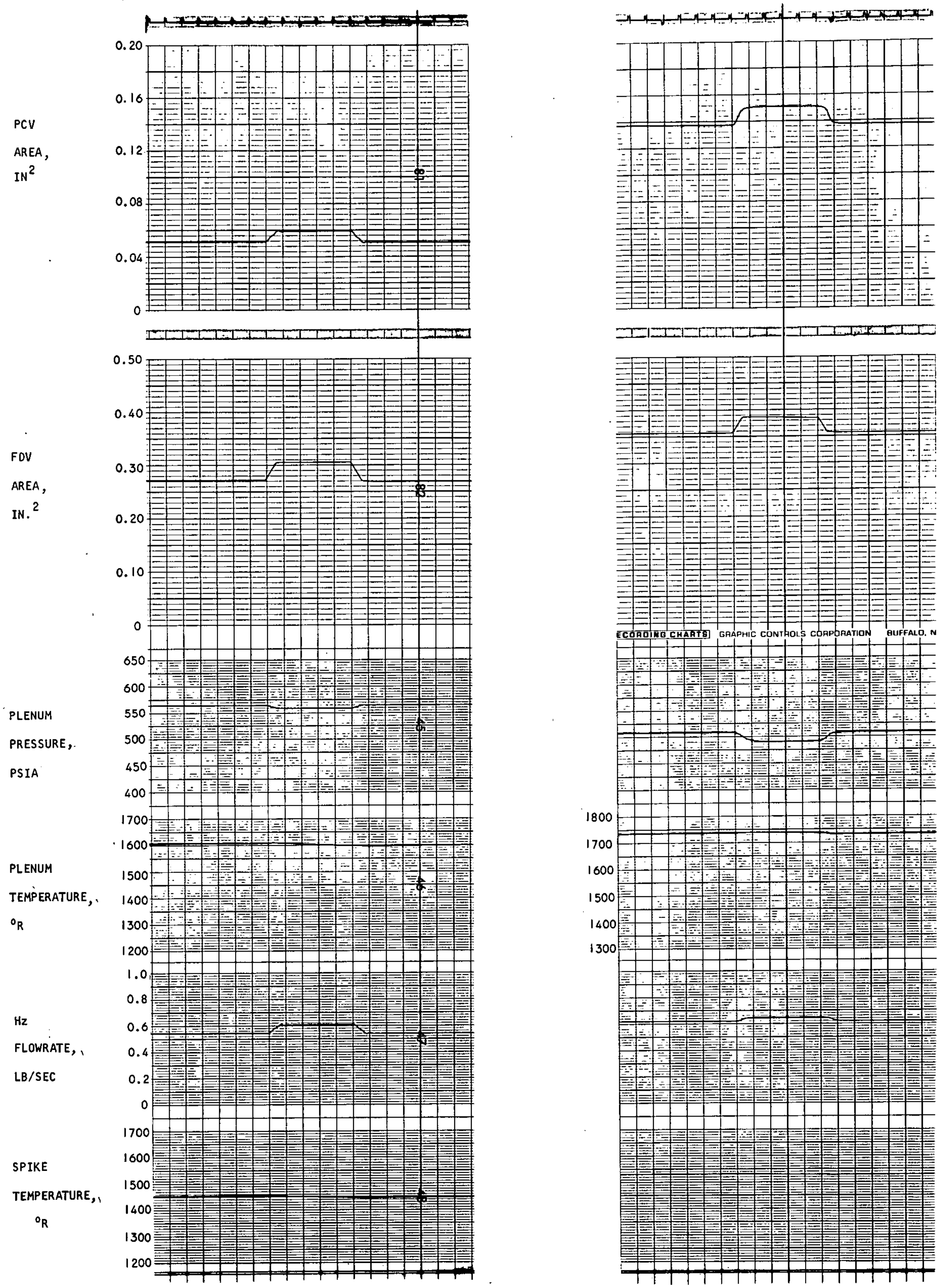

S-58469

Figure 5.3-1. Computer Run for HRE/SAM Temperature/Pressure Control System (100 Percent Heat Load)

INPUT DISTURBANCE: APPROX ±15% FDV AREA 530°R
INLET TEMP: 200°R
HEAT LOAD 50%

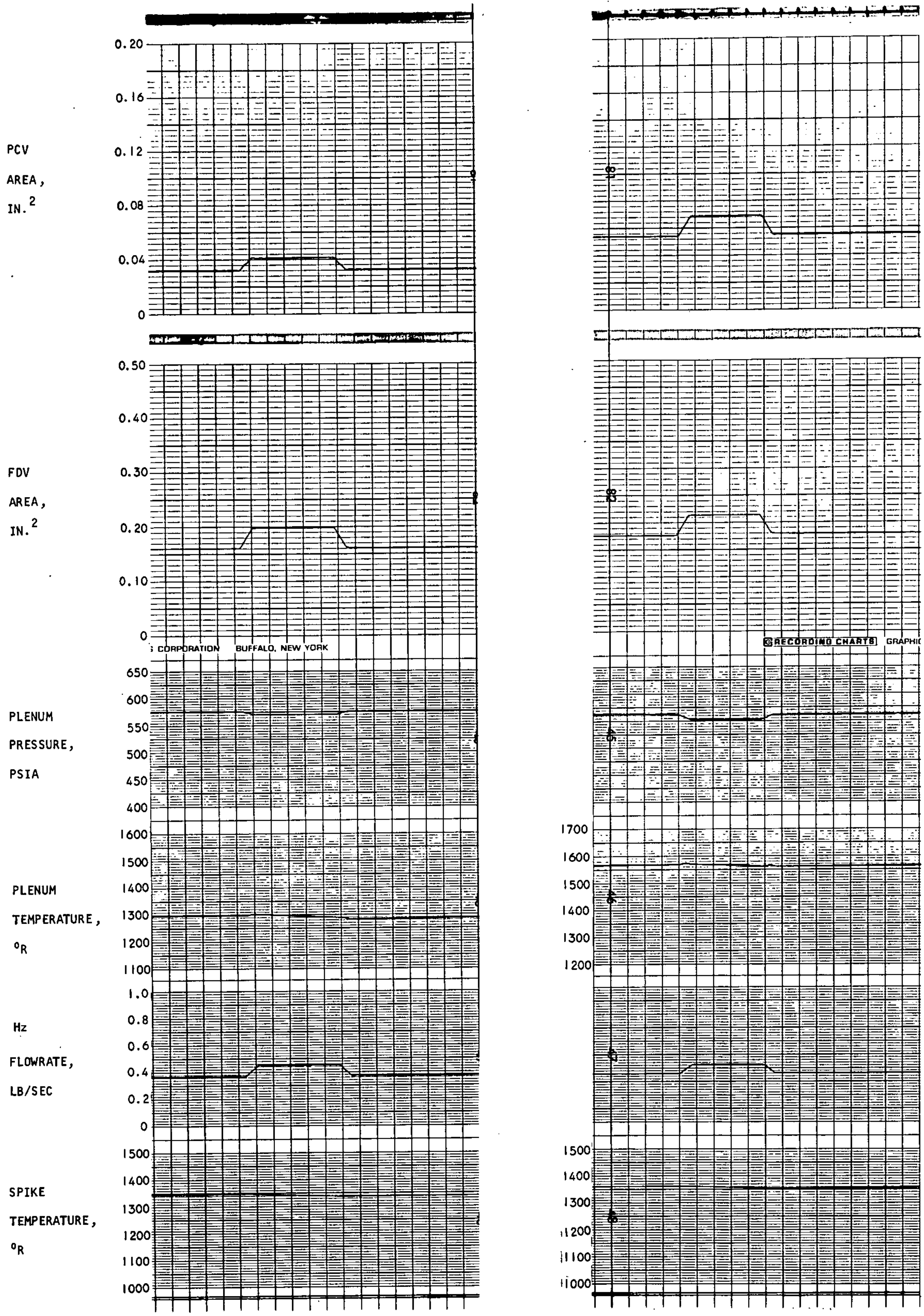

S-58470

Figure 5.3-2. Computer Run for HRE/SAM Temperature/Pressure Control System (50 Percent Heat Load)

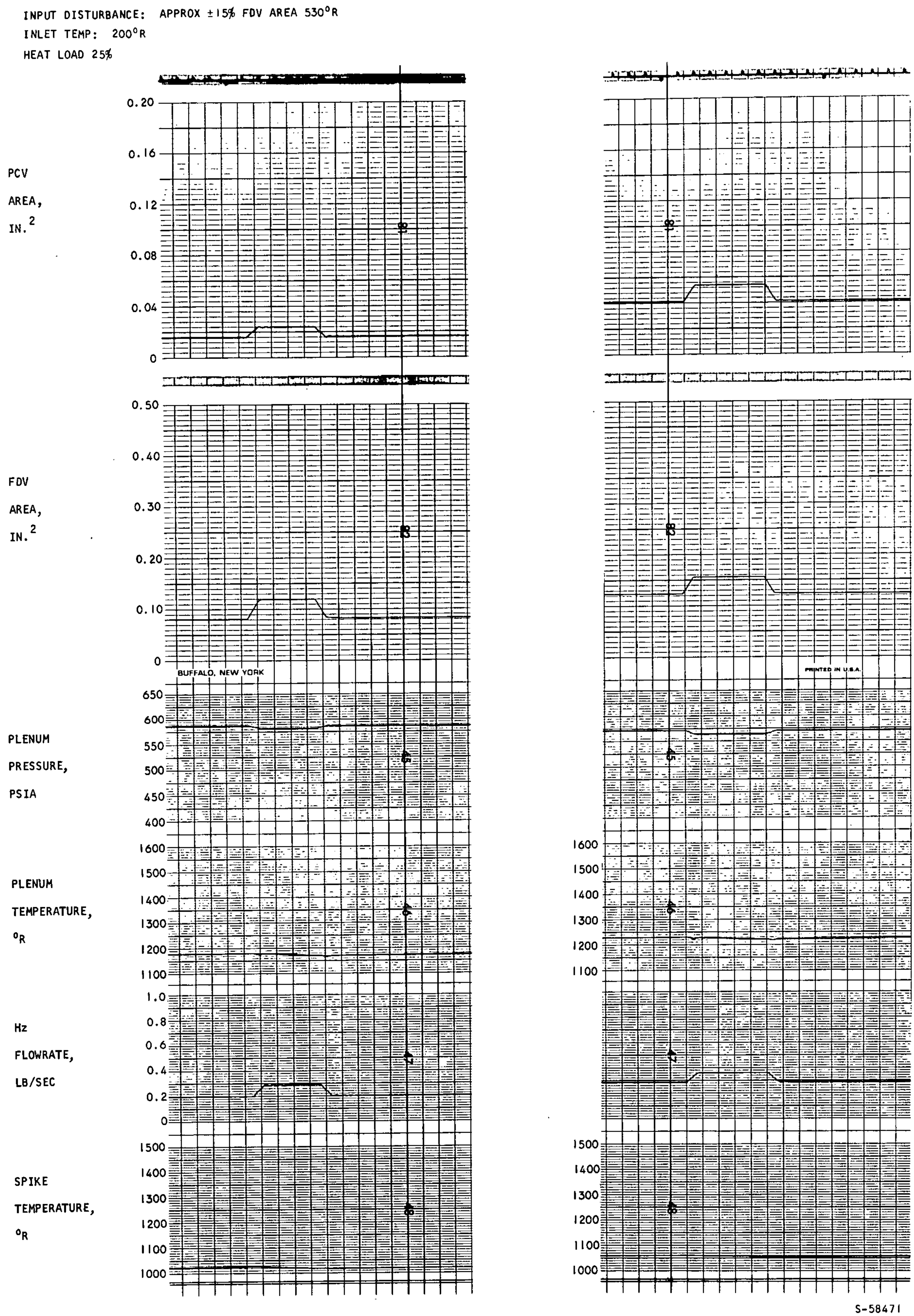

Figure 5.3-3. Computer Run for HRE/SAM Temperature/Pressure Control System (25 Percent Heat Load)

6. DESIGN EFFORT

All design activity has been completed. Drawings have been updated to reflect modifications introduced during assembly of the components. The design of the pressure control valve is based on the use of commercial parts. The mechanical details of this valve are described in the following section. The performance of the valve and its associated controls is discussed in Section 5 as part of the analog simulation.

7. MANUFACTURING

All manufacturing effort has been completed. During the reporting period this effort has involved assembly operations, primarily. The specific areas of work are discussed in the following sections.

Figure 7.0-1 shows the nomenclature used for the major components of the SAM.

7.1 ENGINE ASSEMBLY

The assembly of the various hydrogen-cooled components of the SAM, shown in Figure 7.0-1, is performed in a specific sequence to permit proper alignment and joining of the complex plumbing. The major assembly milestones required are, in chronological order:

(a) Alignment of inner shell assembly and outer shell, and final machining of struts

(b) Alignment of outer shell and leading edge

(c) Alignment of actuator with inner shell, and machining for dowel pins

(d) Final assembly of inner and outer shells and plumbing

(e) Installation of suspension frame, spike, and spike actuator

(f) Assembly and plumbing of leading edge

(g) Installation of nozzle

During the reporting period, the final three of the milestones listed above were completed and the engine assembly was connected to the fuel/coolant manifolding to make up the final SAM assembly.

7.1.1 Installation of Suspension Frame, Spike, and Spike Actuator

The operations prior to installation of the suspension frame, spike, and spike actuator were described in the Thirteenth Interim Technical Data Report (AP-70-6202).

Installation of the suspension frame, made while the assembly was still mounted on the yoke-type fixture, consisted of attachment of the aft support pads to the engine mounts with eight bolts, and installation of the 3/4-in.-dia pin in the yoke and brackets at the forward end.

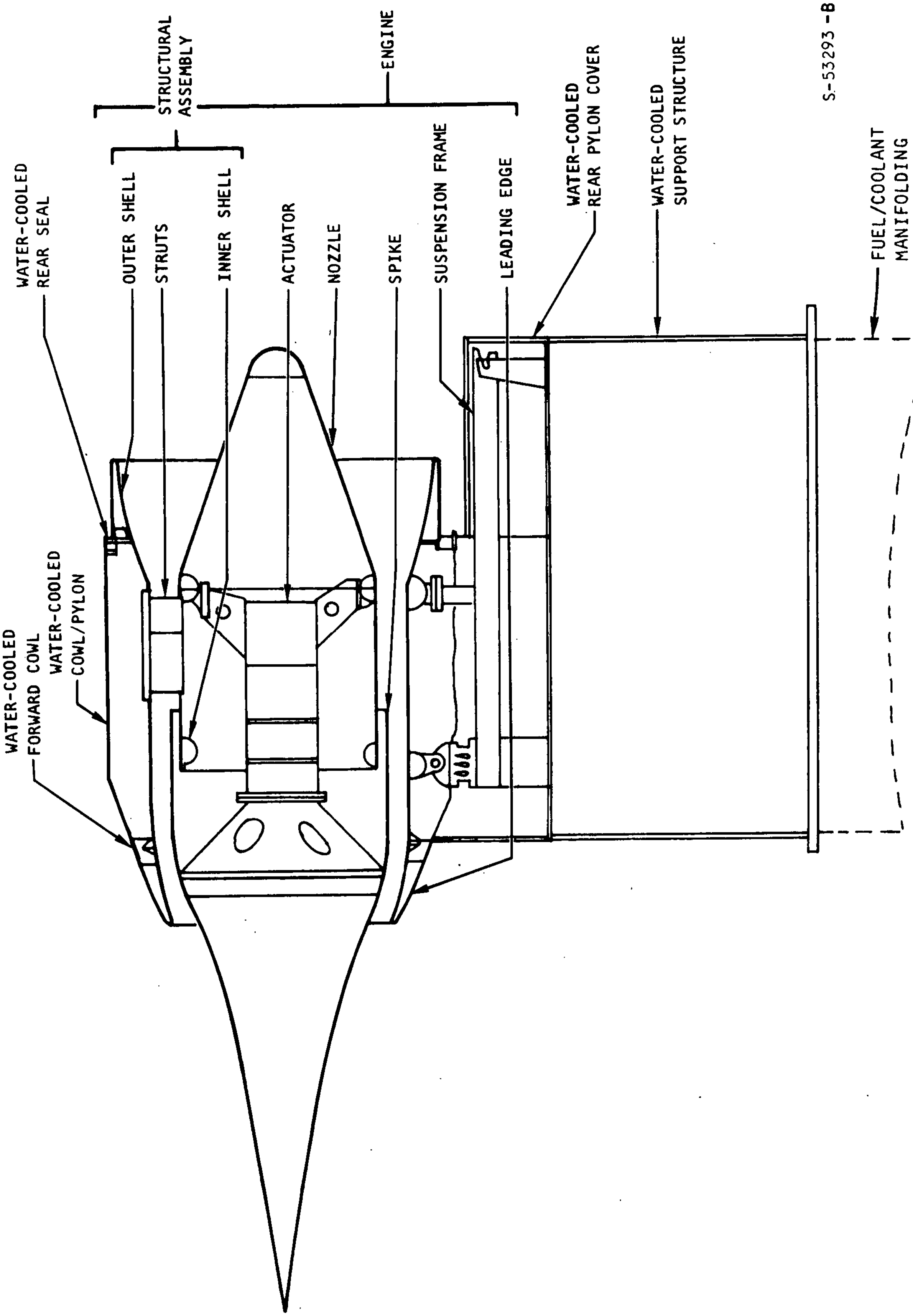

Figure 7.0-1. SAM Components

The unit was then transferred from the yoke fixture to a large, box-frame, tumble fixture, which provided more clearance and positional flexibility, and was positioned with its axis vertical, as shown by Figure 7.1-1.

A dry run installation of spike, actuator, and leading edge was then made, with the packing-type seals, between the spike and inner shell, in place, to confirm concentricity of the components and make final adjustments on tube lengths and fits at the three bellows connections between the spike and inner body.

The final installation of the spike was then performed using the following sequence of operations:

(a) Raising the spike into position corresponding to maximum extension of the actuator, with the large bellows clamped in a compressed position.

(b) Tightening the screws on the packing gland between spike and inner shell by inserting the wrench in the annular gap between the large bellows and the inner shell.

(c) Removing clamps from the large bellows and bolting the large bellows flange to its matching face on the inner body.

(d) Induction brazing the connections between the three small bellows in the spike and the corresponding tubes in the inner shell, and leak-testing the joints.

(e) Insulating tubes and cables.

(f) Lowering the actuator (retracted) into place and bolting to the inner shell, then extending the actuator and bolting it to the spike.

(g) Checking actuator operation and the concentricity of the spike relative to the inner shell.

The arrangement of the unit in the fixture during the above operations is illustrated in Figure 7.1-1.

7.1.2 Assembly and Plumbing of Leading Edge

Following installation and checkout of the spike, the fixture was rotated so as to place the engine axis horizontal for installation of the leading edge assembly. A clamp ring was used to ensure alignment of the flanges and inner surfaces during bolting of the leading edge to the outer shell. The eight 3/8-in.-dia inlet tubes and twenty-four 1/4-in.-dia crossover tubes were then induction-brazed and leak-tested to produce a configuration shown by Figure 7.1-2.

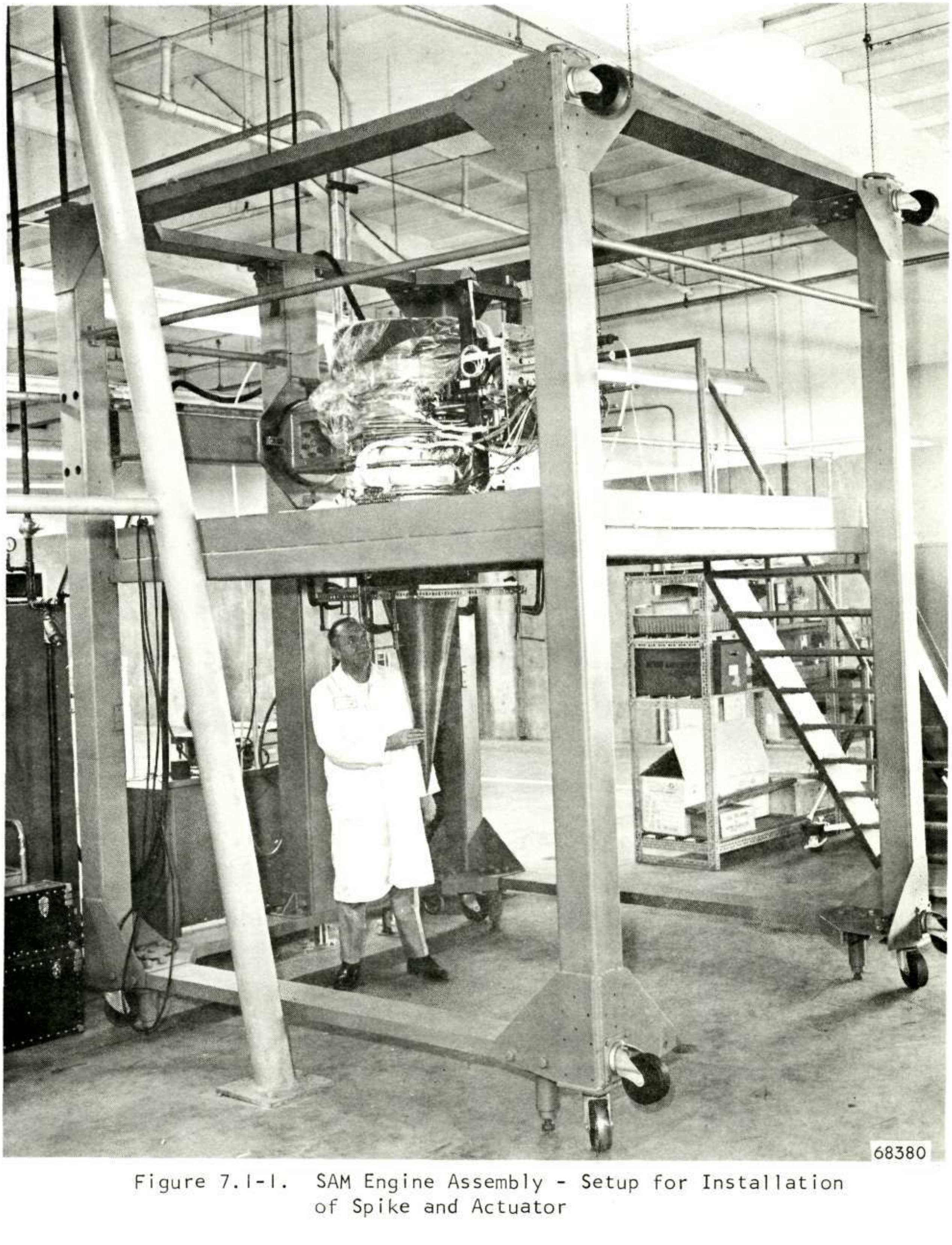

Figure 7.1-1. SAM Engine Assembly - Setup for Installation of Spike and Actuator

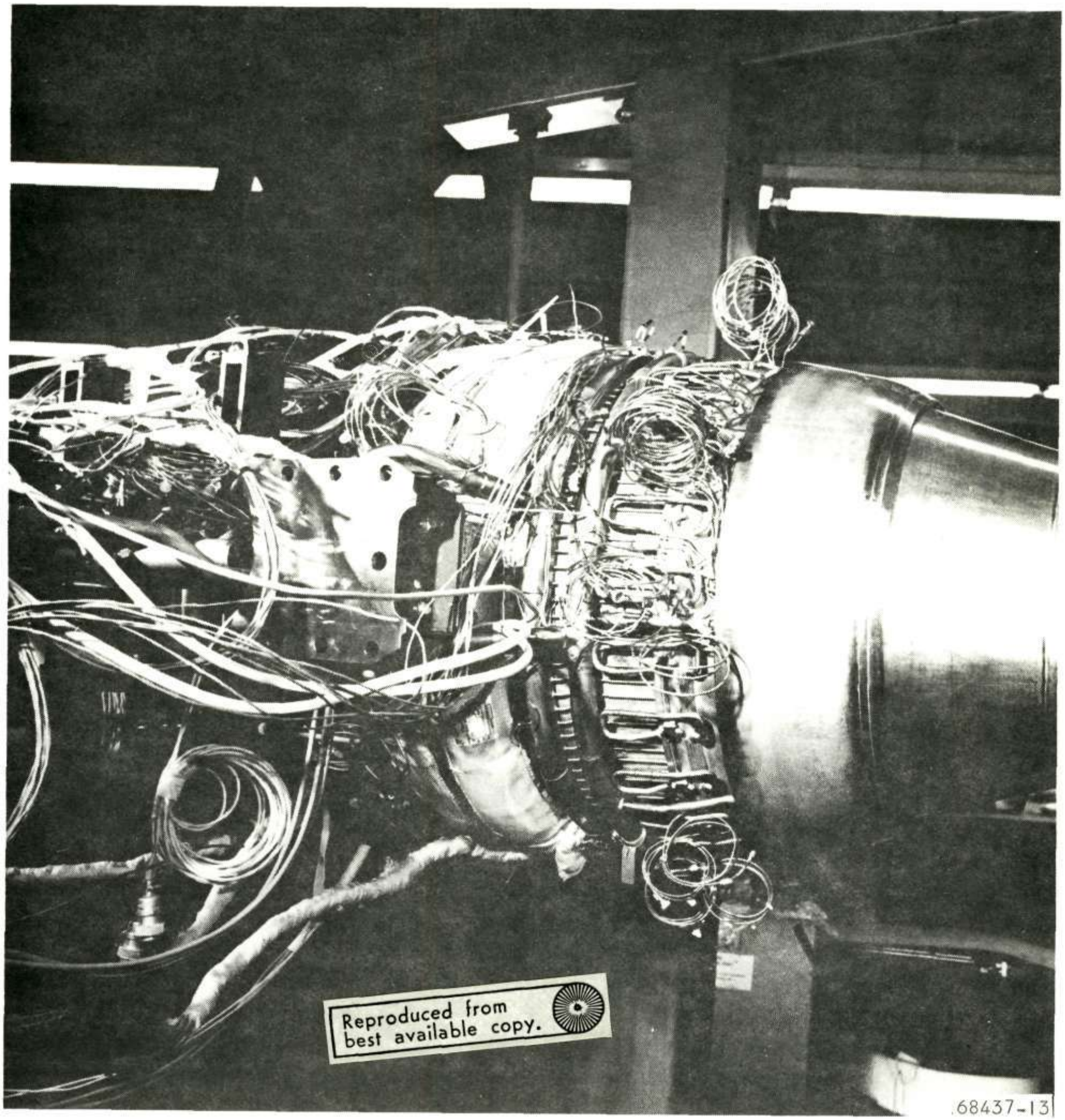

68437-13

Figure 7.1-2. SAM Engine Assembly - Detail of Leading Edge Showing Inlet and Crossover Tubes

7.1.3 Installation of Nozzle

Before the nozzle could be bolted in place, it was necessary to install the manifold which connected the six strut leading edges to the inlet (aft) end of the nozzle. This manifold, in place, is shown in Figure 7.1-3. Also, before bolting the nozzle in place, the six pressure taps which sense air pressure on the surface of the nozzle, were connected to pressure transducers mounted in a housing as shown by Figure 7.1-4. The actual attachment of the nozzle to the inner shell assembly consisted of a series of operations performed while the nozzle was being brought into place for bolting. While in the position shown by Figure 7.1-5, the thermocouple and pressure transducer cable assemblies were first connected, clamped in place, and insulated. Then ten "Omniseals" were installed in the pockets in the nozzle flange, and the nozzle was lined up and bolted to the inner shell. Installation and bolting of the inner cover assembly with its "Omniseals" followed, and then the inner deflector was screwed in place. Finally, the outer cap with its "Omniseal" was screwed on and torqued with a special spanner wrench as shown in Figure 7.1-6. The installation of the bolt and metallic seal in the extreme aft end of the nozzle completed the assembly. After the nozzle was installed, the coolant system was pressurized with helium at 100 psig and a mass spectrometer "sniffer" was applied at all of the seal joints to detect leakage; none was detectable.

7.2 SAM ASSEMBLY

The major assembly milestones required to complete the SAM were:

(a) Installation of bulkhead

(b) Installation of cowl/pylon

(c) Assembly of support wedge

(d) Fitup and connection to fuel/coolant manifolding

The installation of the bulkhead required a series of relatively major operations. The first group, performed with the engine axis horizontal, tubes pointing downward as shown in Figure 7.2-1, accomplished the emplacement of the bulkhead assembly (Figure 7.2-1), the routing of all of the pressure connection tubes (approximately 70) through the correct holes in the bulkhead, and the induction brazing of extension tubes to each of these. Also, all of the cable assemblies (thermocouple, accelerometer, and strain gage) were routed through their allotted holes in the bulkhead and secured. After these operations were completed, the assembly was installed on a stand as shown in Figure 7.2-2 for additional operations. The water tubes for connection to the cowl/pylon were put through the bulkhead for the first time at this point, then the cowl/pylon was slipped into place around the outer shell using a special yoke for support, as shown in Figure 7.2-3. The water pipes through the bulkhead were connected to the pylon, the cowl body was centered relative to the outer shell, and four bolt holes were drilled, reamed, and countersunk in the pylon and matching pads on the suspension frame assembly. After this operation, the cowl/pylon was removed and the bellows used to seal the tubes to the bulkhead were welded to

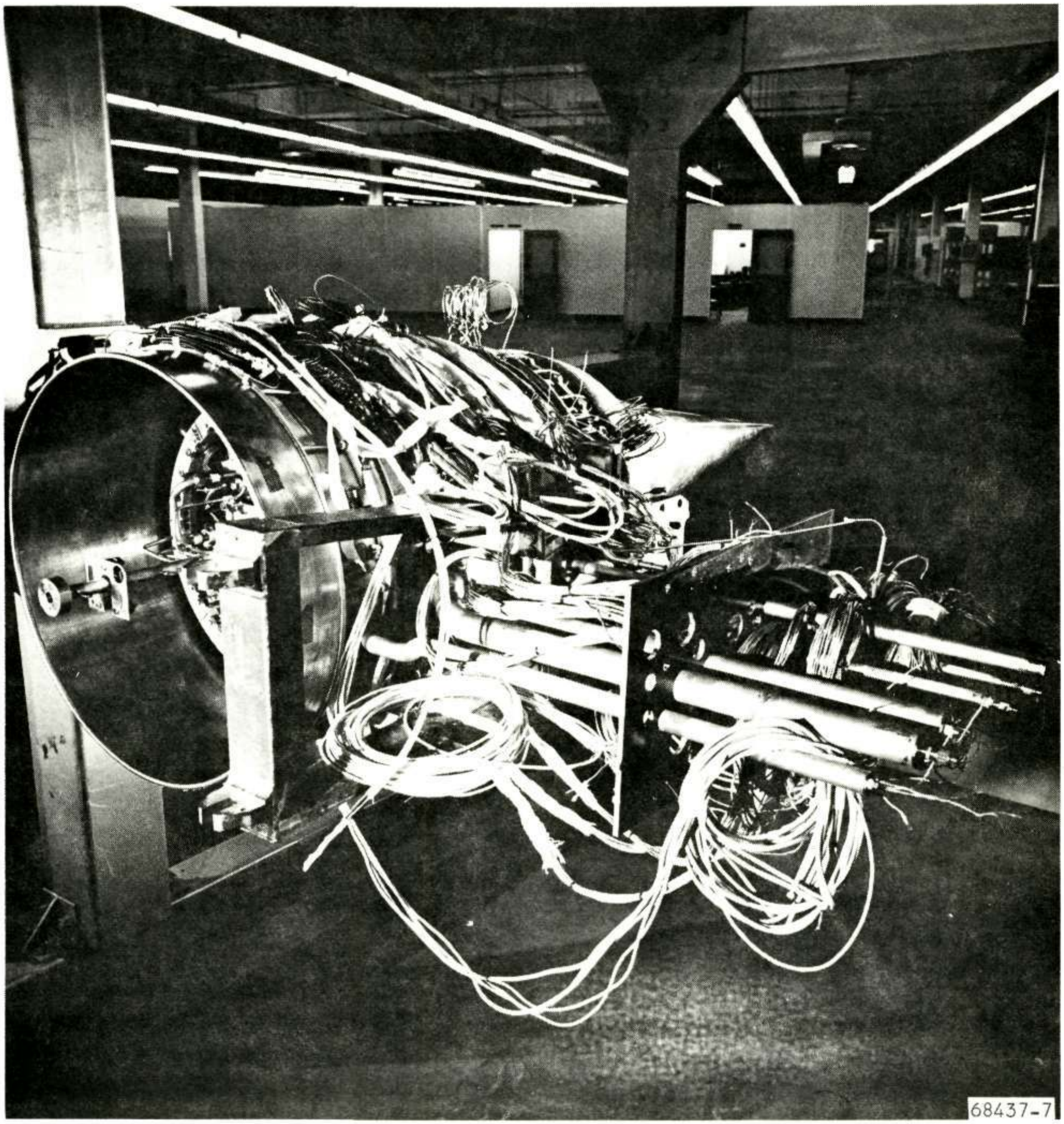

Figure 7.1-3. SAM Engine Assembly - View Into Aft End Showing Strut Leading Edge Coolant Outlet Manifold

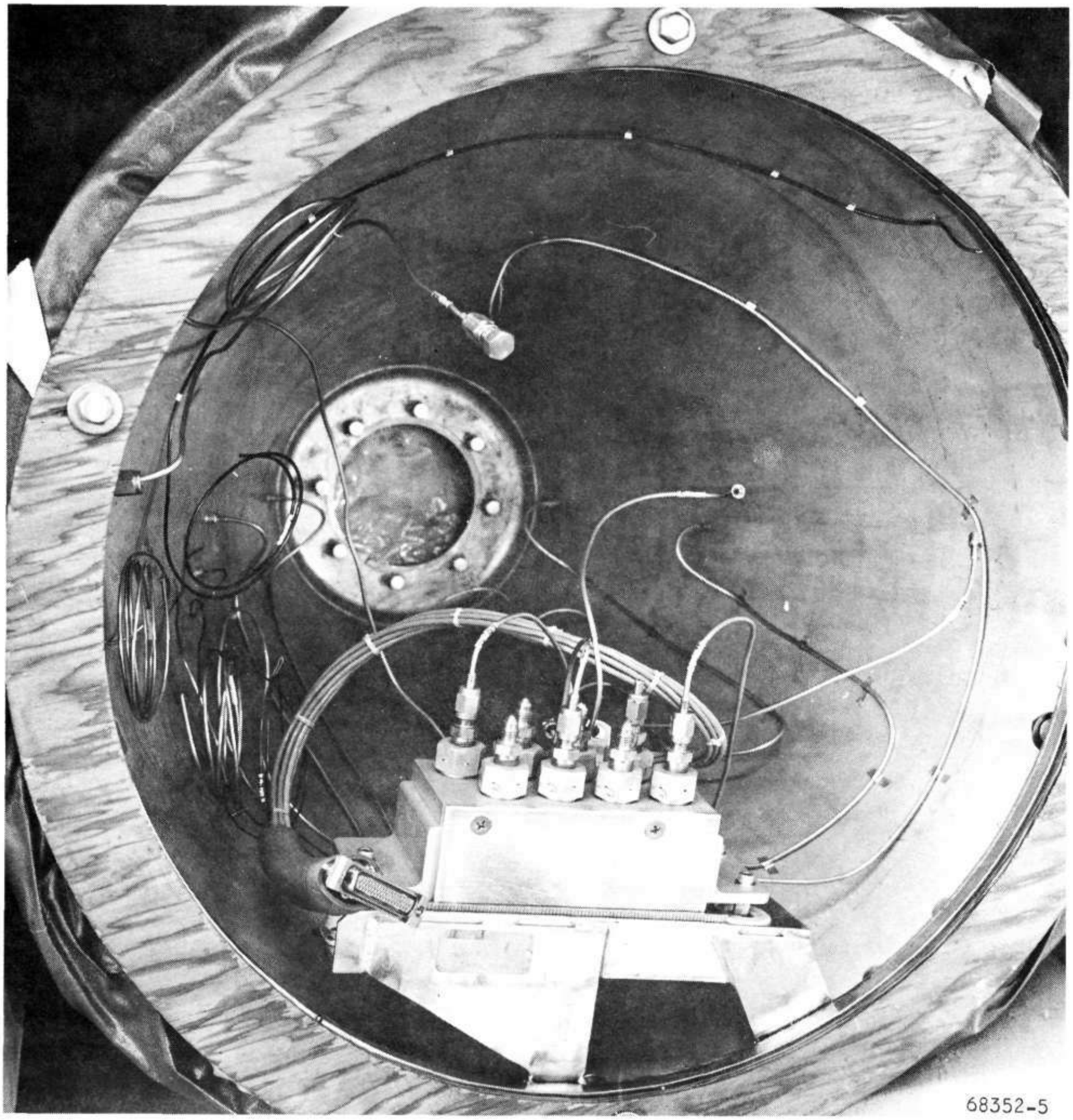

68352-5

Figure 7.1-4. Aft Nozzle Assembly Showing Transducer Housing and Cable

Figure 7.1-5. SAM Engine Assembly - Nozzle In Place for Connection of Cable Assemblies

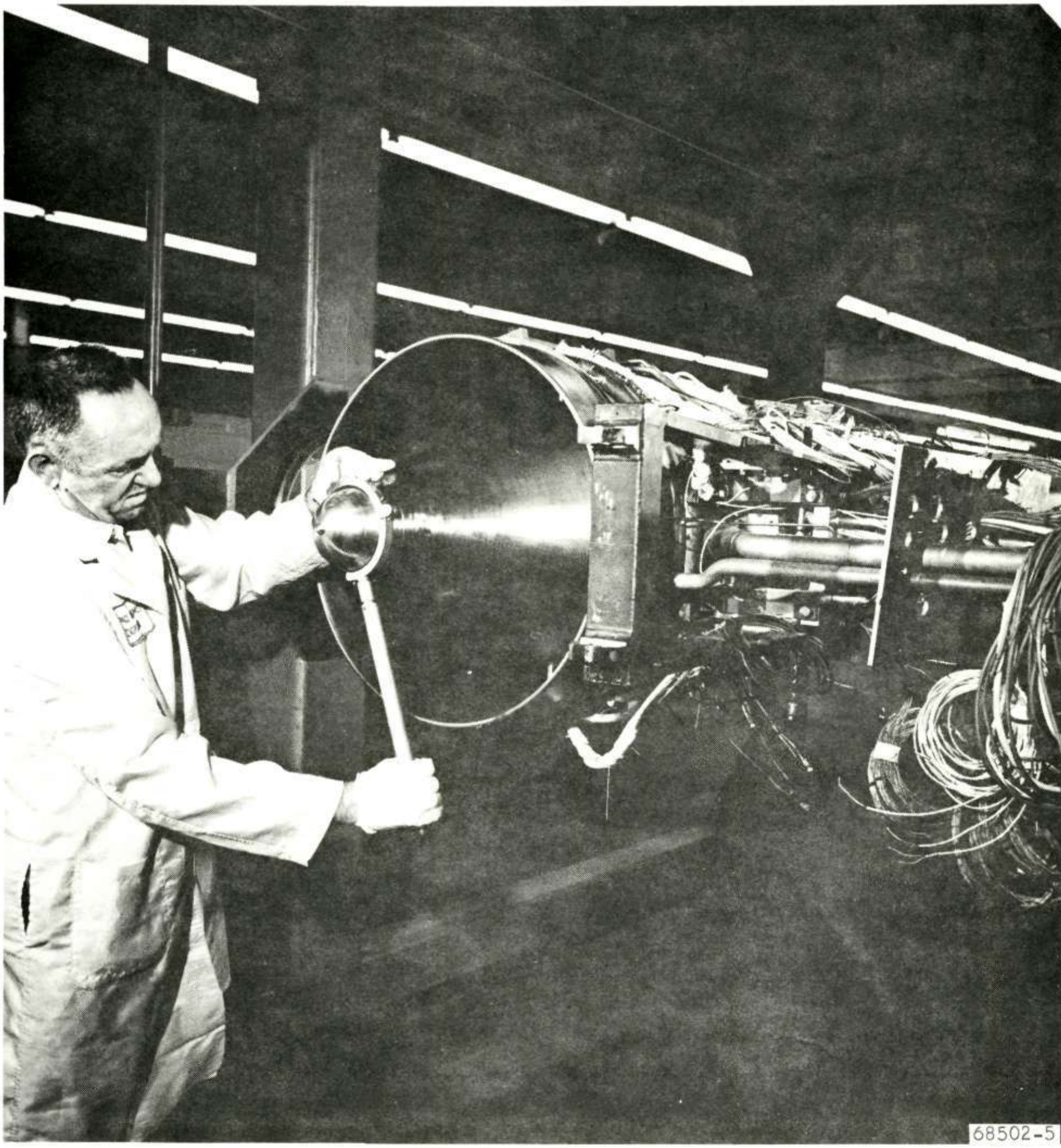

Figure 7.1-6. SAM Engine Assembly - Torqueing of Outer Cap on Nozzle

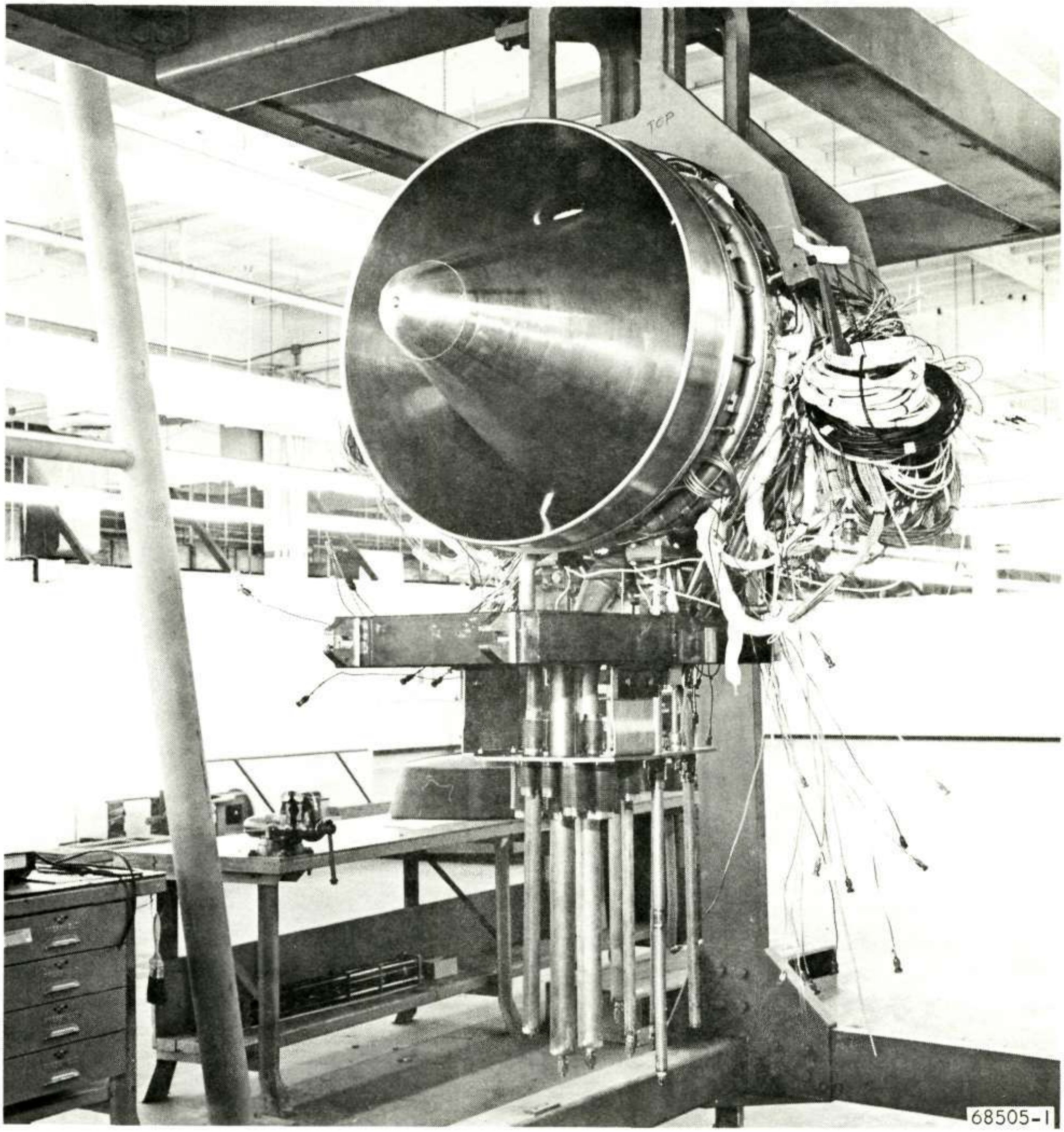

Figure 7.2-1. SAM Engine Assembly Mounted in Position for Routing of Tubes and Cables Through Bulkhead

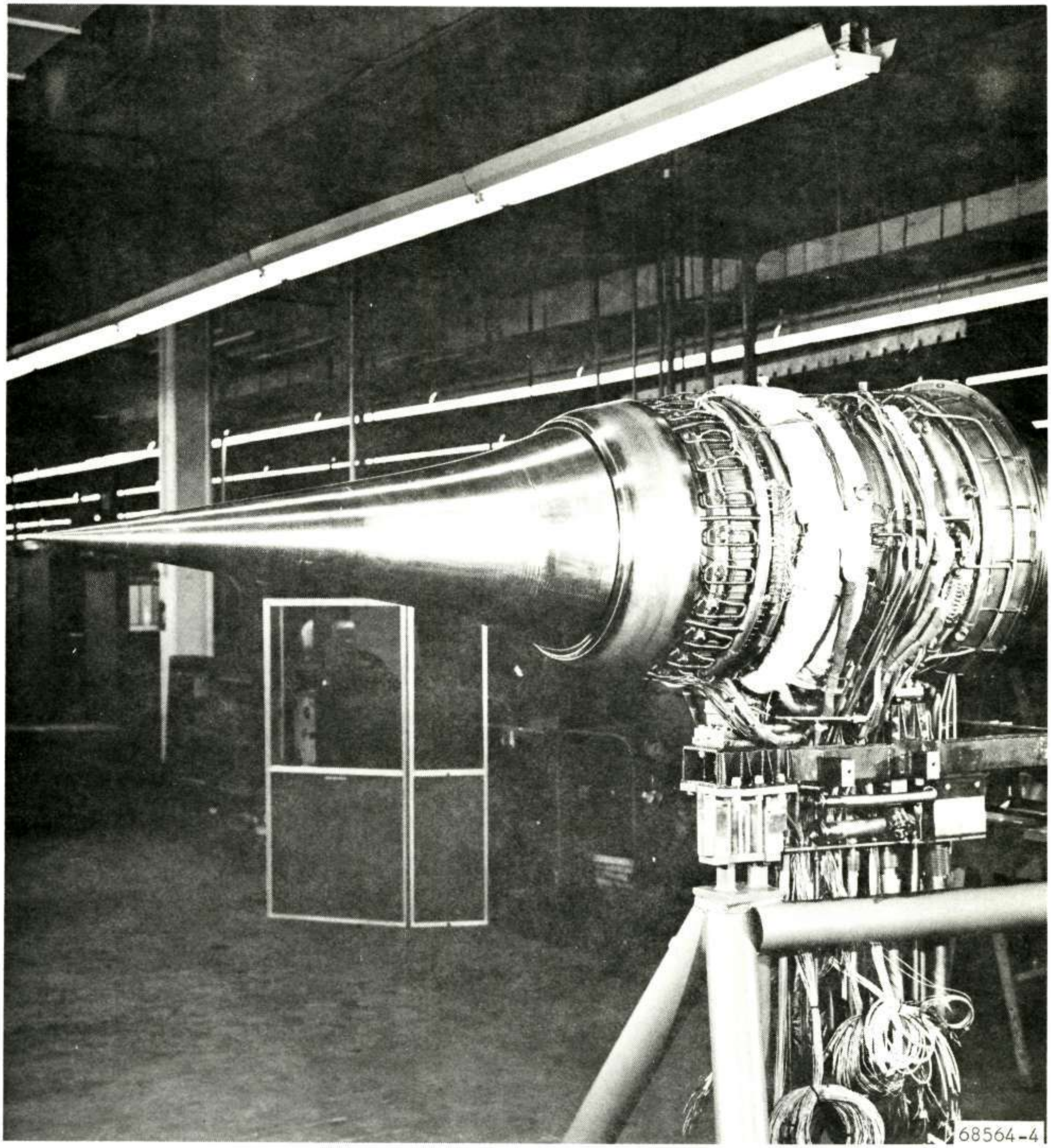

Figure 7.2-2. SAM Engine Assembly Mounted on Stand for Bulkhead Installation Operations

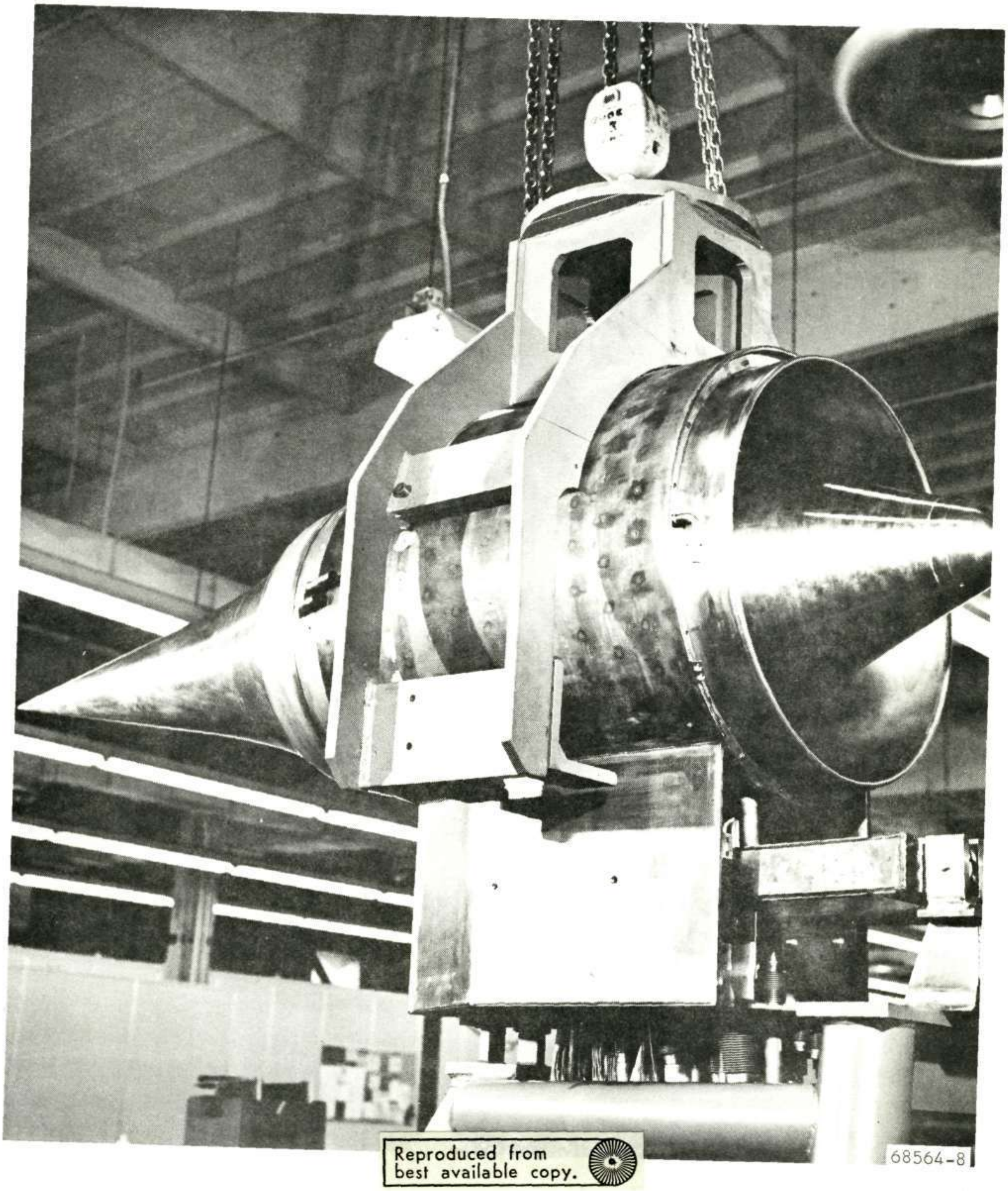

Figure 7.2-3. SAM Engine Assembly - Setup for Fitup of Cowl Pylon to Engine, and Machining of Bolt Holes Into Suspension Frame Assembly

the tubes. Three bellows were welded in the position shown in Figure 7.2-3 and the balance (15) were welded after reinstalling the assembly in the tumble fixture and rotating it to position the tubes pointing upward.

The unit was next re-mounted on the stand and the outer shell was insulated with a blanket of "Refrasil" approximately 1/4-in. thick and an outer membrane of silicone-impregnated fiberglas cloth. Then the cowl pylon, the aft sealing ring, and forward panel were permanently installed with their silicone O-rings in place. The aft pylon cover, with its seals, was then installed, and all of the water connections to the cowl/pylon, forward panel, and aft sealing ring were secured.

The next group of operations consisted of the fitup and connection of all of the tubes between the engine and fuel/coolant manifolding. First the suspension yoke was attached to the cowl/pylon assembly and a table-type fixture of the same height as the support wedge was bolted to the bottom of the unit, after which the matching tubes on the engine and manifold were all trimmed to the correct length for use of tubular couplings and induction brazing. The engine was lowered onto the manifold assembly, as shown in Figure 7.2-4, where all tubes were fitted and any misalignments corrected. To facilitate the sealing of the tube joints, all of the couplings were first T/G lap-welded to the manifold tubes in inert atmosphere bubbles, then the units were re-assembled, and the joints between the couplings and engine tubes were induction brazed in an argon atmosphere with Nioro filler wire. After this operation, all of the joints were leak-tested; those in the hydrogen circuits at 700 psig and those in the water circuits at 100 psig.

The final group of operations covered the mechanical assembly of the remaining components. First the locating jig under the cowl/pylon was removed and the unit was lowered onto the support wedge, Figure 7.2-5, and bolted into place, Figure 7.2-6. The engine assembly as shown in Figure 7.2-6 was used by itself for calibration testing of the spike actuator.

The general appearance of the completed SAM unit is shown by Figure 7.2-7.

7.3 FUEL/COOLANT MANIFOLDING

Figure 7.2-7 shows the completed fuel/coolant manifold assembly with the engine in place on top of the base plate. The coolant inlet and outlet lines, turbine flowmeters, coolant regulating valves (above flowmeters), the two by-pass valves at the forward end of the manifold assembly, and the two fuel dump valves on the aft end of the manifold assembly can be seen in this figure. The inlet flange for the high pressure water system is visible above the by-pass valve and the outlet lines for the high pressure system, as well as the inlet and outlet lines for the low pressure water system, are not installed at this point. They were removed for installation of the engine assembly. The nitrogen purge inlet manifold (2-in. half-coupling) for the two nitrogen circuits is located just below the base plate, at a point forward of the coolant outlet line.

Figure 7.3-1 shows the fuel/coolant manifold assembly as viewed from the aft end. The "Annin" valve on the left of the figure is one of the fuel dump

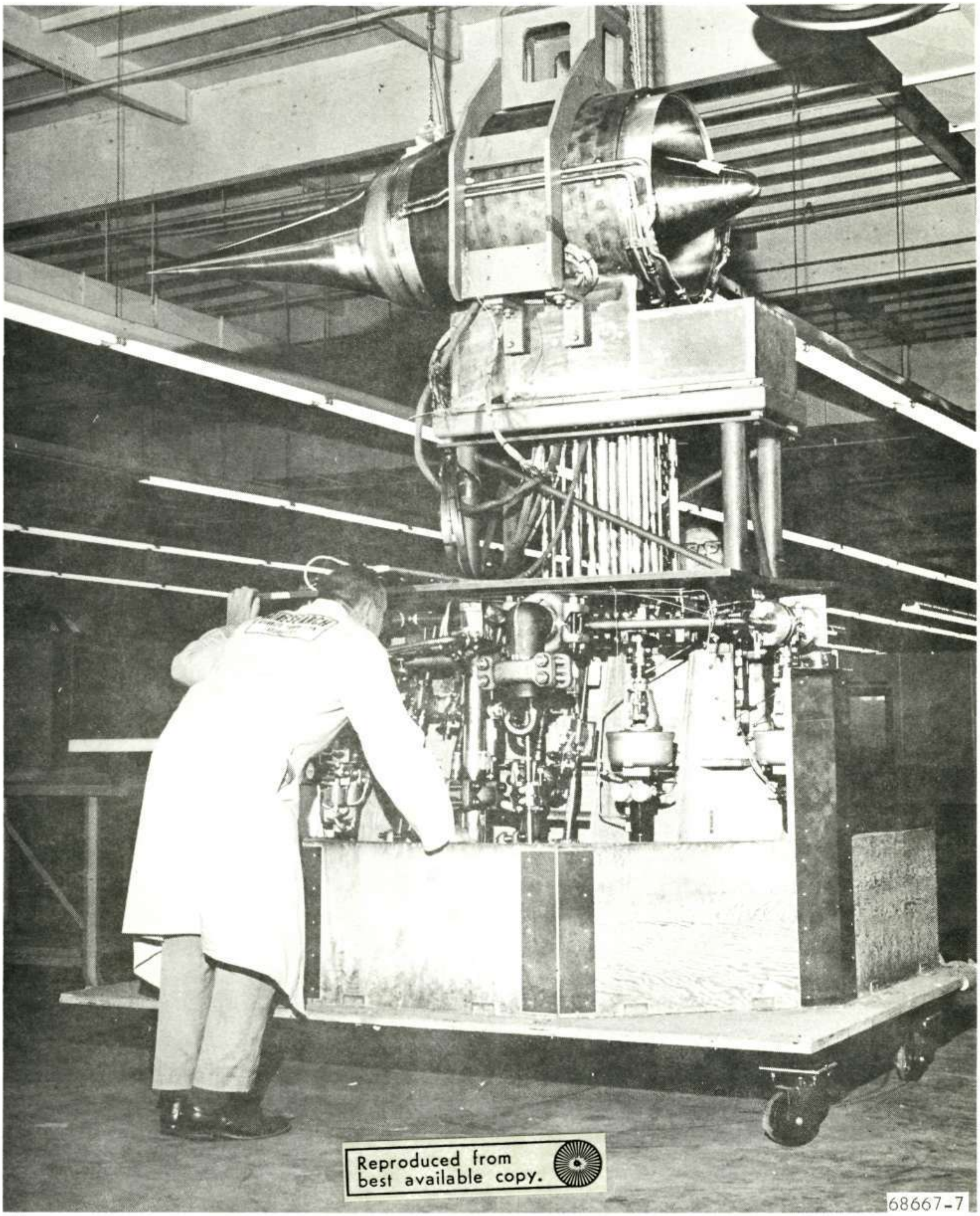

Figure 7.2-4. SAM Engine Assembly - Setup for Brazing Connecting Tubes Between Engine and Manifold Assembly

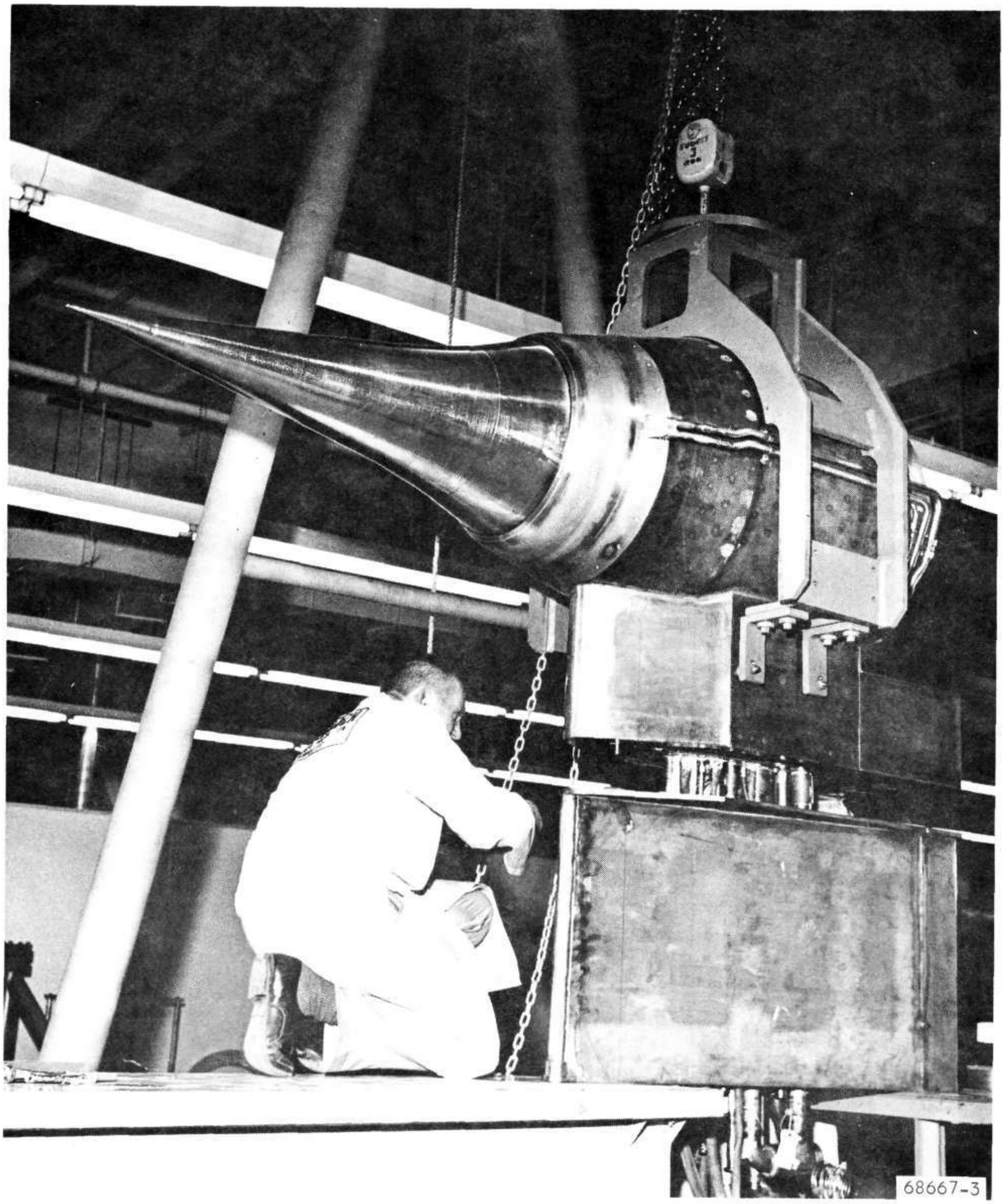

Figure 7.2-5. SAM Engine Assembly Being Lowered on Support Wedge After Brazing of Connecting Tubes

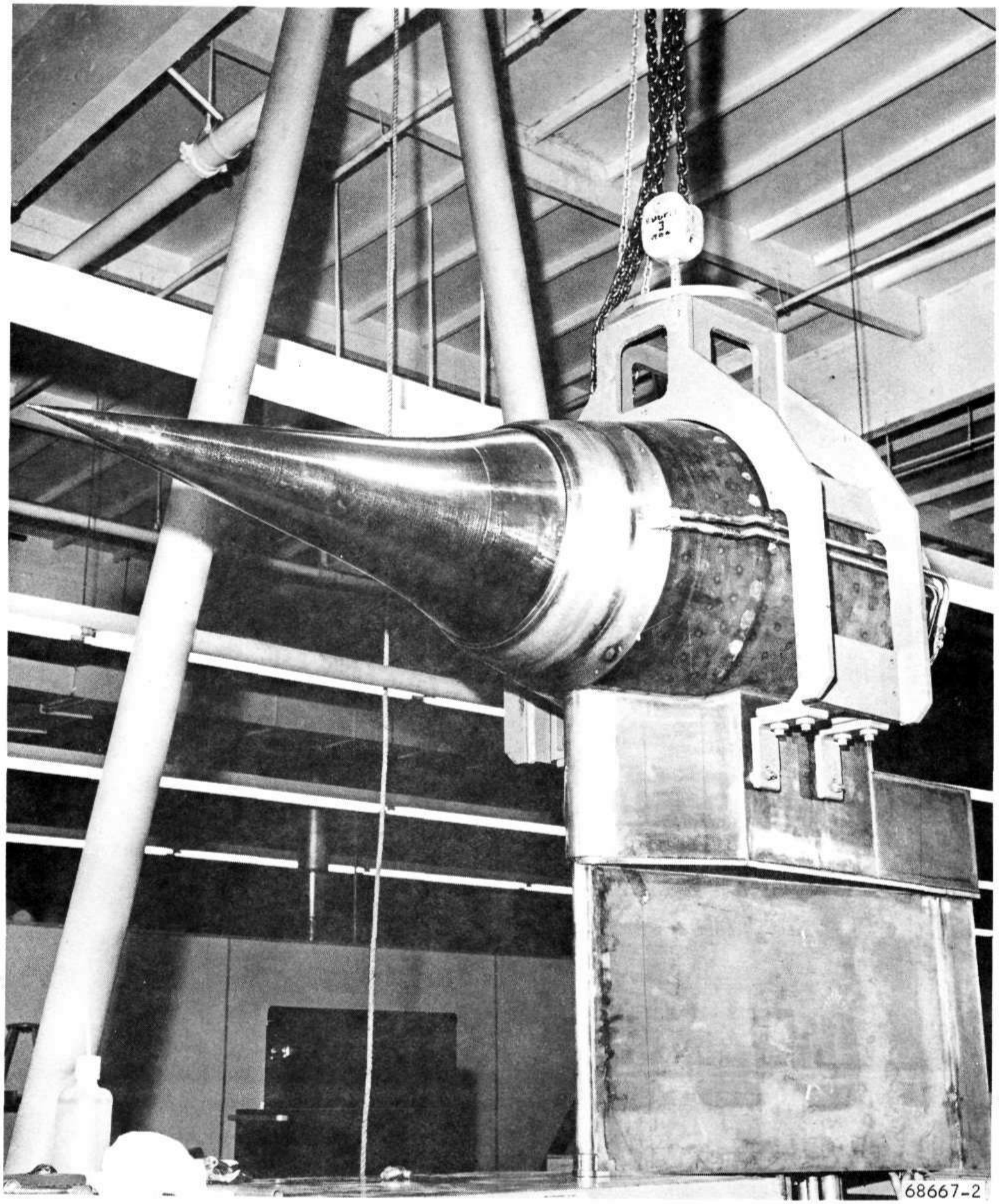

Figure 7.2-6. SAM Engine-Cowl-Support Wedge Assembly

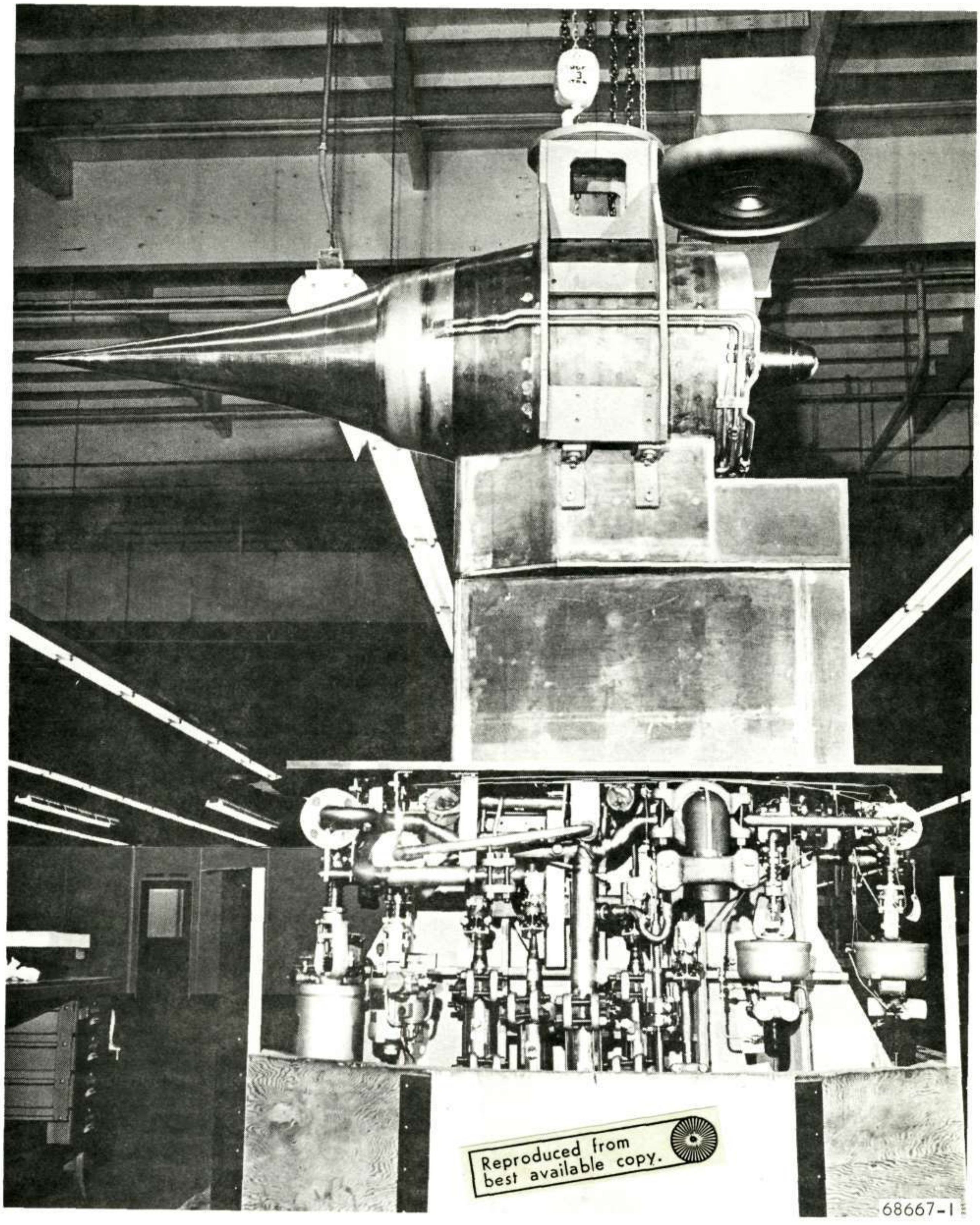

Figure 7.2-7. SAM Engine and Water-Cooled Structures Mounted on Piping Assembly

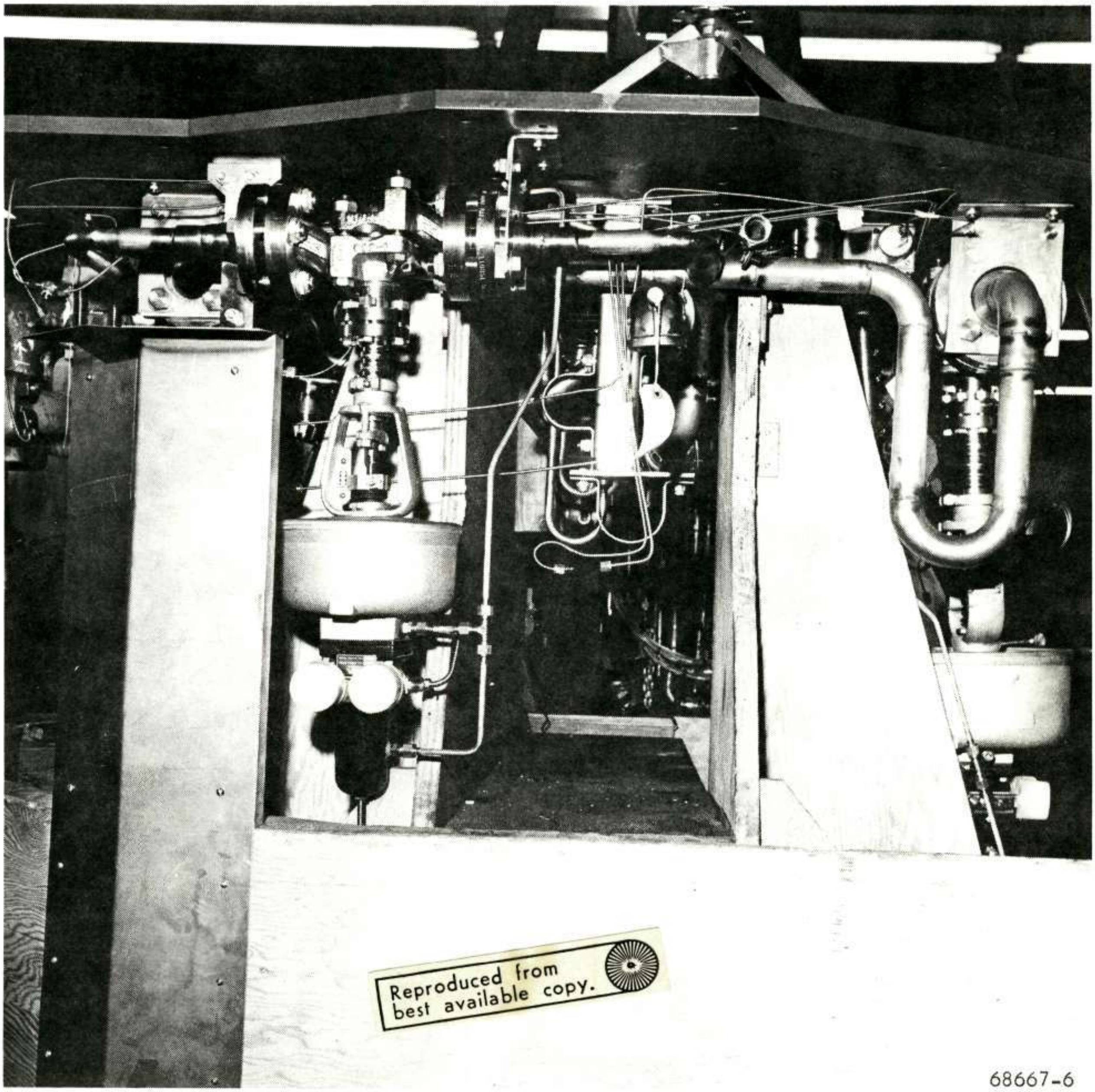

68667-6

Figure 7.3-1. Fuel/Coolant Manifold Assembly Viewed From the Aft End valves, and the valve visible on the right of the assembly is the injection control valve. One of the five differential pressure switches used on the water circuits is attached to the base plate just inboard of the injection control valve. The bracket attached to the base plate in the center of the support carriage mock-up is for supporting the water lines that were removed for installation of the engine assembly.

Figure 7.3-2 shows a view of the fuel/coolant manifold assembly from the forward-starboard side. The four "Moore" regulators for the "Annin" valves and their electrical/pneumatic transducers are shown mounted in the same bracket as the "Groove" pressure regulator. The by-pass valves are supplied with pneumatic pressure from a manifold (not shown) on the downstream side of the "Groove" pressure regulator. The pressure control valve is shown just forward of the regulators. The motor for the pressure control valve was not installed at the time of the picture. Static pressure lines are shown coiled just aft of the regulators, as is one of the sea level vent manifolds.

7.4 PRESSURE CONTROL VALVE

As initially fabricated and tested, the pressure control valve consisted of a low-friction ball valve element and a pneumatic actuator. The frequency response and modulation band obtainable with this actuator were considered unacceptable based on the results of analog simulation studies. As a result, the design of the valve was changed to use the same low friction ball valve element with electric torque motor drive. Figure 7.4-1 shows the assembly of the valve drive. The motor is a printed-circuit armature type, direct-coupled to the shaft of the ball valve. A potentiometer is coupled to the other end of the motor shaft and provides position feedback (the error signal that positions the valve is generated by comparison of the output of a strain gage pressure transducer with the set point voltage). The motor and potentiometer assembly are contained in a hermetically sealed cylinder. This cylinder will be vented to sea level pressure in the wind tunnel to ensure satisfactory operation of the motor when wind tunnel static pressures are in "tenths of psia".

All cylindrical parts of the motor assembly are fabricated from heavy-wall aluminum tubing. The coupling connecting motor and valve is fabricated from PH13-8Mo steel, heat treated to Rockwell C43. The tongue and groove interface between this coupling and the valve allows for misalignment. A hardenable material was selected to minimize wear and, hence, backlash in actuation of the valve.

Figure 7.4-2 shows a photograph of the completed valve and drive assembly, the power amplifier, and the electronic controller.

Figure 7.3-2. Fuel/Coolant Manifold Assembly Viewed From Forward Starboard Side

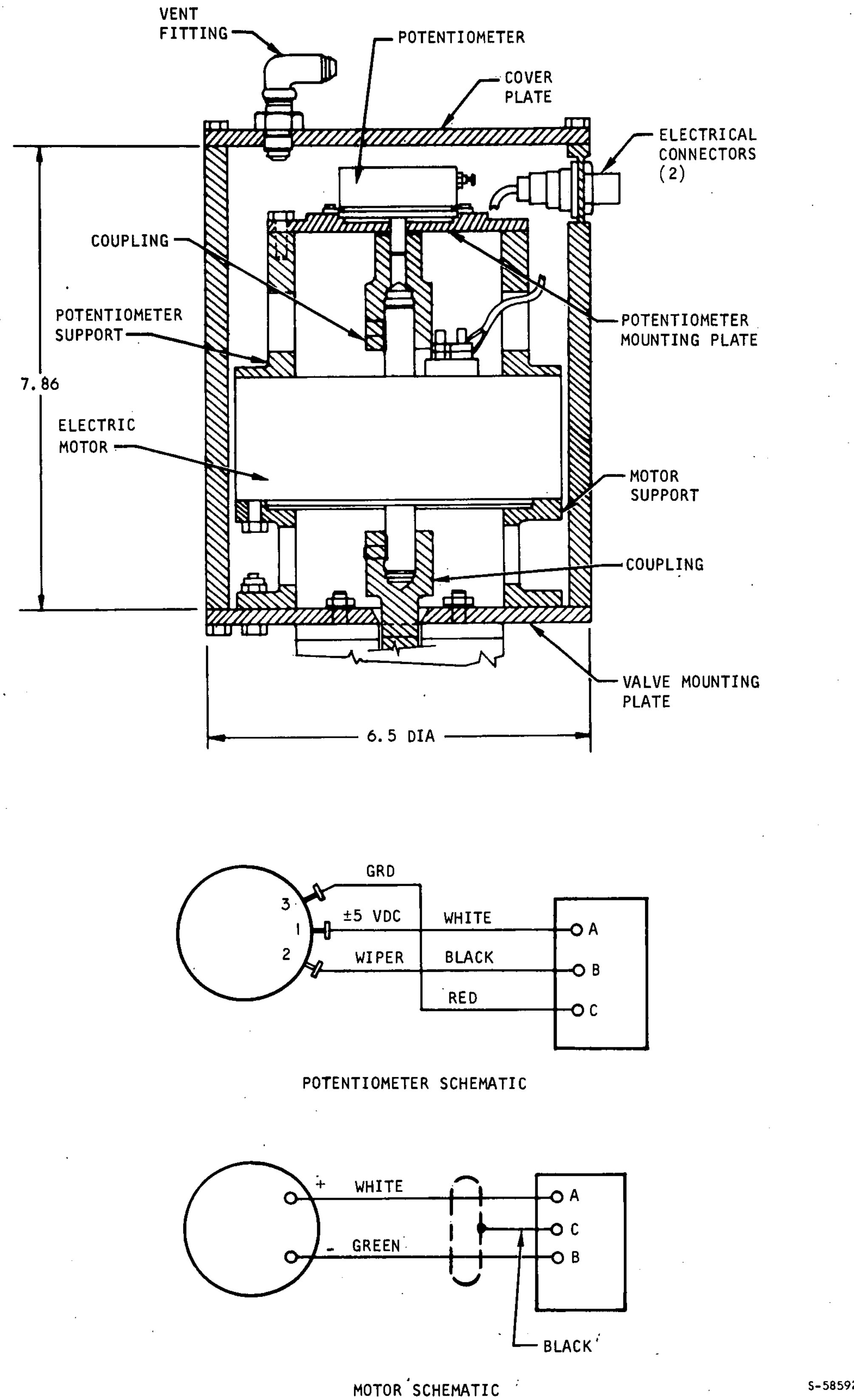

Figure 7.4-1. Pressure-Control Valve Drive Assembly

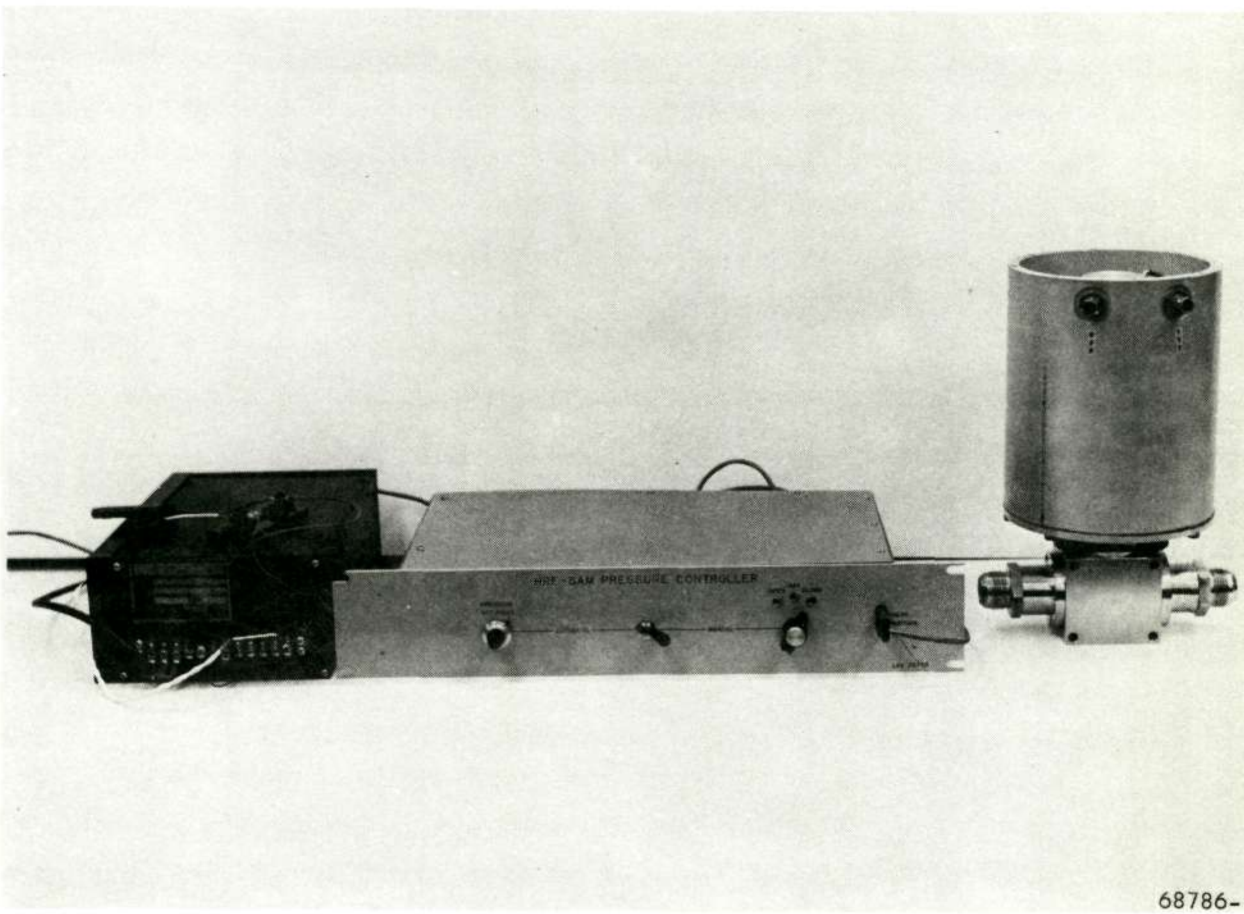

Figure 7.4-2. HRE/SAM Pressure-Control System

8. TESTING

8.1 PRESSURE CONTROL SYSTEM

The pressure control system was evaluated by itself to establish its frequency response characteristics. These were used as inputs to the analog simulation of the SAM coolant system.

8.1.1 Test Setup

Figure 8.1-1 is a schematic of the test setup; Figure 8.1-2 shows a photograph of the test setup. The setup allowed for testing of the valves in two ways. Using a 900-psig air supply, the valve was tested with isothermal air flow from left to right in the figure, with the control sensor located near the downstream needle valve (P3). Steps in flow were introduced into the system by using a solenoid to bypass the downstream needle valve. The orifice section was used for setup and monitoring.

The second test configuration involved the use of two high pressure cylinders as accumulators, maintained at different pressure levels. Using a three-way solenoid across these cylinders, step changes in pressure were applied directly to the control sensor. This configuration was used to evaluate the response of the system to step changes in pressure, for use in the analog simulation.

The test configuration using flowing air was used primarily to evaluate system stability, to adjust the feedback circuit elements for the controller, and to evaluate noise problems and solutions.

8.1.2 Results and Conclusions

Figure 8.1-3 shows the response of the system to a step change in control pressure. The various traces are identified and pertinent values are indicated. The position signal generated by the potentiometer mounted to the valve indicates a system open-loop response of approximately 25 Hz, and a damping factor of approximately 0.1. Prior work with the analog simulation had indicated that a frequency response greater than 10 Hz would be sufficient to ensure a satisfactory system; that is, would result in a system with the potential for adjustment to obtain satisfactory operation. Results of the analog simulation using test results for this system indicated the need for increased damping, to a damping factor of approximately 0.7, with rate feedback. Both modifications were incorporated in the existing circuitry. Results of the analog simulation are discussed in Section 5 and show the response of the valve when used in the engine hydrogen system with hydrogen as the fluid.

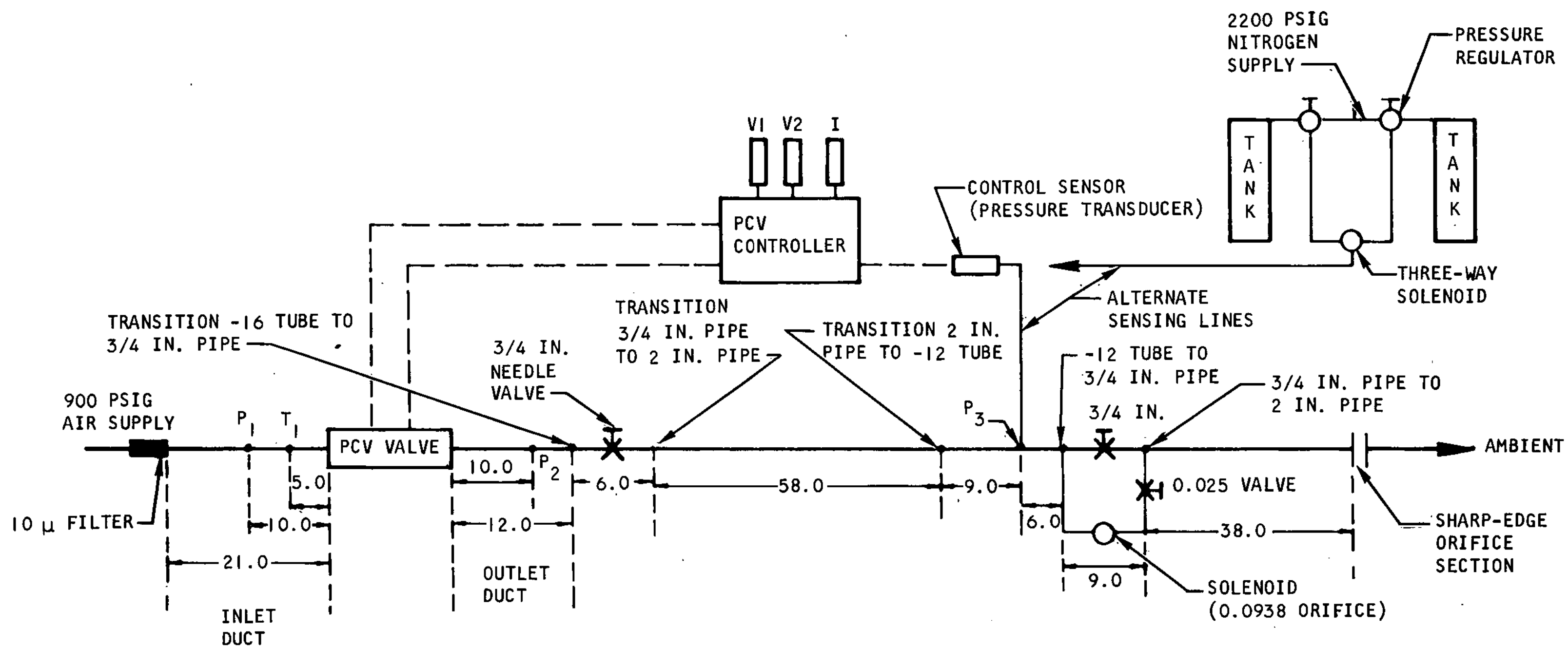

NOTES:

1. ALL MEASUREMENTS ARE IN INCHES
2. INLET AND OUTLET DUCTS ARE 1.00 x 0.035 WALL TUBING
3. SENSING LINES ARE COPPER, (A) 0.0625 ID x 120 IN. LONG: AND (B) 0.180 ID x 12 IN. LONG
4. RECORD P_1, P_2, P_3, I (MOTOR CURRENT), V_1 (VALVE POSITION VOLTAGE), V_2 (SETPOINT VOLTAGE)

S-58593

Figure 8.1-1. Test Setup for HRE/SAM Pressure-Control Valve and System

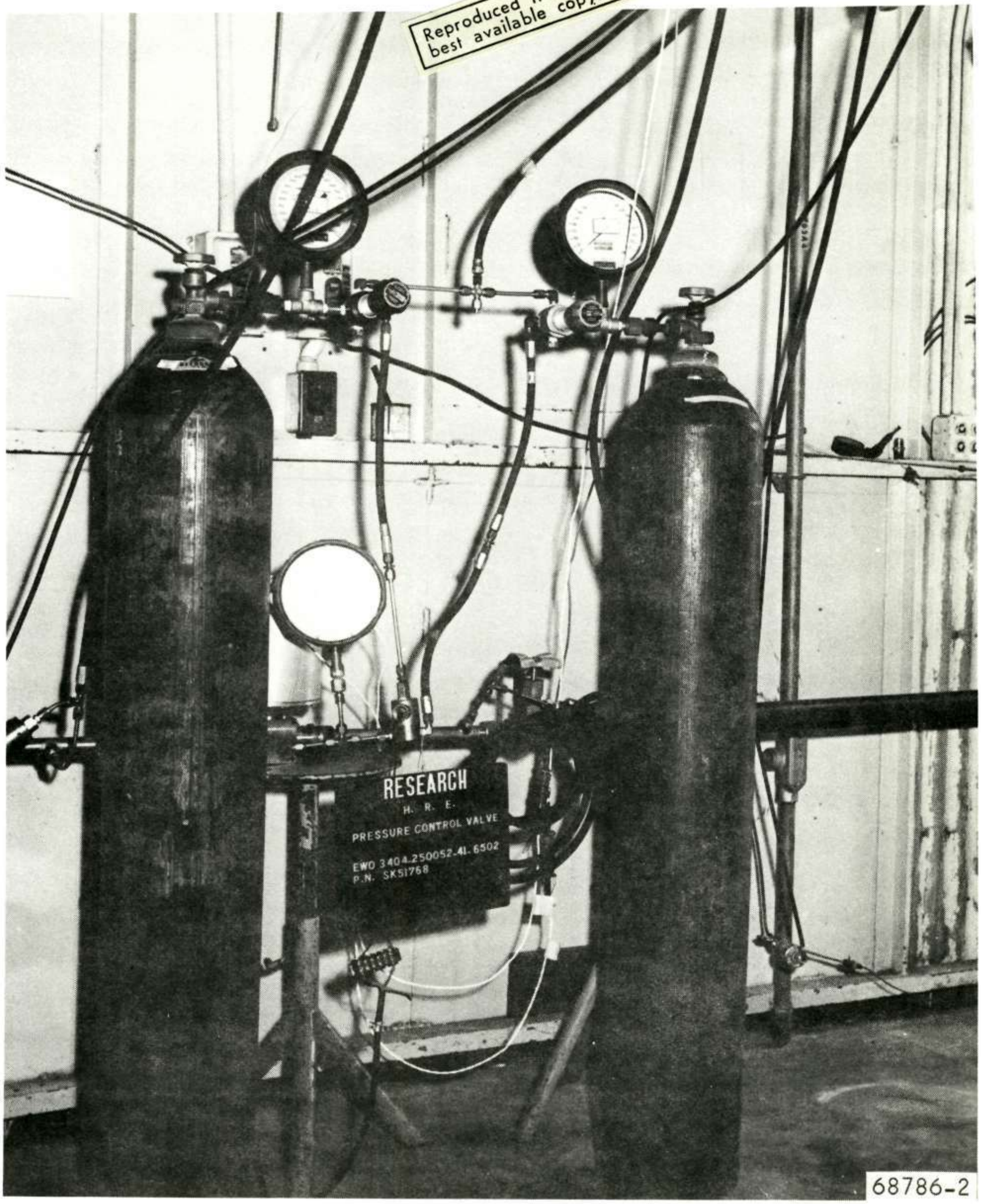

Figure 8.1-2. Test Setup for Pressure-Control System Evaluation

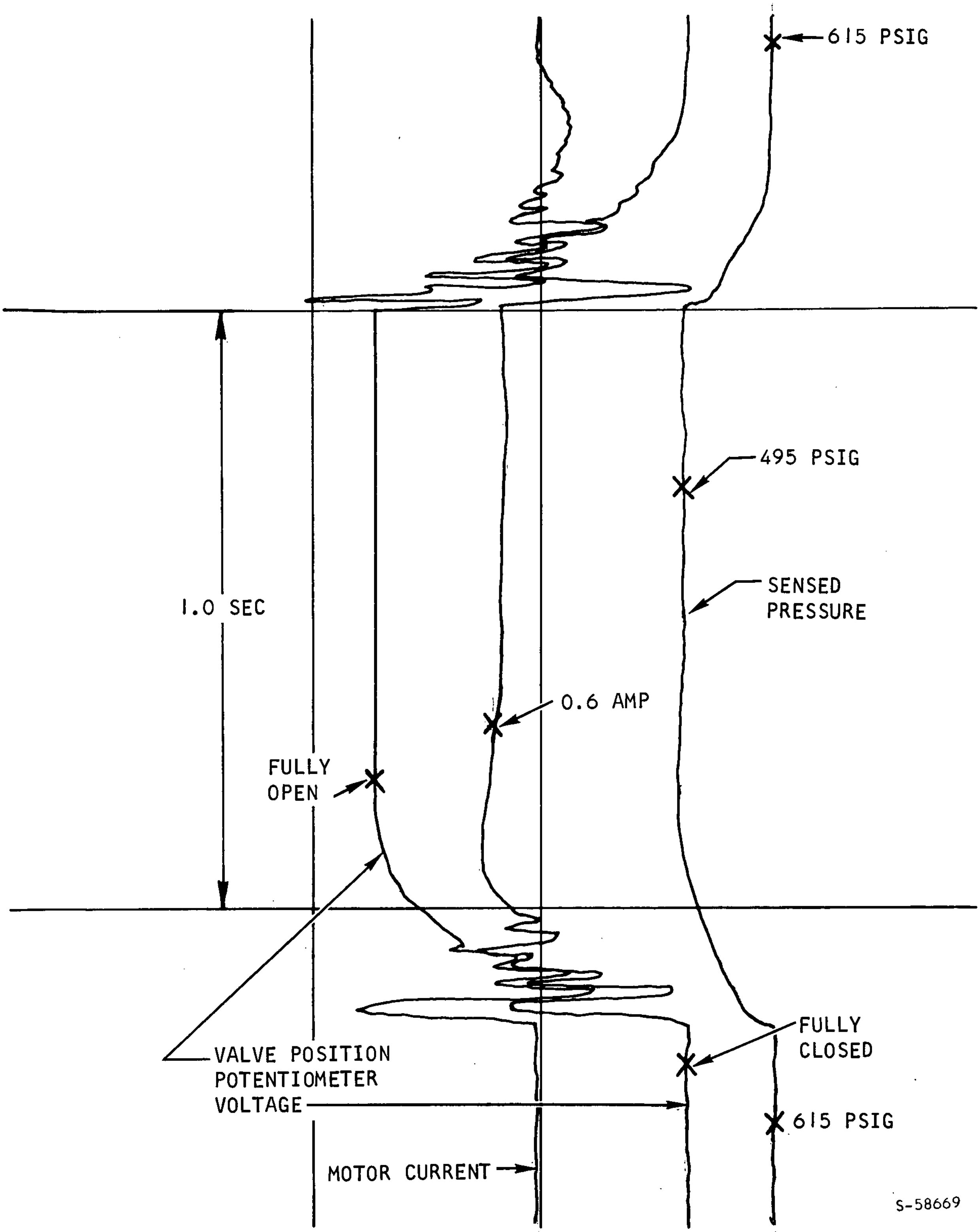

Figure 8.1-3. Pressure Control System Response to Step Change in Sensed Pressure

Figure 8.1-4 shows a typical response characteristic for the flowing air system for a step change in flow. Results for this system indicate stable operation. When the same system was used with hydrogen in the analog simulation, valve system operation was unstable. A similar result was obtained when the SAM system was operated with air and hydrogen. The results of these tests, therefore, can only serve as a first approach to tuning of the system.

Both systems were run with short and long sensing lines (12-in. long, 0.180-in. ID and 120-in. long, 0.0625-in. ID) to assess the effect of sensing line lag on controller performance. No significant differences in response characteristics were noted for the two extremes, indicating relative insensitivity to the line configuration. A similar insensitivity is expected for the actual installation where hydrogen will be the controlled fluid.

The general conclusion drawn from the test results was that the pressure control system was satisfactory. It required modification of electronics, that is, the addition of rate feedback damping, to ensure stable operation with hydrogen under the range of flow conditions anticipated (0.621 lb/sec maximum and 0.2 lb/sec minimum total flows).

8.2 INLET SPIKE CONTROL SYSTEM

The description of refurbishment and calibration testing of the SAM spike actuator was presented in the Thirteenth TDR. After completion of the SAM assembly, the actuator and its electronic control module were retested to calibrate the control system and to determine any acoustic or resonance effects from vibrational inputs in the range of 0.1 to 45 Hz.

8.2.1 Test Setup and Procedure

Figure 8.2-1 shows the SAM engine assembly and instrumentation arrangement for the actuator calibration and frequency response tests. During this test the control setup was identical with that used previously and described in the Thirteenth TDR. The engine assembly was mounted in the shipping cart which, in turn, was bolted to the floor. A 5-in. stroke dial indicator was mounted to the cart as shown in the figure to measure the spike travel directly. The hydraulic power supply, seen in the foreground of Figure 8.2-1 contained Houghto-Safe 1010 hydraulic fluid rather than MIL-H-5606 used in previous testing.

The functional schematic of the components used in the frequency response testing is shown in Figure 8.2-2 and the actual instrumentation can be seen in the foreground in Figure 8.2-1.

8.2.2 Test Results

The same parameters, actuator stroking, latching in the extended position, and LVDT calibration and positioning accuracy, were measured as were determined for the actuator alone. It was found that a pressure of approximately 800 psig was required to disengage the latch and a pressure of 1000 psig produced a balance of mechanical and hydraulic forces at a spike displacement of 4.7-in. aft

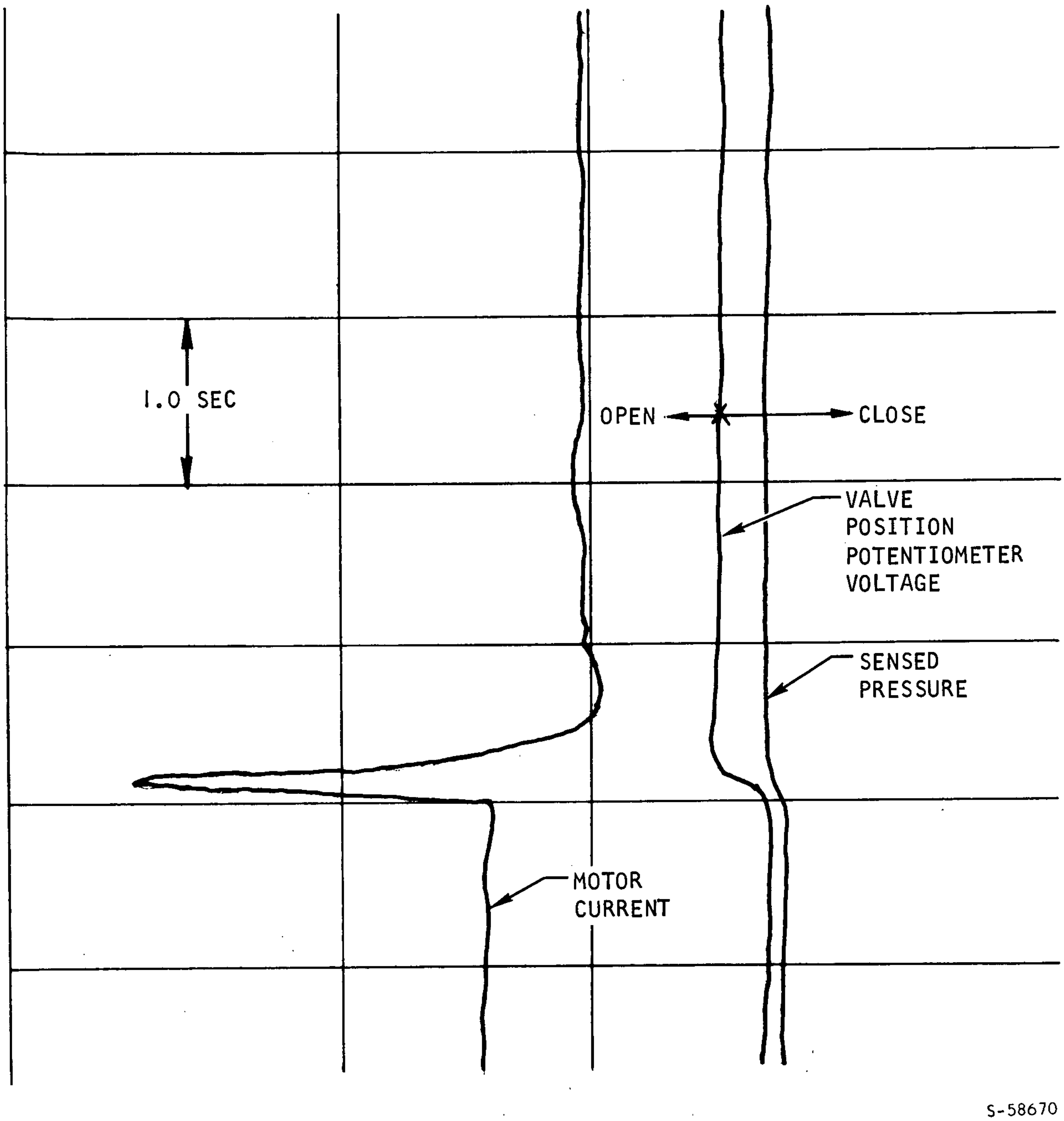

Figure 8.1-4. Pressure Control System Response to Step Change in Flow

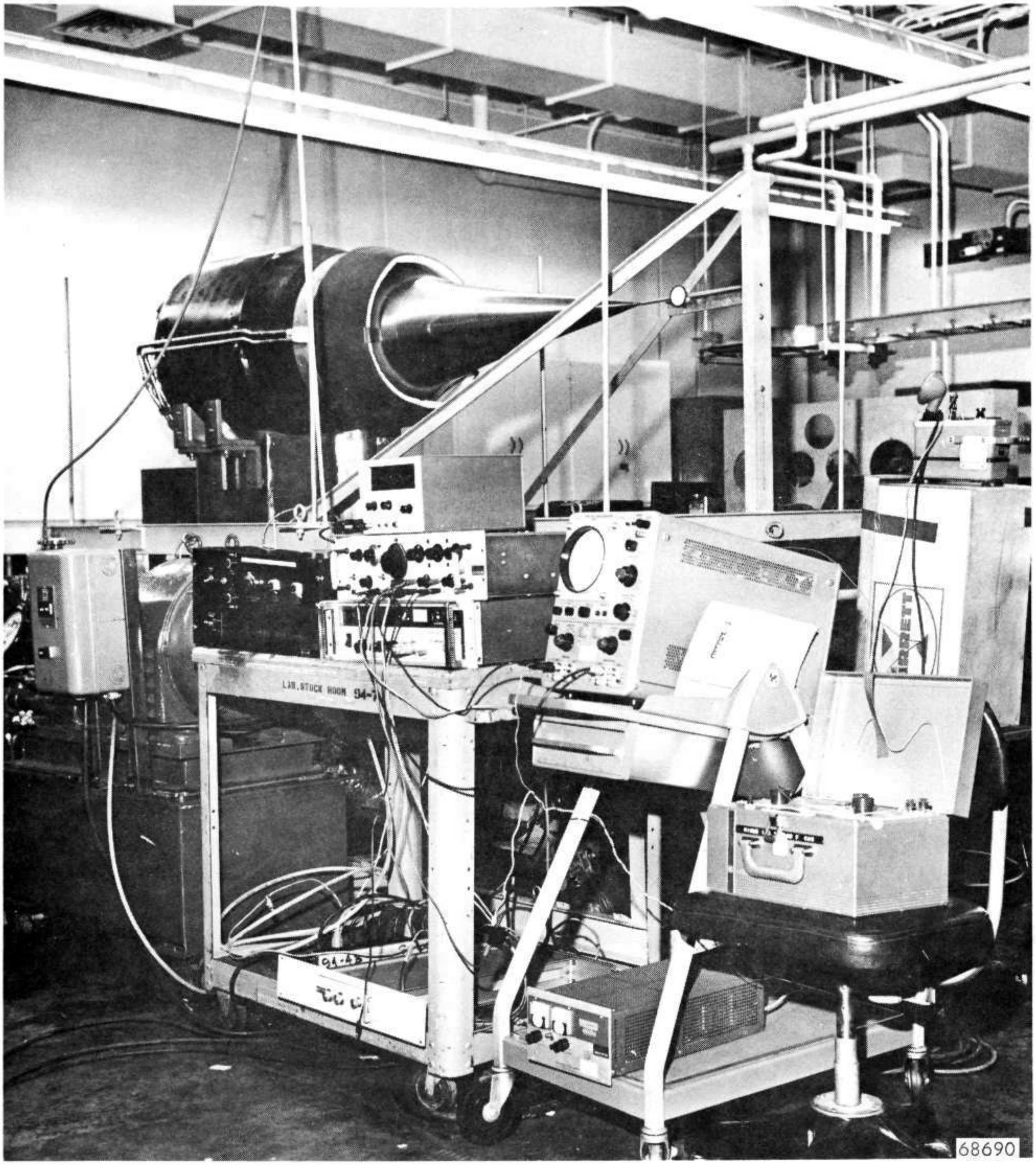

Figure 8.2-1. Test Setup - SAM Spike Control System Tests

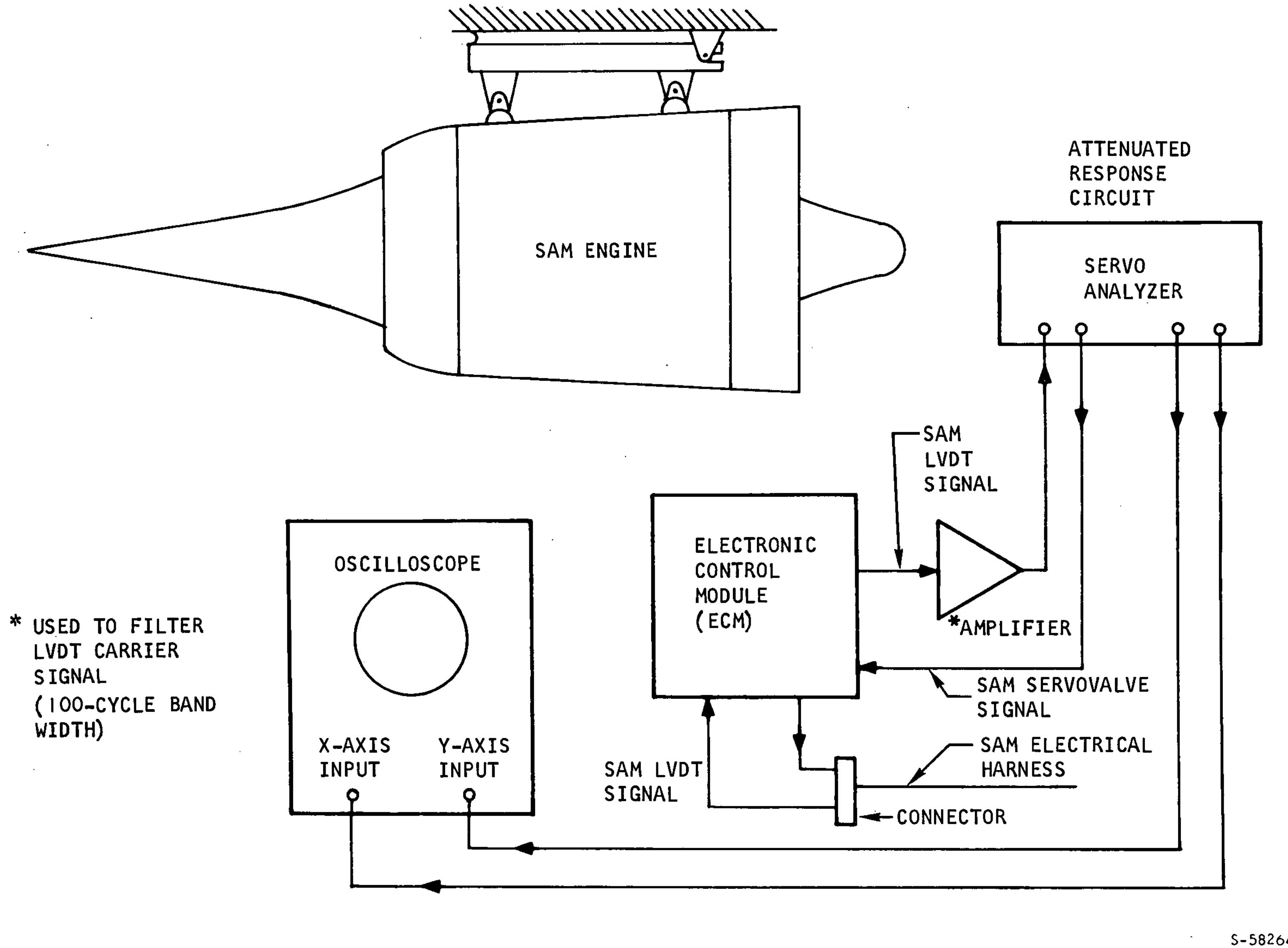

Figure 8.2-2. SAM Frequency Response Test Functional Schematic

from the latched position. The LVDT calibration was identical to that shown in the Thirteenth TDR. An enlarged calibration curve from the SAM test data has been prepared to use during wind tunnel testing.

The amplitude ratio and phase lag corresponding to the range of input frequencies to the hydraulic system are shown in Figure 8.2-3. A spike displacement of 0.01 in. was imposed in the frequency range of 0.1 to 40 Hz, and a displacement of 0.007 in. was used for the last point read. A system hydraulic pressure of approximately 2500 psig was maintained during the frequency response tests.

8.3 SAM FLOW CALIBRATION

The purpose of these tests was to perform leakage, calibration, and checkout tests of the SAM prior to delivery to the 8-Foot High Temperature Structures Tunnel (HTST) at NASA-Langley. These tests consisted of the following:

(a) Pressure drop versus water flow rate in each of the five water flow routes.

(b) Calibration of differential pressure switches in each of the five water flow routes.

(c) Overall pressure drop versus airflow rate in each of the four hydrogen flow routes, for different valve settings. Pressure drops in the regeneratively-cooled shells were previously obtained and reported on a component basis.

(d) Overall pressure drop versus airflow rate in the fuel injection circuit, for different valve settings. The flow characteristic without external plumbing was previously obtained and reported.

(e) Checkout of the TCS when integrated with the SAM, including the flow measuring subsystem, the abort and interlock functions, and the valve control functions.

(f) Nitrogen purge gas flow versus inlet pressure.

The complete assembly, tested in the laboratory, consisted of the following items:

(a) The engine assembly.

(b) The manifold assembly. This assembly was assembled to the engine assembly for testing.

(c) The temperature control system (TCS).

8.3.1 <u>Hydrogen System</u>

The hydrogen system calibration consisted of steady-state runs to check

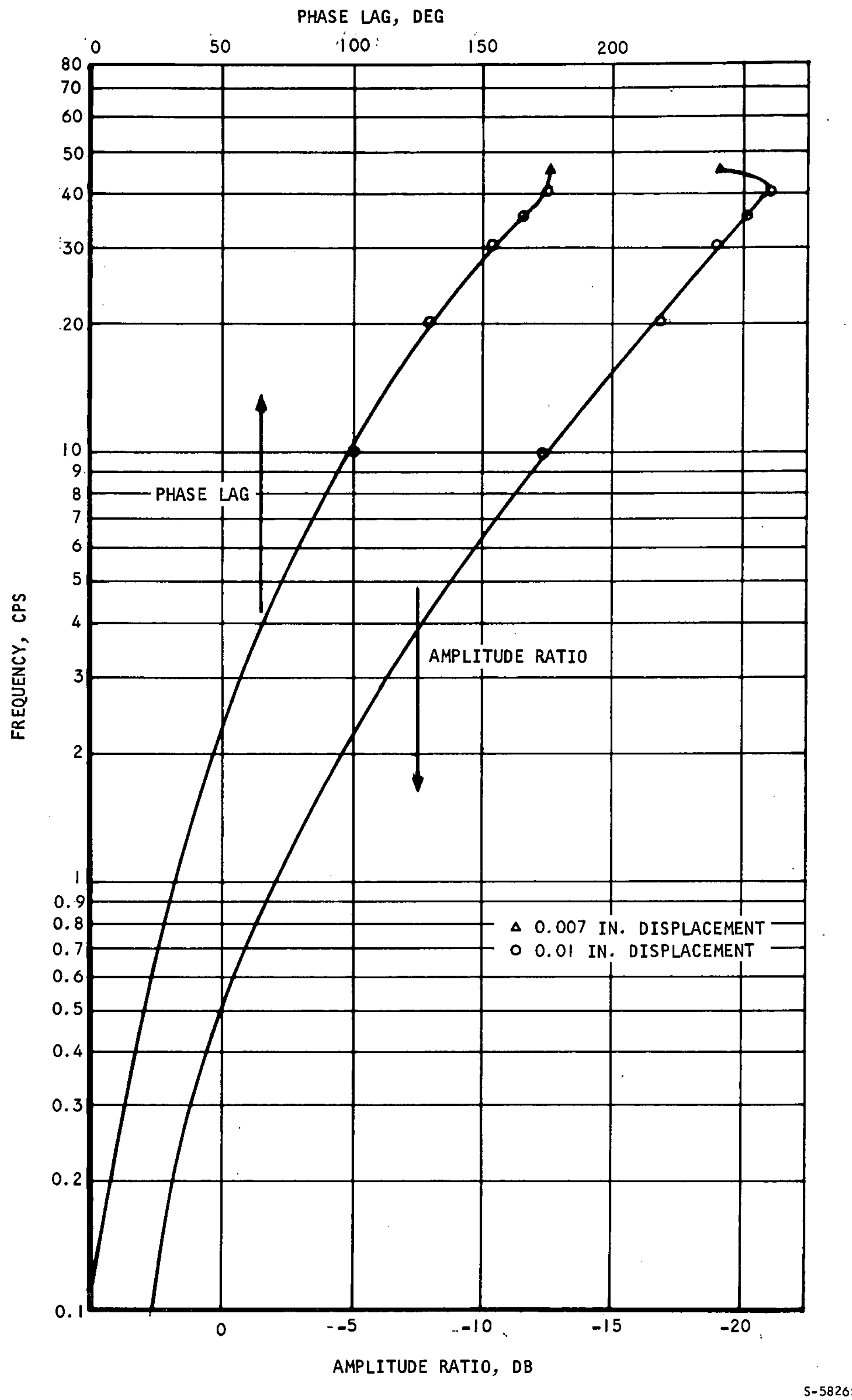

Figure 8.2-3. SAM Inlet Spike Actuation System Frequency Response

the pressure drop in the hydrogen coolant circuit and in the fuel injection circuit. The TCS was checked to confirm proper functioning.

8.3.1.1 Hydrogen Coolant System

An isothermal air flow test was performed on the hydrogen coolant system. The fuel dump valves and the coolant regulating valves were controlled by the controls located in the TCS console. Figure 8.3-1 shows the facility setup for this test. The SAM was tested with all its actual plumbing in the final configuration, as used in the wind tunnel. The procedure for establishing the coolant flow rate was to set the pressure downstream of the pressure control valve (PCV) with the coolant regulating valves (CRV) in the fully open position. One fuel dump valve (FDV 2) was used as the running valve, with the other fuel dump valve (FDV 1) electrically-positioned in the fully closed position. The FDV 2 was opened to obtain the desired flow rate by adjusting the potentiometer setting on the TCS console. The coolant regulating valves were adjusted to obtain the flow split as follows in each coolant circuit:

Spike	41.2%
Innerbody	9.3%
Leading edge	29.0%
Trailing edge	17.8%
Strut	2.7%

Data was recorded at five levels of airflow ranging from 46.2 lb/min to 14.4 lb/min at a system inlet pressure of approximately 270 psig and at three settings of the CRV's with flow splits maintained the same.

Results of the isothermal airflow tests are summarized below. Figure 8.3-2 schematically shows coolant system pressure levels for a typical test run. The indicated flow percentages in each route are approximately equal to those proposed for nitrogen calibration of the SAM in the wind tunnel. Figure 8.3-3 presents the average density-pressure drop product ($\rho\Delta P$) for the spike. Included is the curve obtained from component tests performed on the spike (Reference 5-2). Acceptable agreement is noted (pressures were measured with built-in 1000 psi transducers, giving a possible error in ΔP of ±7 psi). Pressure drops were checked for two other flow routes (innerbody and leading edge) and are adequately within the range of prediction when the accuracy of the pressure measurements were considered. For most test runs the innerbody and leading edge pressure drops were approximately equal to or less than the instrument and reading accuracy of the pressure gauges (±2 psi). Similarly small pressure drops are predicted in the two innerbody, leading edge, outer shell, and strut routes during hydrogen testing. Differential pressure transducers will be used in several of these routes during wind tunnel tests to improve data accuracy.

The total flow rate through the SAM as measured by the turbine flowmeter (Cox Model GM-32, SN 13664) was compared with the flow measured by a 4 by 2 in.

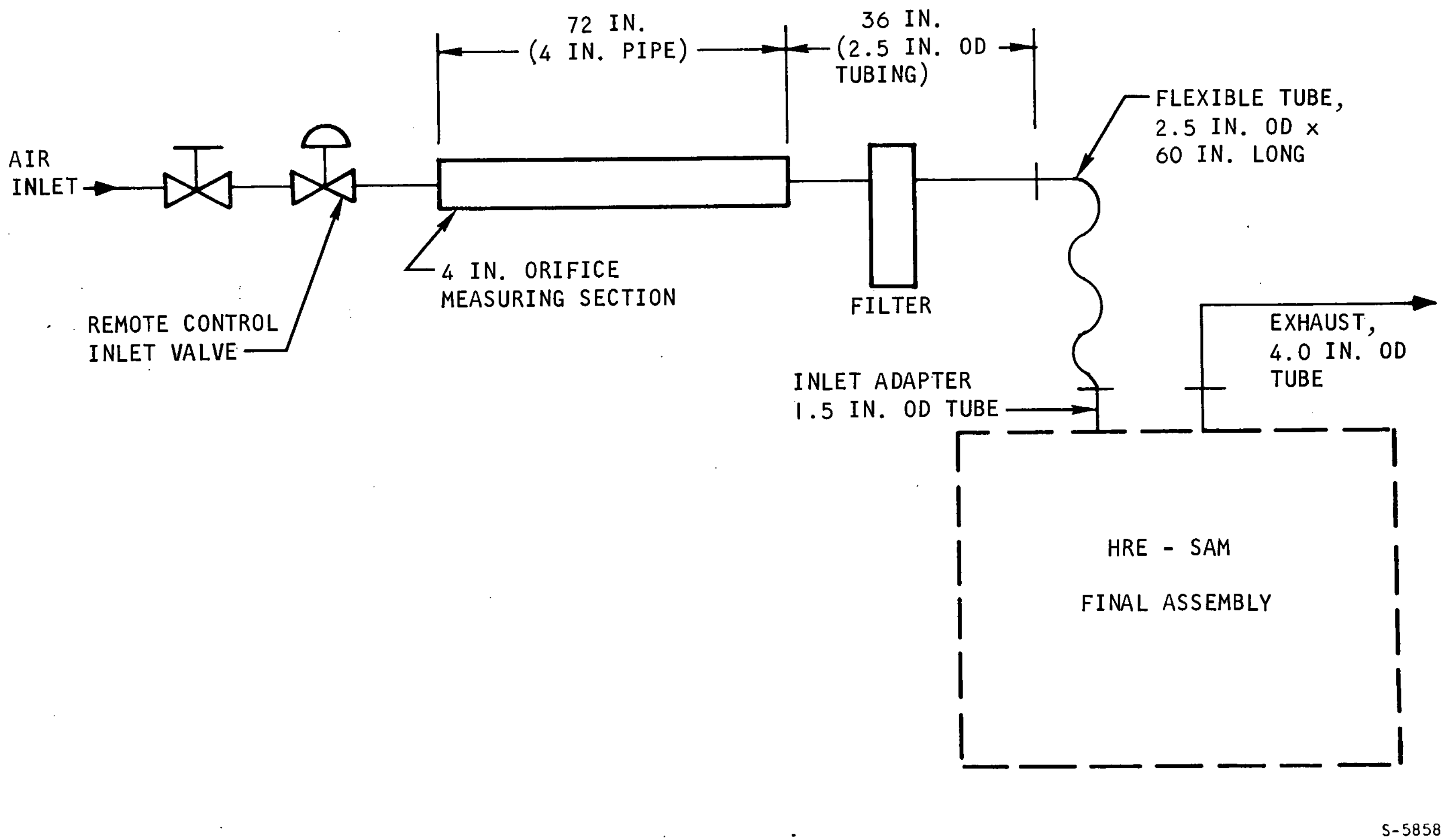

Figure 8.3-1. Hydrogen System Calibration - Test Setup

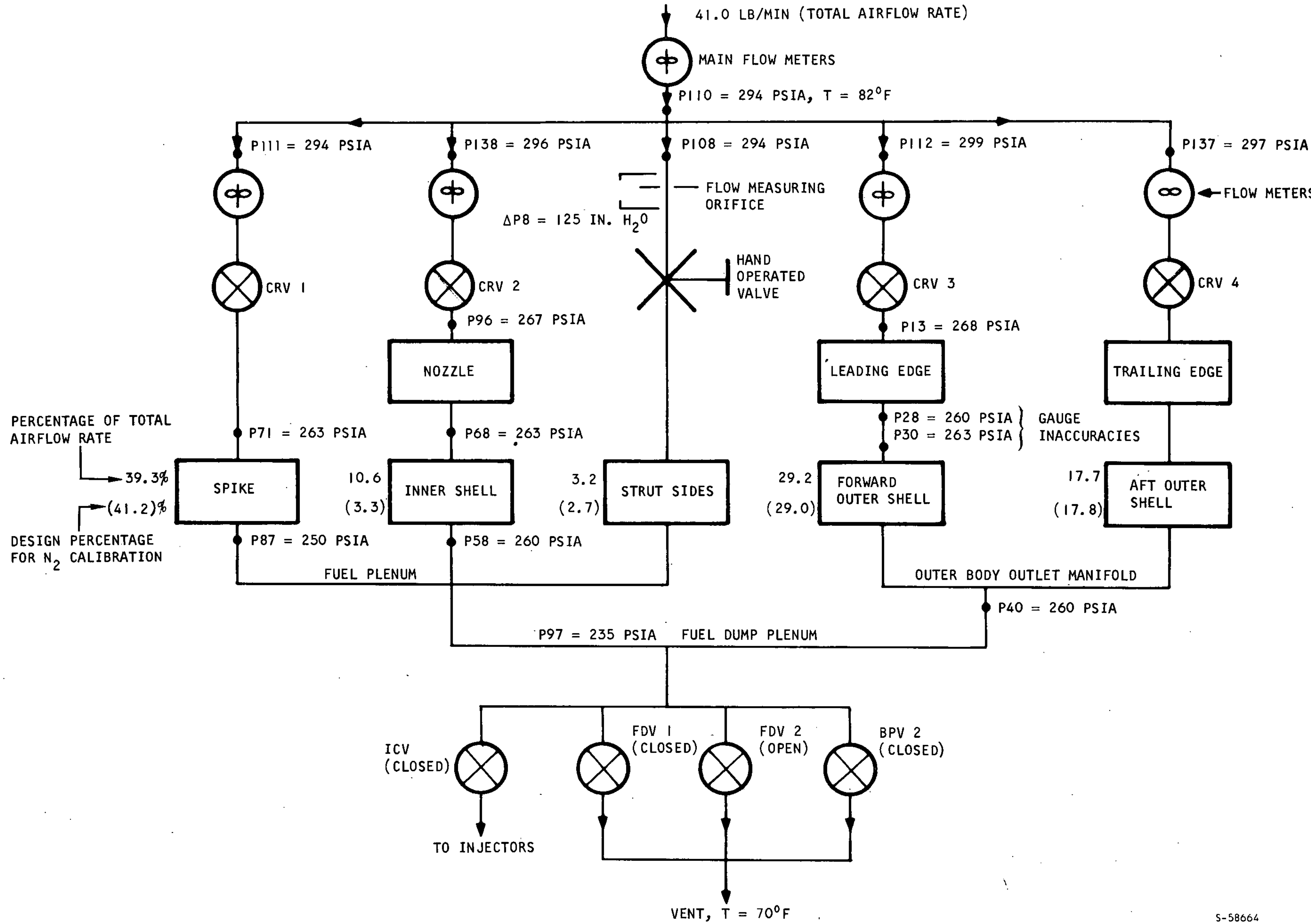

Figure 8.3-2. Coolant System Parameters for Typical Air Test Run

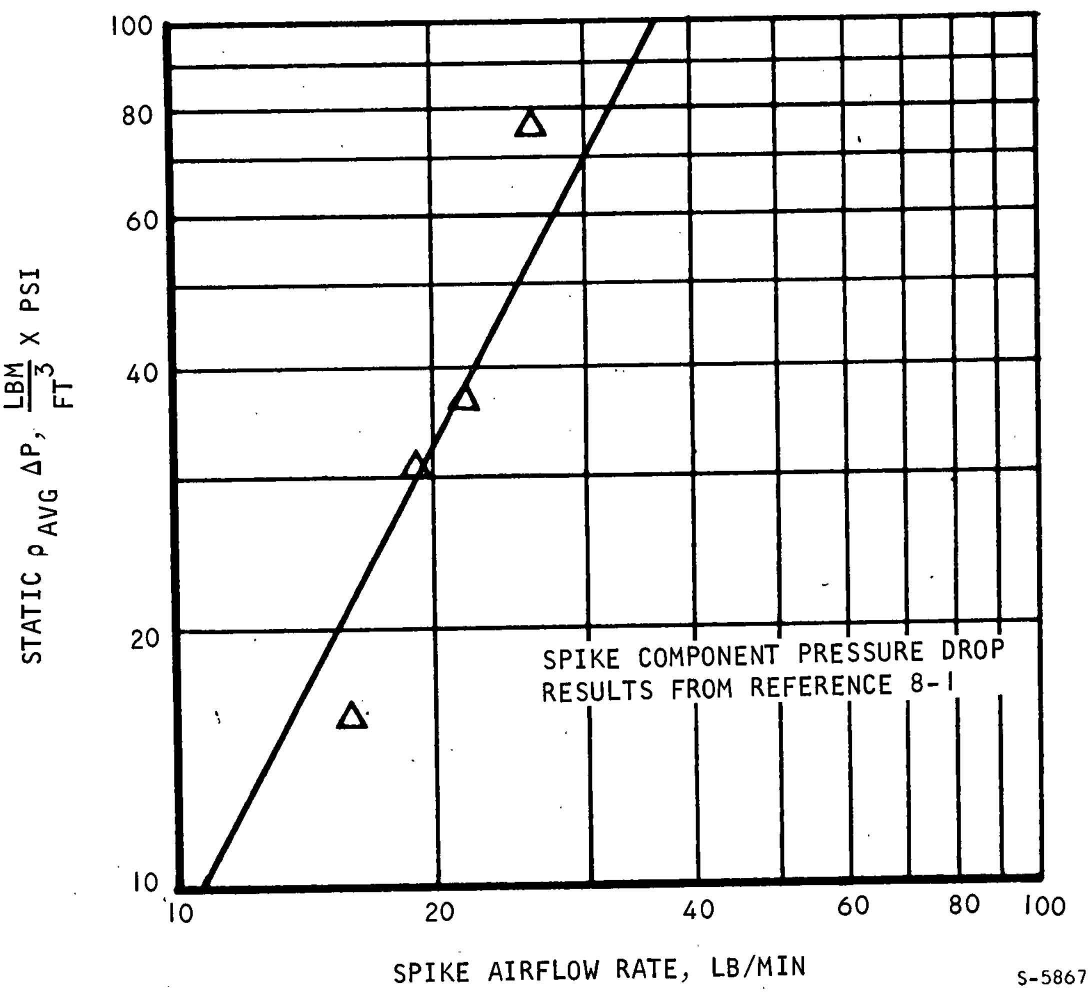

Figure 8.3-3. SAM Spike Air Pressure Drop Test Results

flange top orifice upstream of the SAM. Results are reported in Figure 8.3.4. The standard deviation error is ±1.2 percent for the thirteen test points sampled. The largest error (3 percent) occurred at 18.6 lb/min. If this data point is deleted, the standard deviation error is reduced to ±0.8 percent. Mass flow rate through the flowmeters was calculated by multiplying the volume flow rate (as determined by the frequency reading of the flowmeters) by the air density at the flowmeters.

Static pressure taps were located adjacent to each of the flowmeters (spike, innerbody, leading edge, outer shell, and total) and the strut-sides flow-measuring orifice. For all flow test runs, these six pressures were sufficiently close to each other that a random error analysis was performed. The standard deviation between these six pressures for all test runs was ±2.2 psi at an average pressure level of 270 psig or ±0.8 percent. Thus, any one of these pressures can be used to calculate any of the flows if the deviation of up to ±0.8 percent is acceptable. This deviation will be accepted for SAM data reduction since pressures adjacent to the innerbody and trailing edge flowmeters (P137 and P138) will not be measured during SAM testing.

The total engine flow rate percentage to each of the five flow routes is plotted versus total engine flow rate in Figure 8.3-5. The CRV potentiometer settings were fixed for the range of total engine flow rates shown and were set to give the design percentages for N_2 calibration indicated in Figure 8.3-5. With the CRV positions fixed, the FDV position was changed from run to run to vary the total engine flow rate. The maximum flow deviations between the flow rates shown are 1.9 percent (of total engine flow) for the spike, 2.5 for the innerbody, 1.7 for the leading edge, 0.7 for the trailing edge, and 0.5 for the strut sides. The flow percentages were set using flow percentage gauges that are accurate to ±2 percent of total engine flow. These settings were not refined from run to run and gave flow percentages that were as much as 2-1/2 percent away from the design setting for N_2 calibration. Additional adjustment of the CRV settings (particularly the spike) would have reduced these differences.

8.3.1.2 Injection System Test

An isothermal airflow test was performed on the injection system circuit. Airflow rates varying from 46.21 lb/min to 14.4 lb/min were used to calibrate the fuel injection circuit. The flow rates in the coolant routes were maintained the same as in the coolant circuit tests. For the fuel injection tests, the desired flow rate was established by flowing air through the coolant circuit and FDV and then making the transition from the coolant circuit to the injector circuit by means of the TCS (i.e., close FDV and open injection control valve (ICV)).

To maintain coolant system pressures (120 to 300 psia) and airflow rates (15 to 60 lb/min) equal to those using the FDV only, the transition to the injection system required that the injector control valve (ICV) be positioned at small openings. These small openings choked the flow through the ICV and created pressure ratios across the spike and outer shell injectors that were just equal to or less than the critical choking ratio. Flow through the spike and outer shell injectors was estimated from the recorded pressures in the

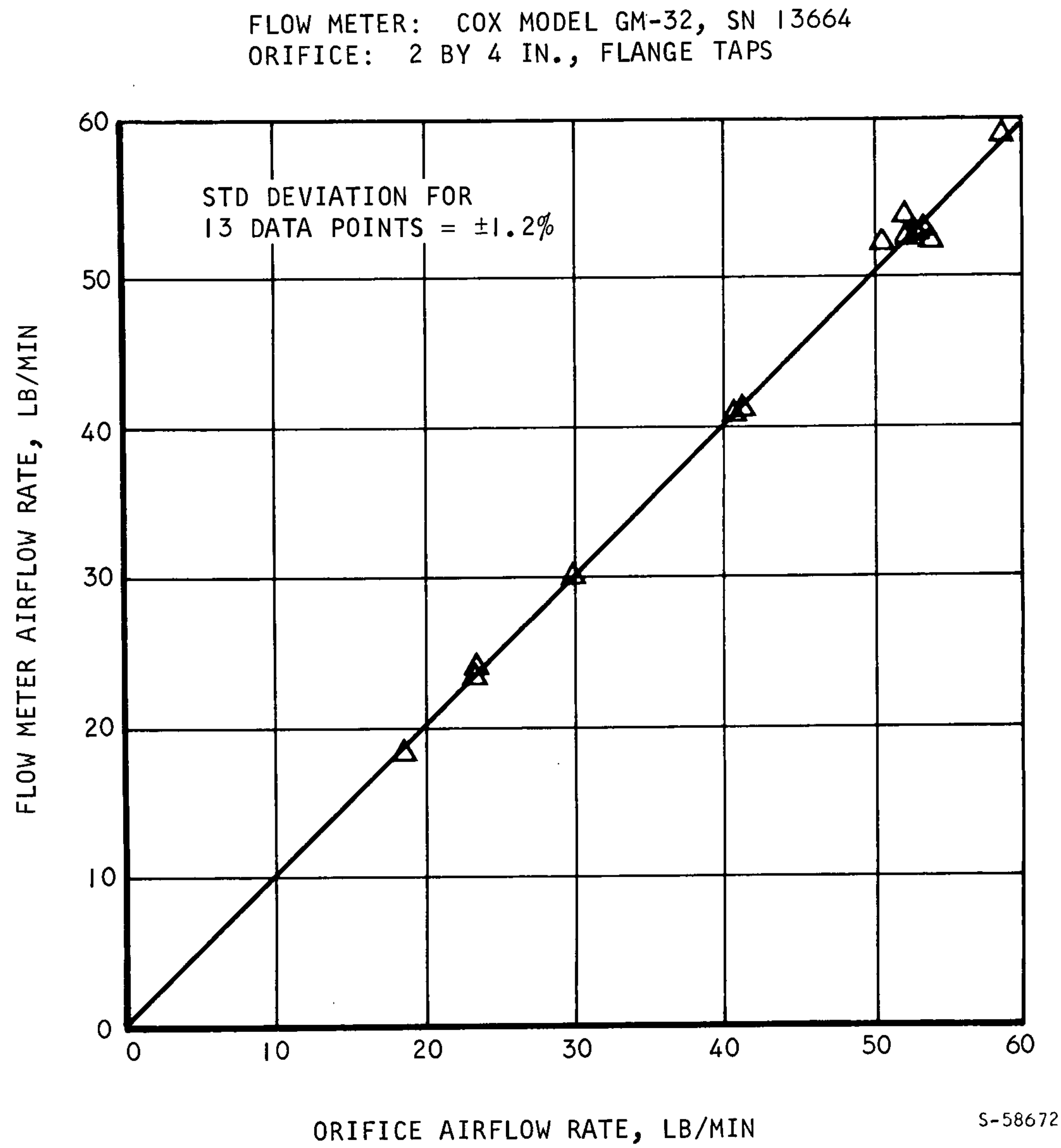

Figure 8.3-4. Measurement Accuracy of Total Flowmeter

NOTE: FIXED CRV POTENTIOMETER SETTINGS

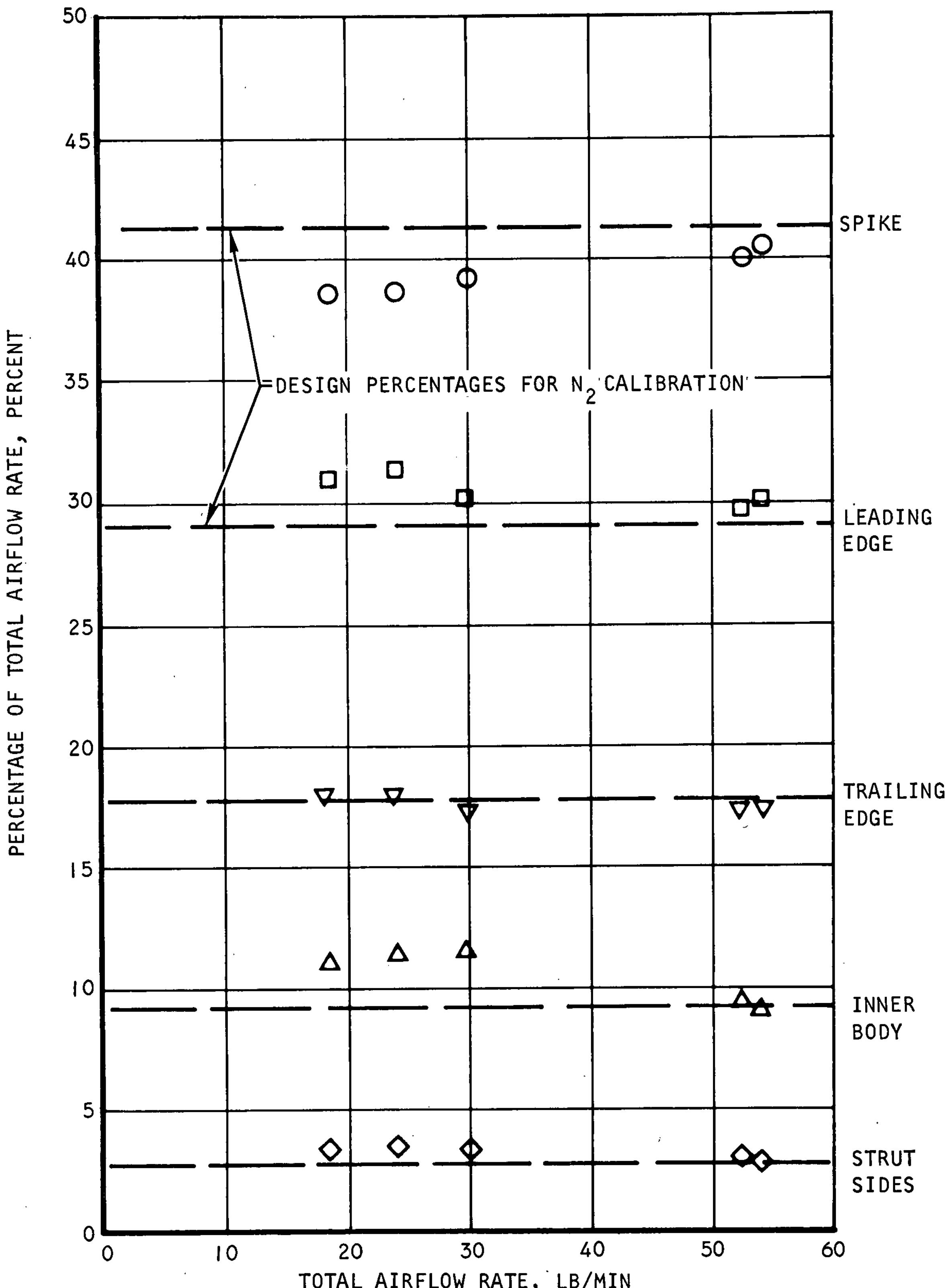

S-58673

Figure 8.3-5. Coolant Route Flow Rate Percentages injector manifolds (P84 and P34, respectively) and the injector calibration data (discharge coefficients) in Reference (5-2). However, the sum of the estimated injection flow rates differed from the total airflow rate (as measured by the orifice upstream of the SAM) by 3 to 100 percent. These differences were caused by pressure gauge (P34) and pressure transducer (P84) inaccuracies at pressure levels from 20 to 30 psia. For injector flow rates that agreed fairly well with the total flow rate (3 to 6 percent), it is estimated that approximately 54 to 62 percent of the total engine flow was routed through the spike injectors while the remainder was routed through the outer shell injectors. The design objective was a 50-50 split between spike and outer shell injectors, as reported in Reference (5-1).

8.3.1.3 Temperature Control System (TCS)

The TCS functions and operating modes were checked out during the course of the isothermal airflow testing.

The external purge command from the facility was simulated to verify that the BPV's, FDV's, and the ICV opened upon command and returned to their previous settings when the signal was removed.

The ICV permissive signal from the facility was simulated to ensure that the ICV valve would open only when the enabling signal from the facility, showing that the engine was at the tunnel centerline, was sent to the TCS panel.

The low-hydrogen flow abort system was checked by first presetting the potentiometer on the low flow switching mechanism and establishing a flow rate in the coolant circuit. A step change was then imposed on FDV area. As the valve closed and the coolant flow was reduced, the two solenoid controlled BPV's opened. System inlet pressures, the dump plenum pressure, and system flow rates were continuously recorded. Figure 8.3-6 shows typical traces of the flow rates during one of the runs. From the dynamic recordings, an undershoot in total flow of approximately 25 percent was observed relative to the preset trip values in the low flow switch. This was consistent at all flow rates tried. For slow changes in flow, the trip flows match the calibration values. Actual settings during test will be based on an intermediate trip flow to provide protection during step change and also avoid unnecessary aborts.

The FDV to ICV transition was dynamically checked both with and without the PCV valve functioning. Again, only the one FDV valve was used, with the upstream FDV closed electrically. The transition was not satisfactory without the pressure control system functioning. Figure 8.3-7 shows the flow rates and dump plenum pressure during a typical run. Results are considered satisfactory, i.e., the total system flow rate is maintained near constant (about 6 percent excursion from steady state) during transition.

The pressure control system and fuel dump valve interaction was determined by applying a step change to the FDV electropneumatic transducer. This was accomplished by electrically switching from the use of one FDV valve to both valves open to the same setting. Valve area change is at the maximum possible rate. Figure 8.3-8 shows the flow rates and dump plenum pressure during a typical run. The pressure control system damping factor was 0.1 for this run.

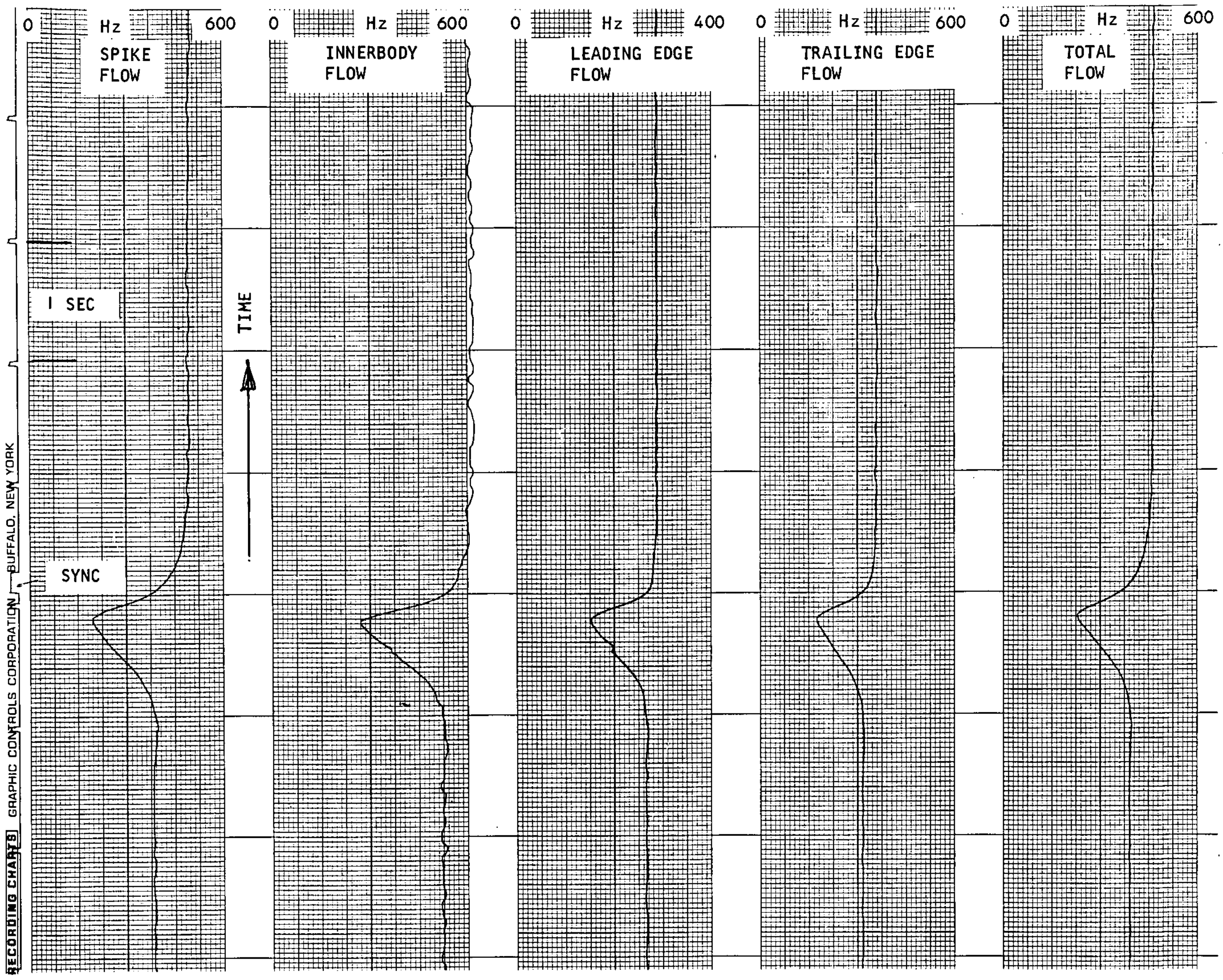

Figure 8.3-6. Low Hydrogen Flow Abort

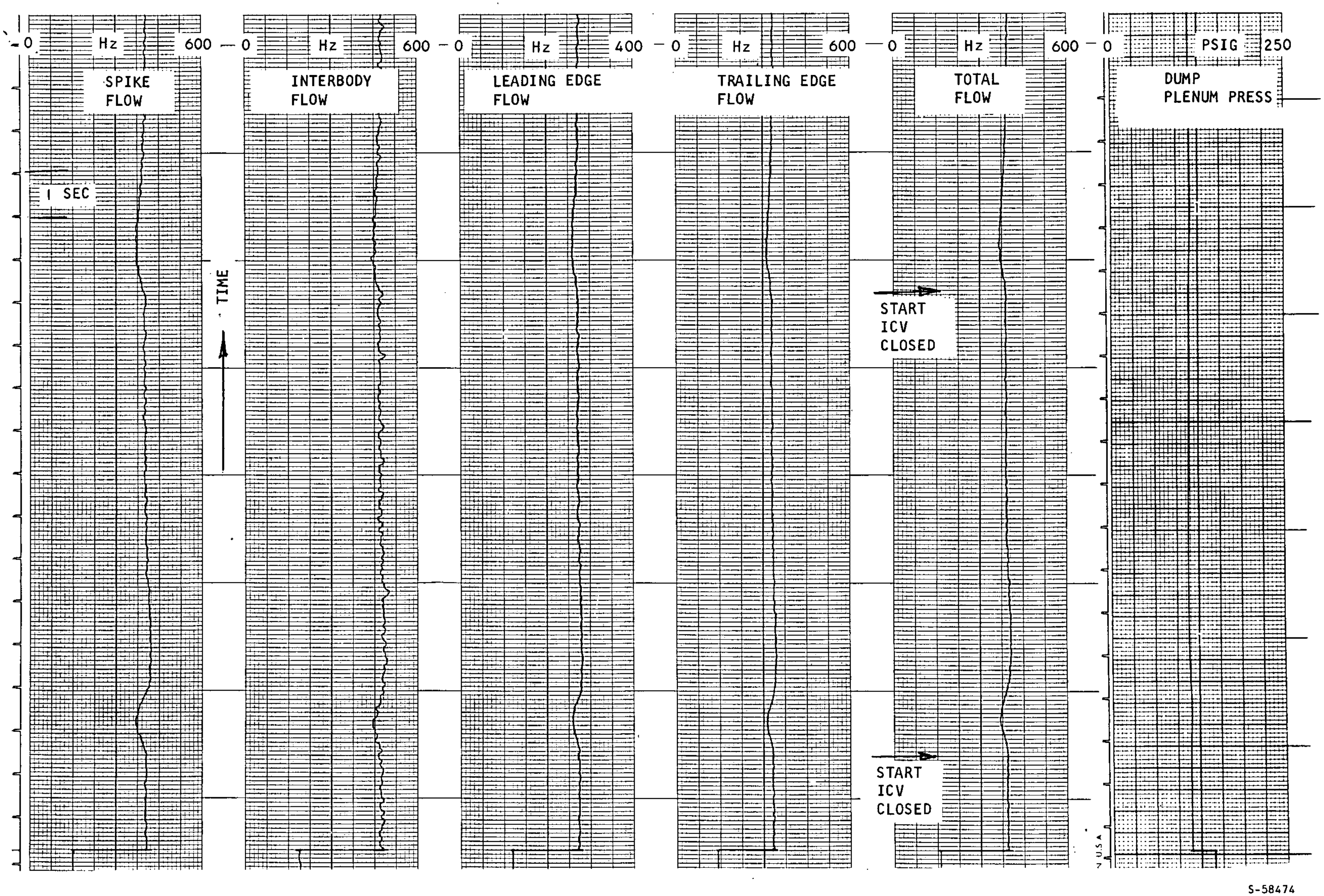

Figure 8.3-7. FDV-ICV Transition with PCV Operative

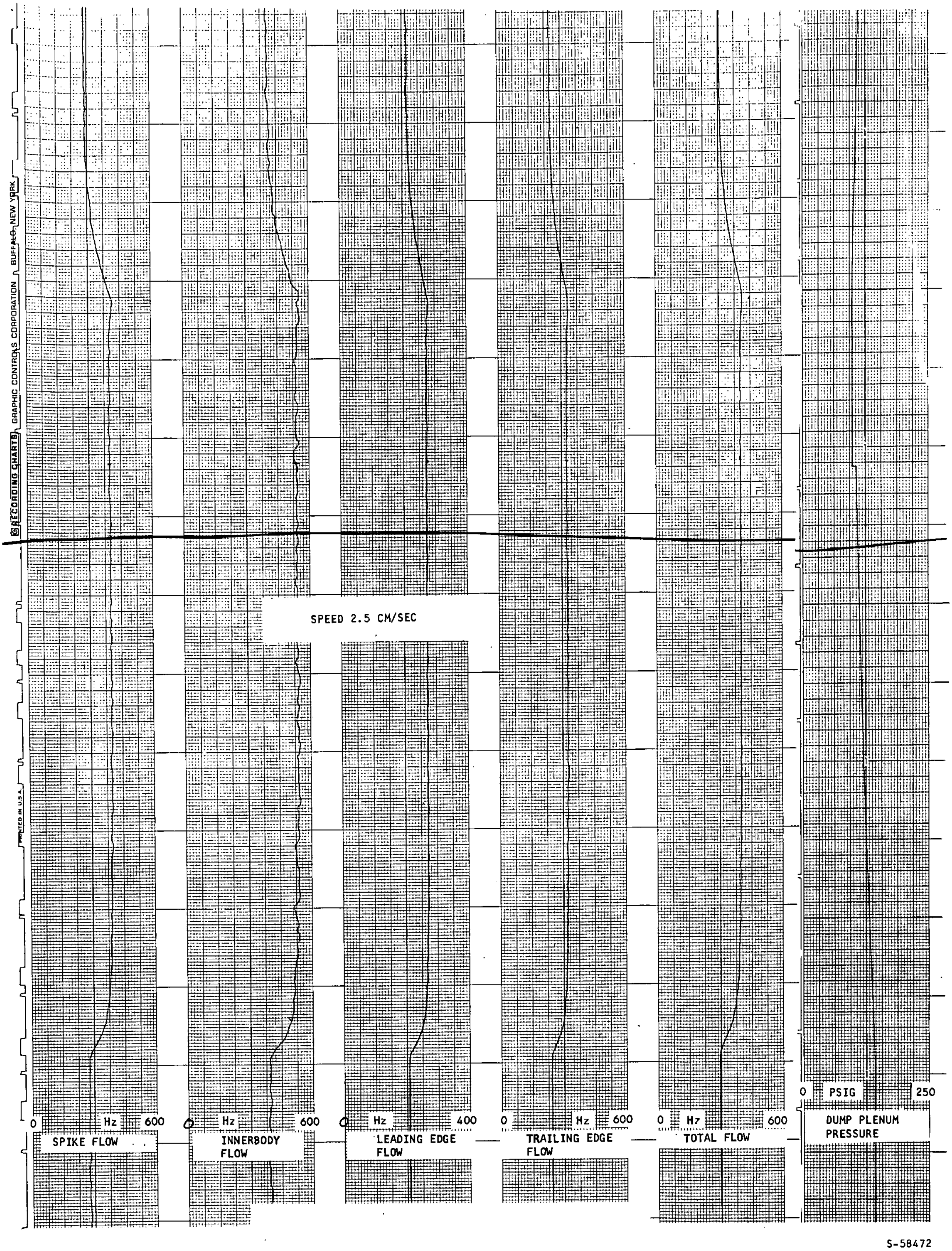

Figure 8.3-8. FDV-PCV Interaction

Performance shown is satisfactory, but not directly applicable to performance with hydrogen.

8.3.2 Water Systems

8.3.2.1 Flow Versus Pressure Drop

Pressure drop tests have been performed on the five water-cooled routes of the SAM. The flow routes are shown pictorially in Figures 8.3-9, 8.3-10, and 8.3-11. A schematic of the test setup is shown in Figures 8.3-12 and 8.3-13. Test results (route pressure drop versus water-flow rate) are presented in Figure 8.3-14 (routes 1 and 2) and Figures 8.3-15 (routes 3, 4, and 5).

Test pressure drops of flow routes 1 and 2 (low pressure system) are 41 and 18 percent lower than predictions, respectively, at the design point flow rates. Pressure drops of routes 3, 4, and 5 (high pressure system) are 25, 51, and 5 percent higher than predicted values. The predicted pressure drops and flow rates are reported in References (8-1) and (8-2).

8.3.2.2 Differential Pressure Switches

As a result of differences in test pressure drops from predicted values reported above, the differential pressure switch settings and operating pressures of all routes, and the flow rates of route 3 and 4 were modified from those reported in References (8-1) and (8-2). The pressure switch settings and resulting flow conditions based on water test data and the proposed initial settings and conditions for SAM testing are presented in Table 8.3-1. Pressure switch settings for SAM testing are noted in Figures 8.3-14 and 8.3-15. The lower (than predicted) operating flow rates in routes 3 and 4 have been accepted so that the inlet pressure on the high pressure system can be common for routes 3, 4, and 5. It is noted that the predicted water flow rates were based on maximum tunnel heating conditions. As the SAM tunnel heating conditions are increased from test to test, the water routes (and, in particular, routes 3 and 4) will be checked for overheating. Water flow rates will be increased accordingly. Sufficient margin exists in pressure containment strength to use the predicted flow rates if required.

8.3.3 Nitrogen Purge Systems

Tests were performed to measure the airflow through the two circuits that will have nitrogen purge flow during wind tunnel test. One circuit leads into the innerbody cavity and exhausts by means of leakage at the various O-ring seals between the outerbody and cowl/pylon, and between the cowl/pylon and the support wedge. The second circuit leads into and out of the second-stage injector manifold in the inner shell assembly to provide a purge flow for hydrogen leakage into this manifold from one of the strut pads. Exhaust was to sea level ambient in the tests.

Figure 8.3-16 shows the setup schematic for the cavity purge flow test and Figure 8.3-17 the setup for the manifold purge flow circuit test. The

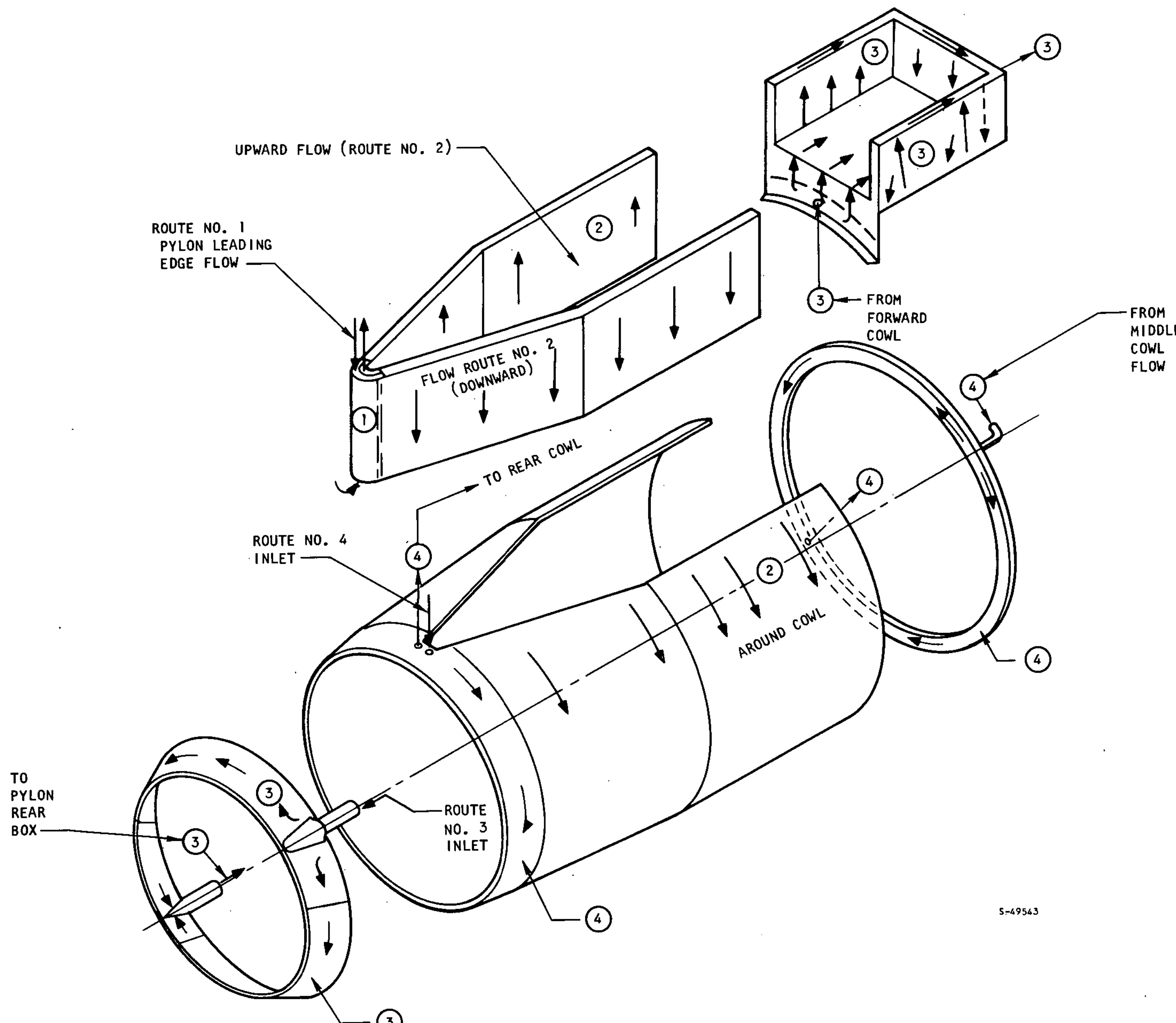

Figure 8.3-9. Coolant Flow Routes 1 Through 4 in SAM Cowl and Pylon

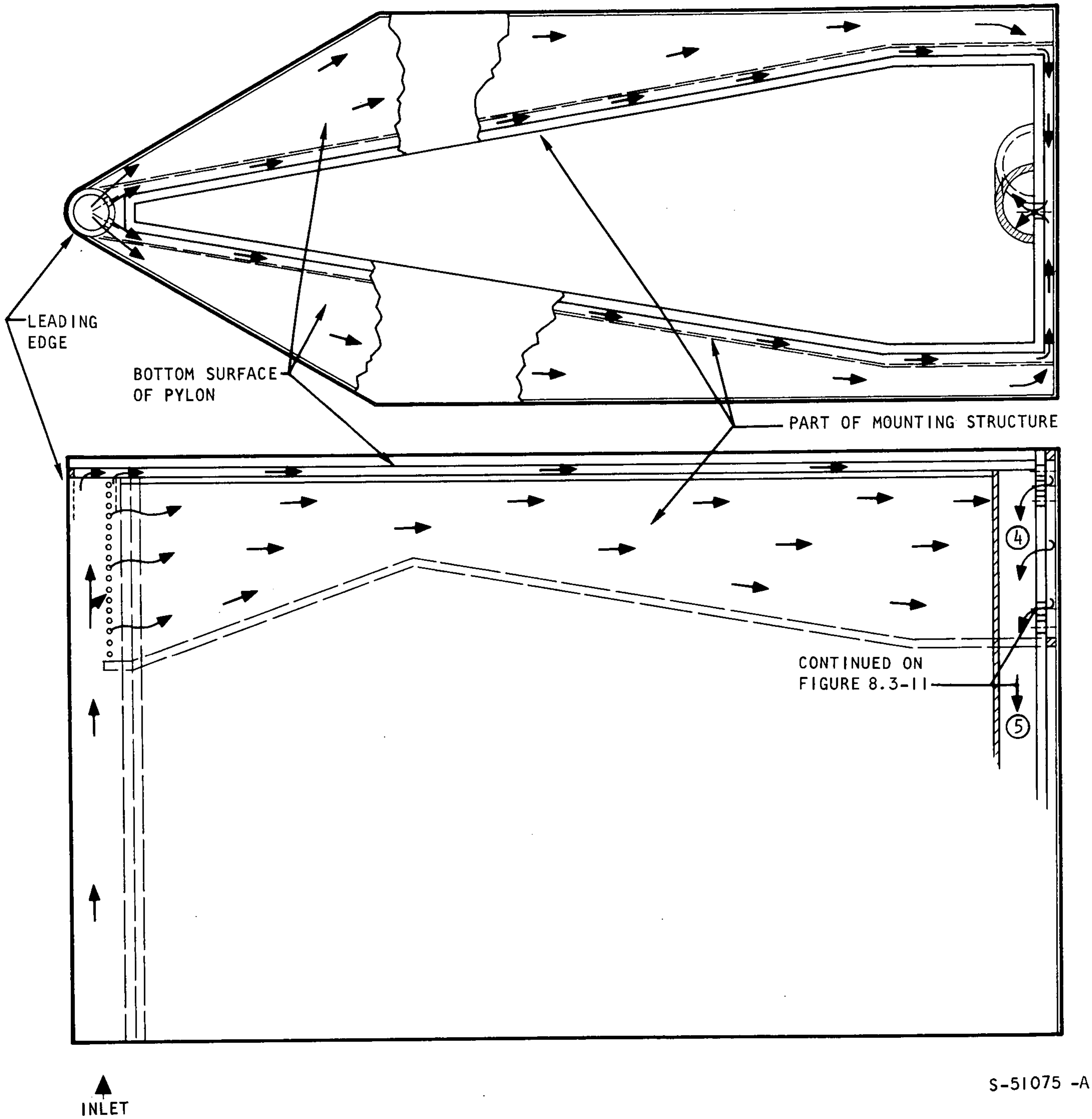

Figure 8.3-10. Support Wedge (Route 5) - Cooling of Mating Surface with Pylon, Leading Edge, and Part of Sides (Reference Figure 8.3-11)

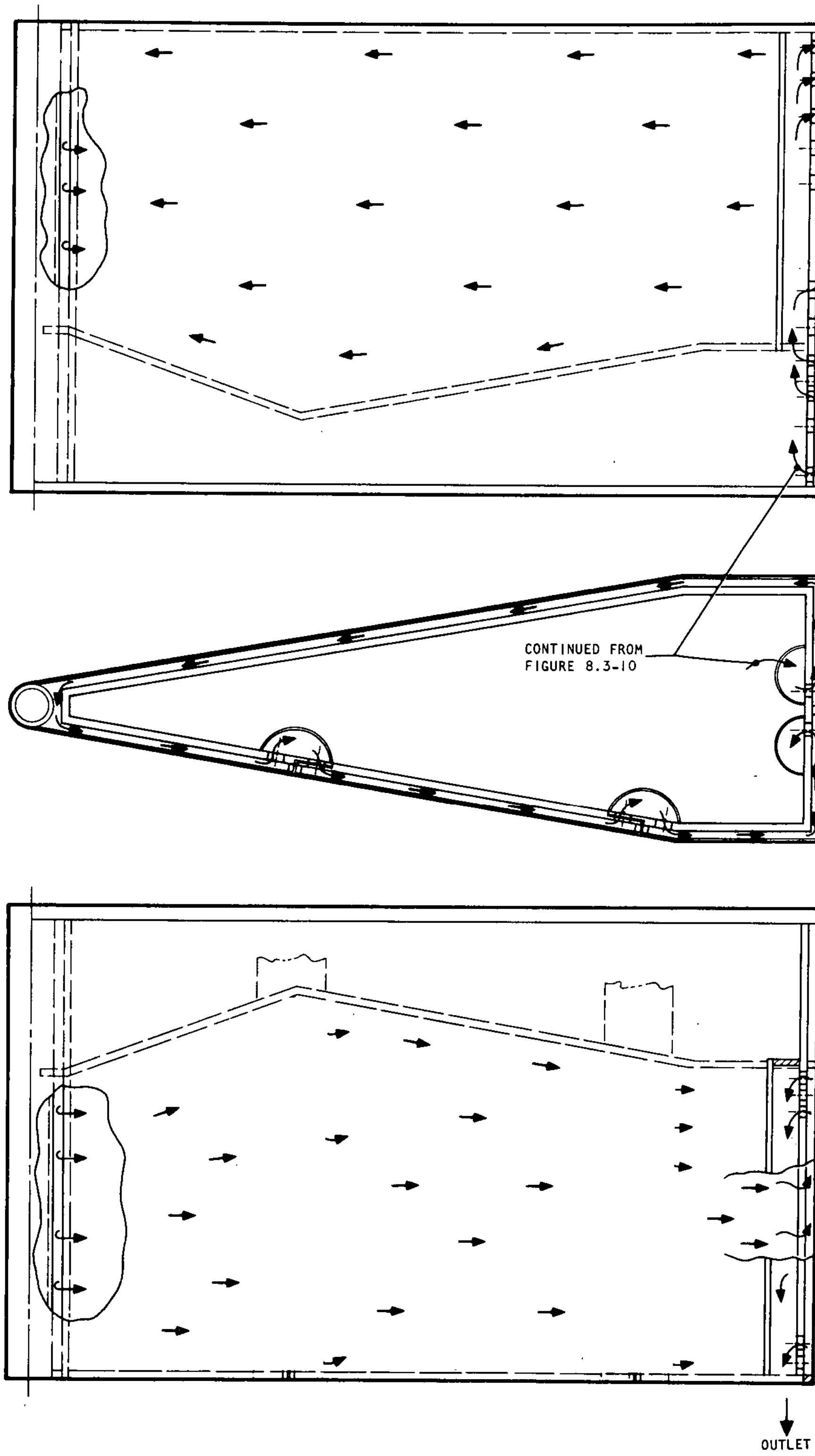

S-51076 -A

Figure 8.3-11. Support Wedge (Route 5) - Cooling of Remaining Part of Sides (Reference Figure 8.3-10)

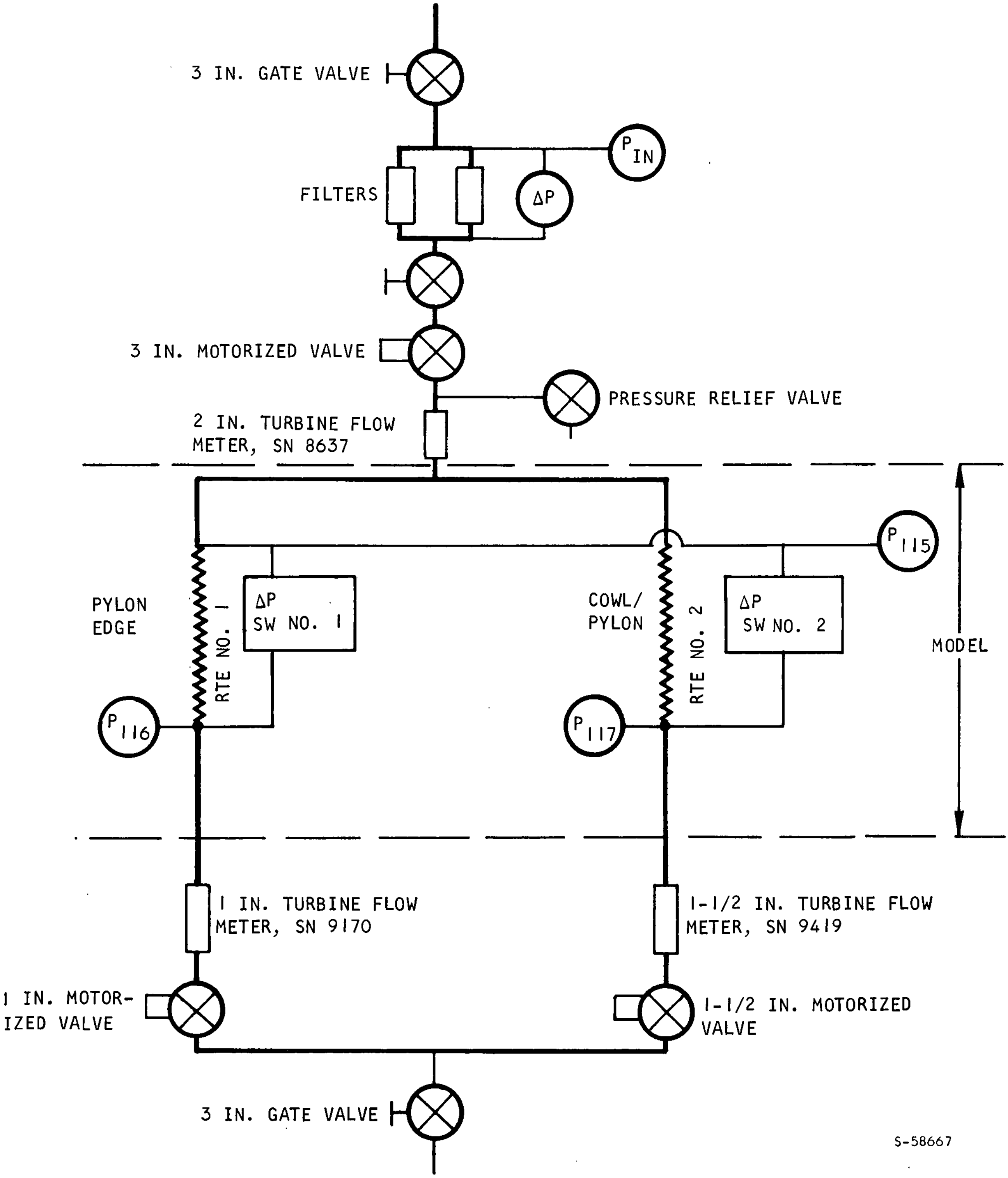

Figure 8.3-12. Low Pressure Water Cooling System

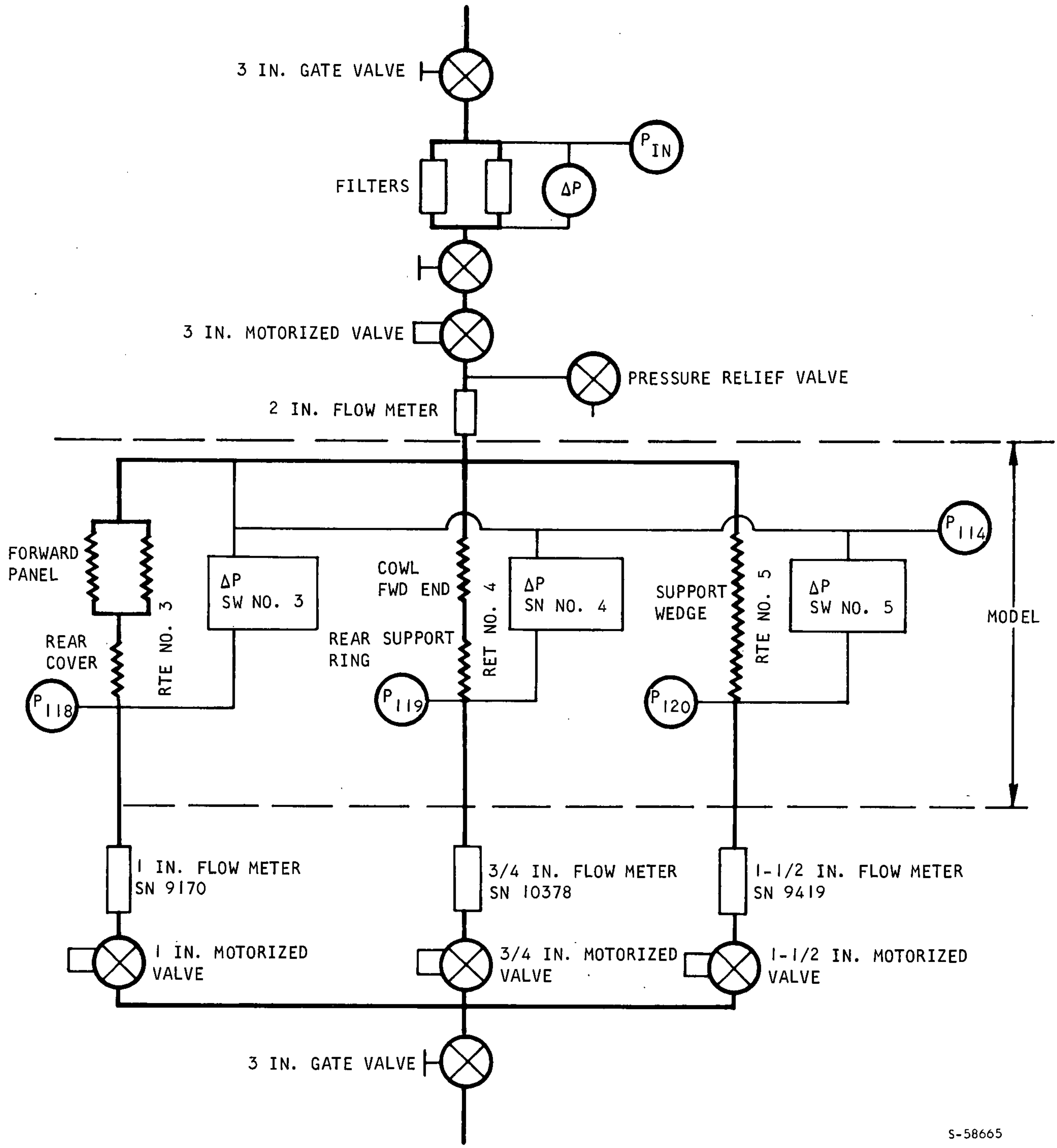

Figure 8.3-13. High Pressure Water Cooling System

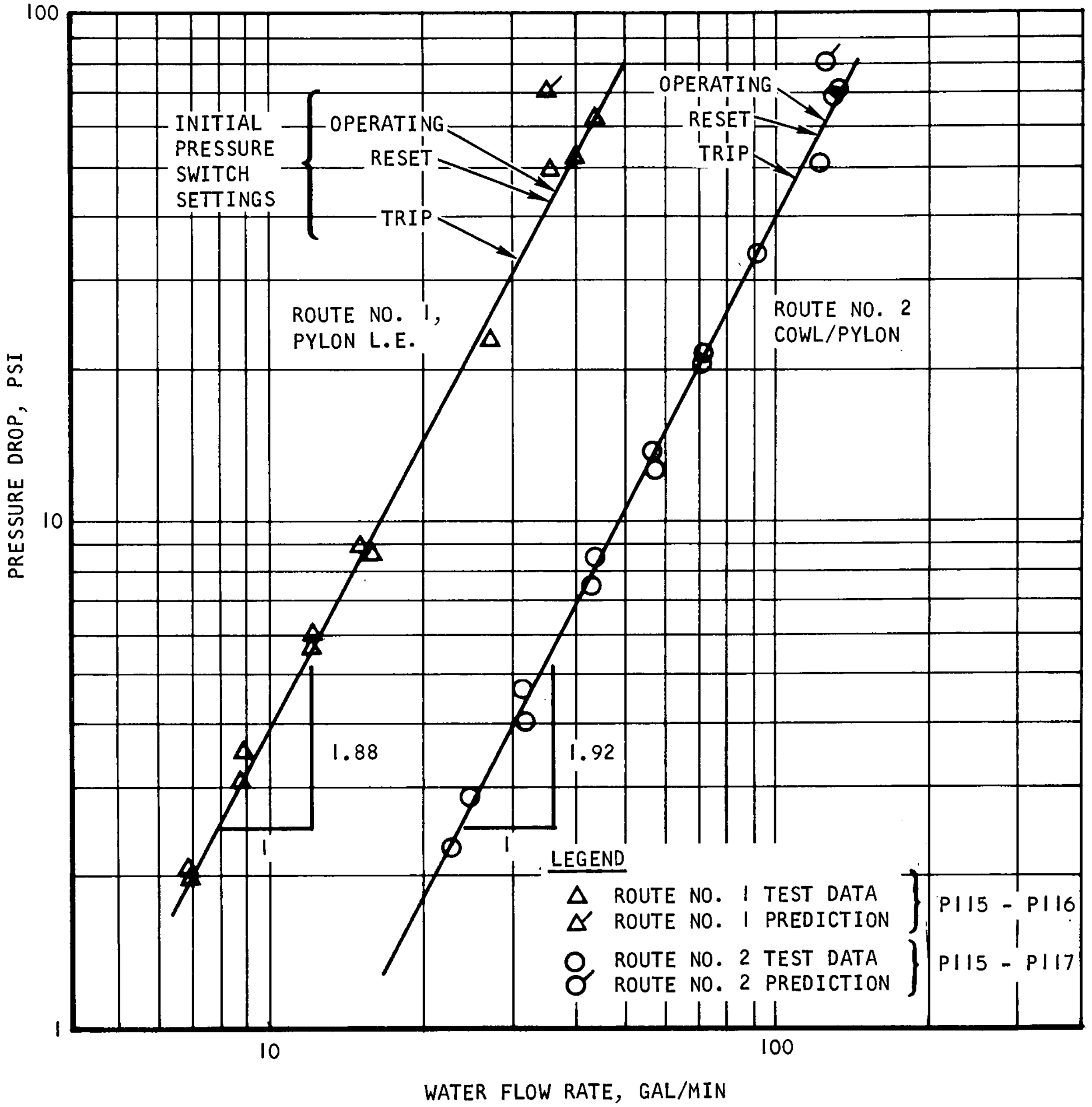

S-58666

Figure 8.3-14. SAM Water Flow Routes 1 and 2 Pressure Drop Test Results

LEGEND

- ○ ROUTE NO. 3 TEST DATA — P114 - P118
- ROUTE NO. 3 PREDICTION
- △ ROUTE NO. 4 TEST DATA — P114 - P119
- ROUTE NO. 4 PREDICTION
- ▽ ROUTE NO. 5 TEST DATA — P114 - P120
- ▽ ROUTE NO. 5 PREDICTION

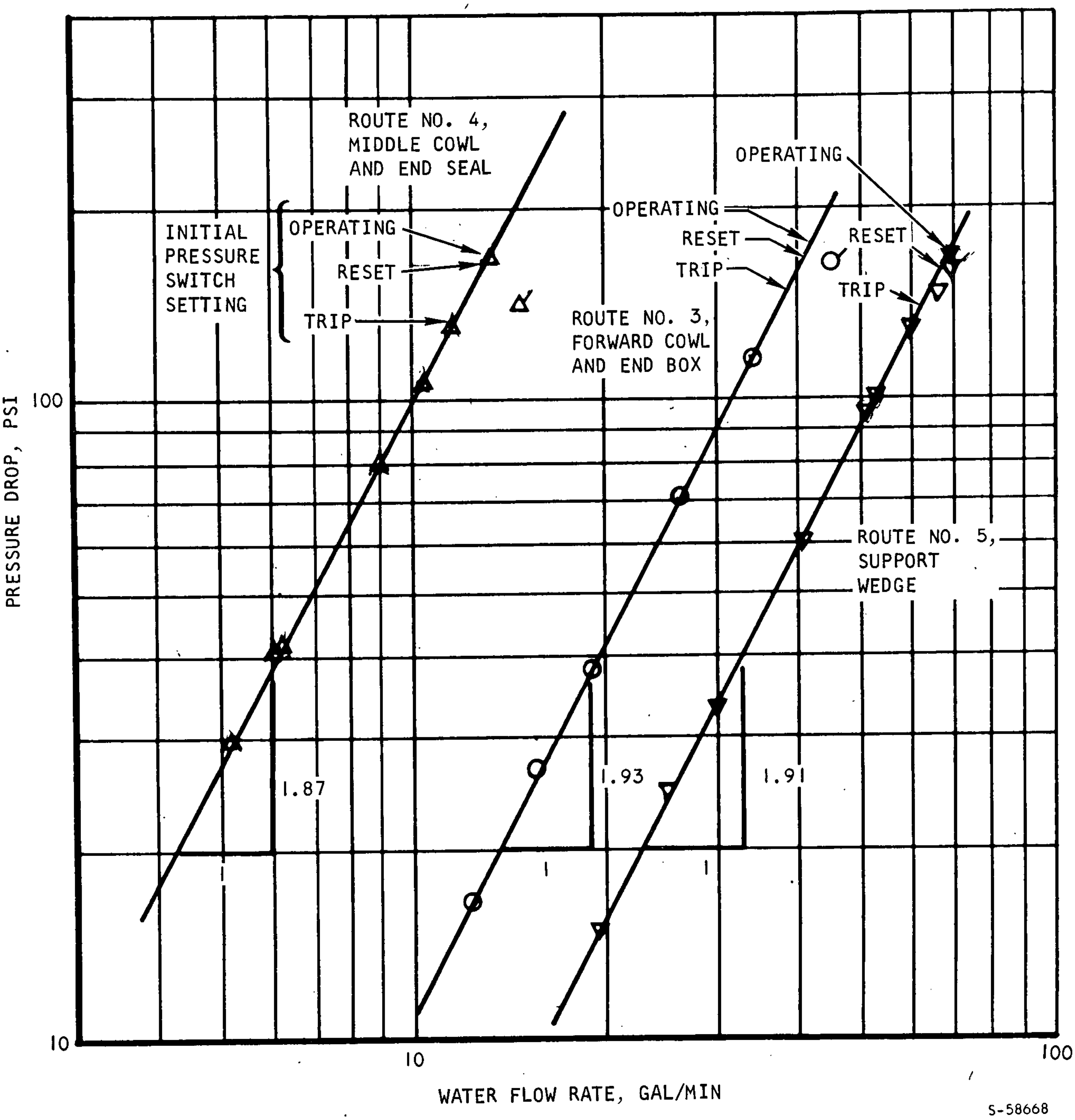

Figure 8.3-15. SAM Water Flow Routes 3, 4, and 5 Pressure Drop Test Results

TABLE 8.3-1

WATER TEST RESULTS AND MODIFIED CONDITIONS FOR SAM TESTING

	Parameter	Route 1	Route 2	Route 3	Route 4	Route 5
Test results at Design flow rate	Design flow rate, gpm	37	125	43	15	70
	Test pressure drop, psi	45 (70)*	62 (80)*	210 (160)*	220 (140)*	170 (160)*
	Trip flow rate, gpm	31	108	40	13	63
	Trip pressure drop, psi	33	47	165	170	139
	Reset pressure drop, psi	43	57	185	190	159
Initial setting and conditions for SAM testing	Operating flow rate, gpm	37	125	42	13	70
	Operating press.drop, psi	45	62	175	170	170
	Trip flow rate, gpm	31	108	39	12	63
	Trip pressure drop, psi	33	47	150	145	139
	Reset press. drop, psi	43	57	170	165	159
	Operating inlet pressure, psig	90	90	190	190	190
	Operating outlet pressure, psig	45	28	15	20	20

*Indicates predicted pressure drop

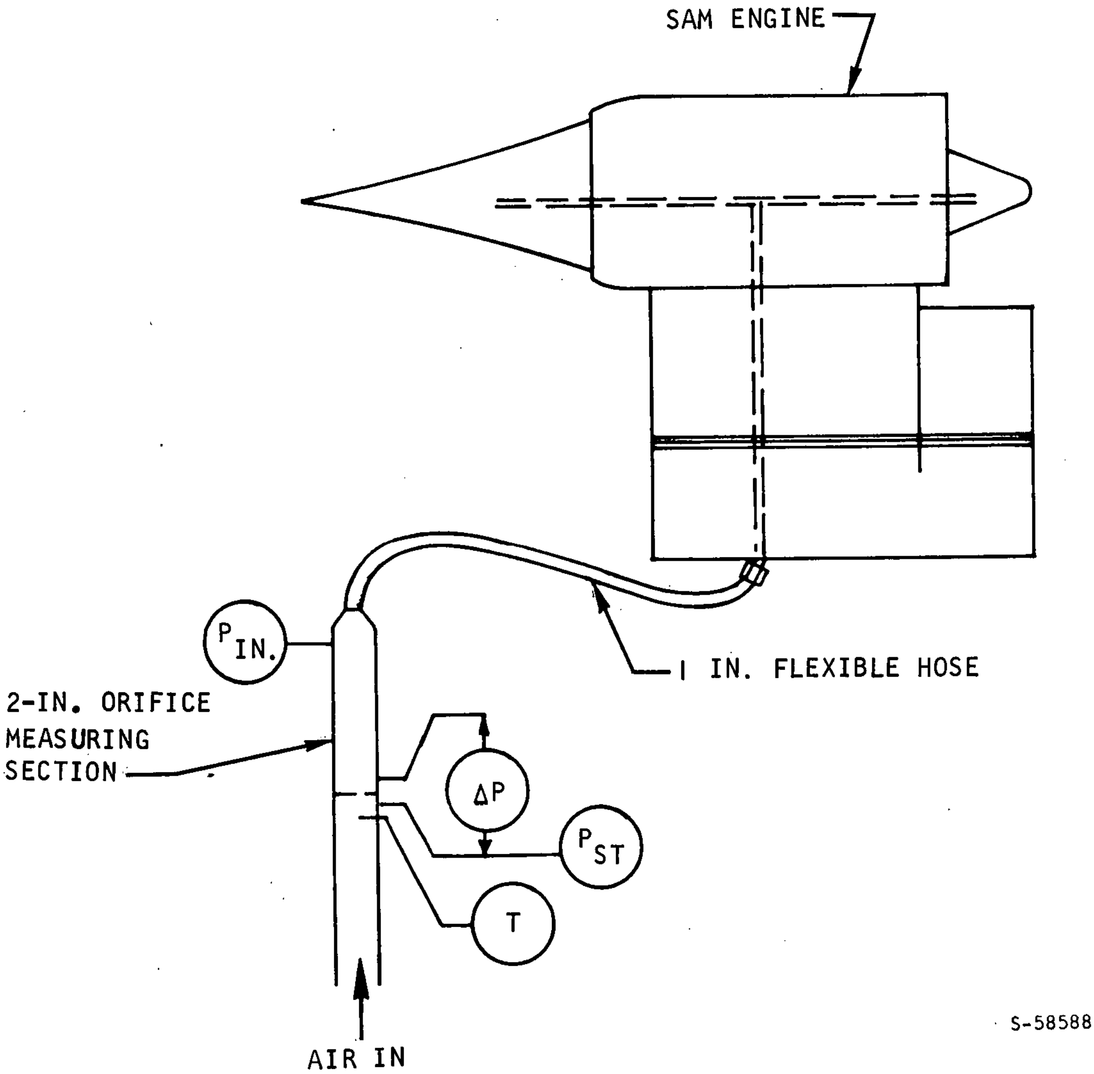

Figure 8.3-16. Test Setup Schematic - Cavity Purge Flow

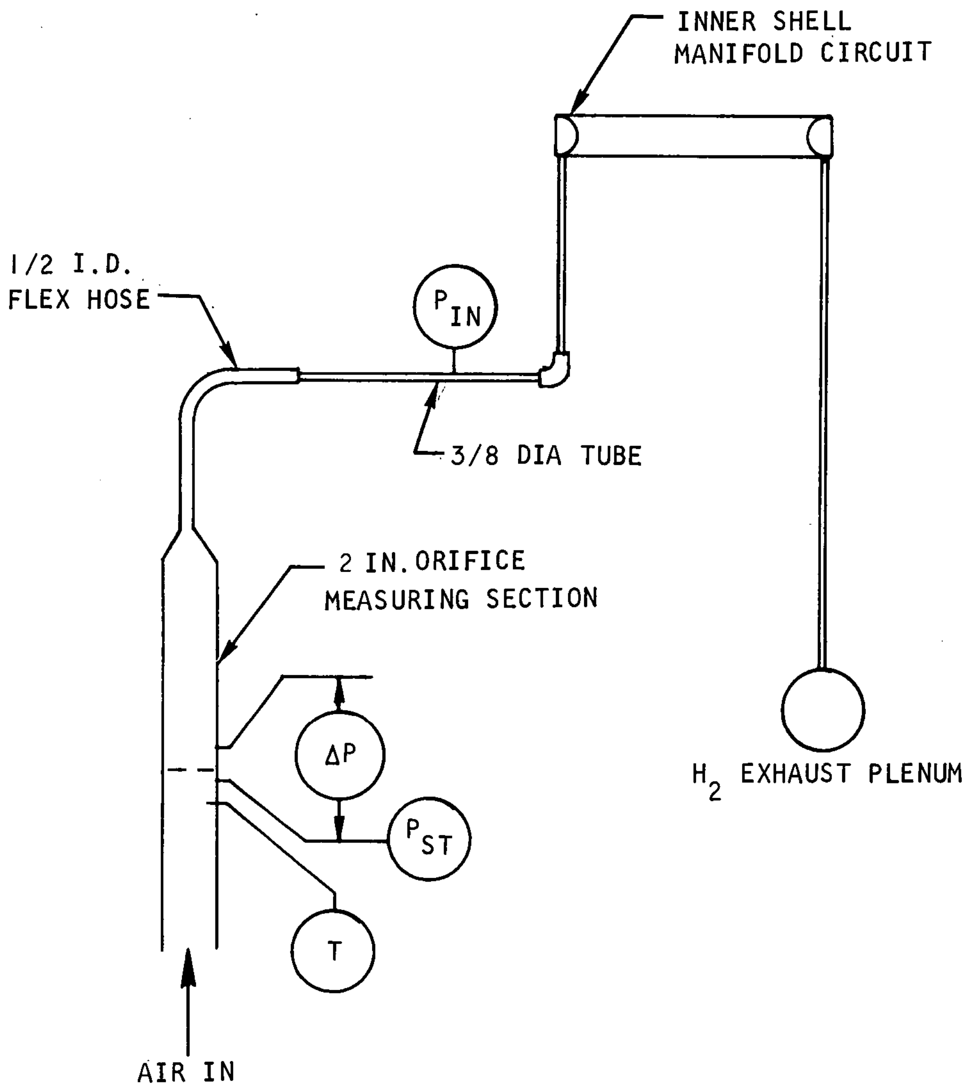

Figure 8.3-17. Test Setup Schematic - Manifold Purge Flow

S-58586

results of the tests are shown in Figure 8.3-18; also shown are relationships of both the cavity and manifold flows to inlet pressure and of the cavity pressure to inlet pressure. These results will be used to set purge flows during tunnel tests. Cavity purge pressure will be limited to 12 psi differential relative to tunnel freestream static pressure. Manifold inlet pressure will be approximately 120 psi. These pressure levels assure outflow of purge gas at all tunnel and coolant operating conditions.

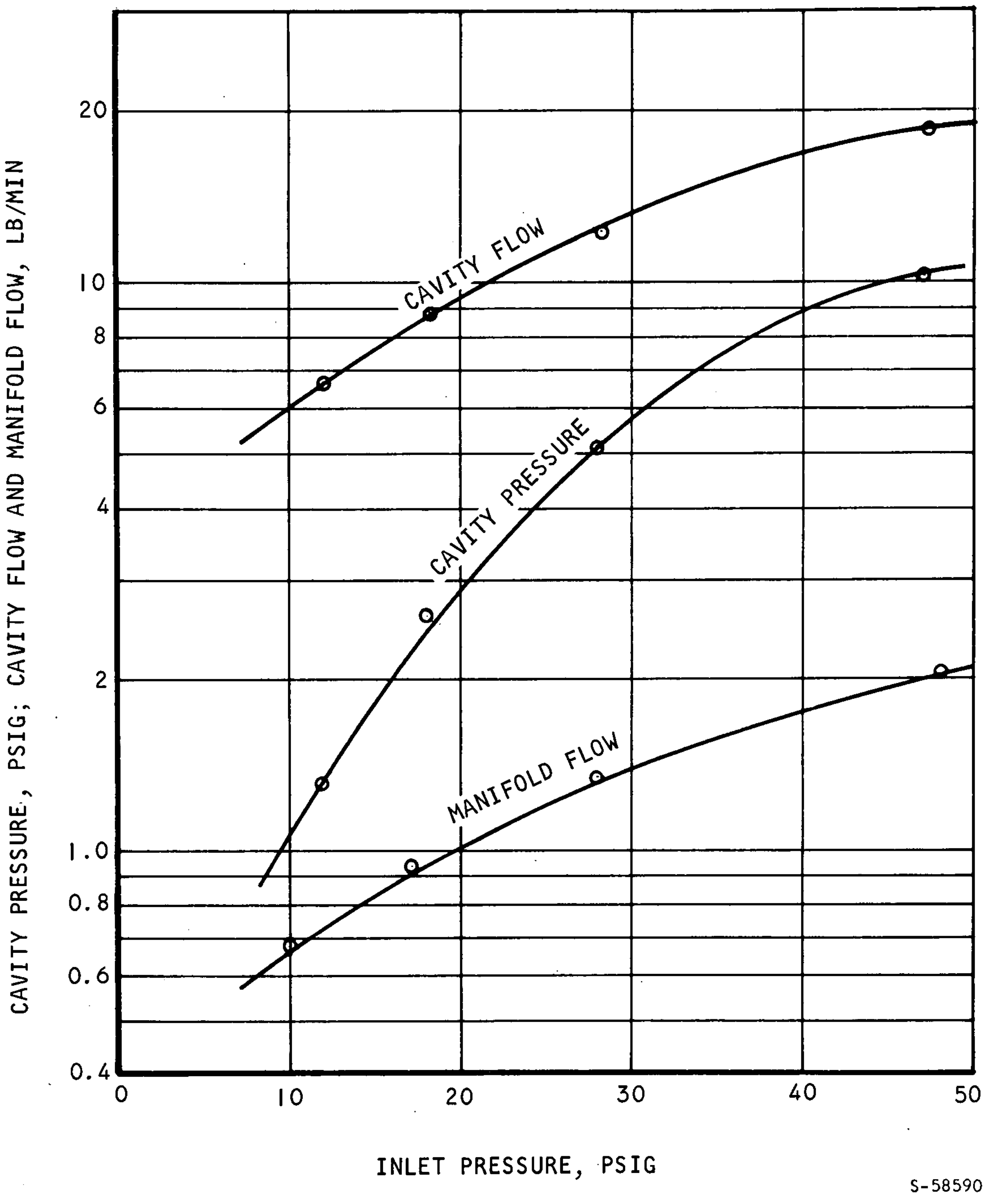

Figure 8.3-18. Nitrogen Purge Flows and Pressures

9. FUTURE ACTION

Scheduled activities for the next reporting period are all related to the testing of the SAM in the NASA-Langley 8-ft-High Temperature Structures Tunnel. Upon the delivery of the model, the engine and manifold assembly will be re-assembled outside of the test section and then installed as a unit. Initial checkouts are expected to begin in October and will be followed by the scheduled test runs.

Preparation of a data reduction program is in process. In addition, the programming necessary to convert the data acquisition system tapes to BCD tapes (engineering units) is in process and will be completed to permit checkout of the data reduction program prior to start of the scheduled test runs. Most of the programming associated with the latter effort involves the calculation of parameters necessary to monitor test operation, such as flow rates, heat fluxes, temperature differences, and selected pressure drops. Detail analysis of test conditions and of performance of the model will be performed by the data reduction program, which will use the BCD tapes as input.

REFERENCES

5-1. Engineering Staff, Hypersonic Research Engine Project - Phase IIA, Structures and Cooling Development, Twelfth Interim Technical Data Report, AiResearch Report No. AP-70-6116, Data Item No. 55-7.12, 11 March 1970.

5-2. Engineering Staff, Hypersonic Research Engine Project - Phase IIA, Structures and Cooling Development, Tenth Interim Technical Data Report, AiResearch Report No. AP-69-5390, Data Item No. 55-7.10, 26 August 1969.

8-1. Engineering Staff, Hypersonic Research Engine Project - Phase IIA, Structures and Cooling Development, Eighth Interim Technical Data Report, AiResearch Report No. AP-69-4759, Data Item No. 55-7.08, 27 February 1969.

8-2. Engineering Staff, Hypersonic Research Engine Project - Phase IIA, Structures and Cooling Development, Ninth Interim Technical Data Report, AiResearch Report No. AP-69-5075, Data Item No. 55-7.09, 3 June 1969.